TRANSCRIPTIONAL REGULATION OF CARDIAC VENTRICULAR DEVELOPMENT

APPROVED BY SUPERVISORY COMMITTEE

Mentor: Deepak Srivastava, M.D. _____

Chairperson: Rueyling Lin, Ph.D. _____

Daniel J. Garry, M.D., Ph.D._____

Eric N. Olson, Ph.D. _____

To my mother and father, for their constant love and support in all my life's endeavors. To my husband Mark for his endless love, encouragement, and friendship. To my family, past and present, for the love, the laughs, and the memories.

TRANSCRIPTIONAL REGULATION OF CARDIAC VENTRICULAR DEVELOPMENT

by

STEPHANIE ANGELO PIERCE

DISSERTATION

Presented to the Faculty of the Graduate School of Biomedical Sciences

The University of Texas Southwestern Medical Center at Dallas

In Partial Fulfillment of the Requirements

For the Degree of

DOCTOR OF PHILOSOPHY

The University of Texas Southwestern Medical Center at Dallas

Dallas, Texas

June, 2004

Copyright

by

Stephanie Angelo Pierce 2004

All Rights Reserved

TRANSCRIPTIONAL REGULATION OF CARDIAC VENTRICULAR DEVELOPMENT

Publication No. _____

Stephanie Angelo Pierce, Ph.D.

The University of Texas Southwestern Medical Center at Dallas, 2004

Supervising Professor: Deepak Srivastava, M.D.

Congenital heart disease is the leading non-infectious cause of death in children. Disruption of cardiac gene expression during development can result in congenital heart defects. Numerous transcription factors regulate specific temporo-spatial events during cardiac differentiation and morphogenesis, however the mechanisms that regulate such events are largely unknown. Using a novel modified subtractive hybridization method to identify early cardiac-specific genes, we found *Bop,* a histone deacetylase-dependent transcriptional repressor. *Bop* was expressed specifically in the myocardium of the heart and somites during development. Targeted deletion of *Bop* in mouse resulted in hypoplasia of the right ventricle and expansion of the extracellular matrix between the myocardium and

endocardium of the embryonic heart, suggesting a persistence of immature ventricular cardiomyocytes. Expression of *dHAND*, the evolutionarily conserved bHLH factor necessary for proper right ventricle development, was downregulated in the heart of the *Bop*-null embryo. In an effort to understand the mechanism by which *Bop* functions in cardiac differentiation and morphogenesis, the yeast two-hybrid assay was used to identify factors that interact with m-Bop in the embryonic heart. The DNA-binding factor, skNAC, and the inhibitor of mitosis, TRB3, were identified. TRB3 enhanced repression of SV40-driven luciferase activity by m-Bop. Disruption of this interaction resulted in the inability of TRB3 to enhance m-Bop's repressive activity, suggesting a novel function for TRB3 as a corepressor of m-Bop in the developing heart. *skNAC* was expressed in the myocardium of the heart and somites, strikingly similar to the expression pattern of *Bop*. While early *in vitro* attempts to study m-Bop and skNAC failed, *in vivo* efforts to study a genetic interaction are ongoing.

TABLE OF CONTENTS

DEDICATION ii

ABSTRACT v

TABLE OF CONTENTS vii

PUBLICATIONS x

LIST OF FIGURES AND TABLES xi

INTRODUCTION 1

CARDIAC CELL FATE SPECIFICATION 1
CARDIAC MORPHOGENESIS AND LOOPING 2
TRANSCRIPTIONAL CONTROL OF CARDIOGENESIS 3
FIGURE 7
REFERENCES 8

CHAPTER 1: Conservation of Sequence and Expression of Xenopus and Zebrafish *dHAND* During Cardiac, Branchial Arch and Lateral Mesoderm Development 11

INTRODUCTION 11
RESULTS 12
DISCUSSION 17
METHODS 18
Zebrafish and *Xenopus* cDNA library screen 18
Whole mount RNA *in situ* hybridization 18
Histologic analysis 19
Reverse transcriptase polymerase chain reaction 19
FIGURES 20
REFERENCES 25

CHAPTER 2: *Bop* encodes a muscle-restricted MYND and SET domain-containing protein essential for cardiac differentiation and morphogenesis 27

INTRODUCTION 27
RESULTS 29
Isolation of chicken m-Bop by subtractive hybridization 29
Bop is expressed specifically in cardiac and skeletal muscle precursors 30
m-Bop can function as a transcriptional repressor 32
Transcriptional repression by m-Bop requires HDAC activity 33
Bop mutant mice show ventricular hypoplasia and expanded extracellular matrix 34

Cardiomyocyte maturation defect in *Bop* mutant mice 36
DISCUSSION 38
Selective and subtractive PCR amplification..... 39
Cardiomyocyte maturation defects in *Bop* mutant mice 39
Chamber-specific functions of *Bop* 40
m-Bop as a regulator of chromatin modification..... 41
METHODS 42
Cloning of chicken m-Bop cDNA 42
Whole-mount and section *in situ* hybridization 43
Cell culture and transient transfections 43
Luciferase assays..... 44
Immunoprecipitation and western blotting..... 45
Targeted deletion of *Bop* 45
Histochemistry..... 46
TUNEL assay 47
FIGURES 48
REFERNCES 56

CHAPTER 3: m-Bop interacts with cofactors that affect its function.....60

INTRODUCTION 60
RESULTS.....62
Yeast two-hybrid library construction and screening.....62
Testing the interactions by co-immunoprecipitation.....66
PART I
Bop and *TRB3* are coexpressed in the embryo 67
TRB3 does not affect subcellular localization of m-Bop.....67
TRB3 does not induce ubiquitin-mediated degradation of m-Bop.....68
TRB3 does not phosphorylate m-Bop by *in vitro* kinase assay.....68
TRB3 enhances transcriptional repression by m-Bop 69
N-terminus of TRB3 is necessary for interaction with m-Bop.....70
PART II
Bop and *skNAC* are coexpressed in the heart and somites.....72
m-Bop and the DNA-binding factor, skNAC 73
Targeted deletion of *skNAC* 74
DISCUSSION 75
Using the yeast two-hybrid as a tool..... 76
A role for TRB3 in cardiac development.....80
skNAC in the embryonic heart 82
METHODS 84
RNA isolation.....84
Yeast two-hybrid library construction and screening..... 85
Plasmid construction..... 86
Immunoprecipitation and western blotting.....86

Whole mount and section *in situ* hybridization 87
Cell culture and transient transcfections 87
Luciferase assay 88
Immunocytochemistry 88
Kinase assay 89
Targeted deletion of *skNAC* 89
FIGURES AND TABLE 90
REFERNCES 100

DISCUSSION 103
FIGURE 105

ACKNOWLEDGEMENTS 106
VITAE 107

PUBLICATIONS

Paul D. Gottlieb*, **Stephanie A. Pierce***, Robert J. Sims III, Hiroyuki Yamagishi, Elizabeth K. Weihe, June V. Harriss, Shanna D. Maika, William A Kuziel, Heather L. King, Eric N. Olson, Osamu Nakagawa and Deepak Srivastava. Bop encodes a muscle-restricted protein containing a MYND and SET domain and is essential for cardiac differentiation and morphogenesis. Nature Genetics, 31:25-32 (2002). *Authors contributed equally.

Stephanie Angelo, Jamie Lohr, Kyu H. Lee, Baruch S. Ticho, Roger E. Breitbart, Sandra Hill, H. Joseph Yost, Deepak Srivastava. Conservation of sequence and expression of Xenopus and Zebrafish *dHAND* during cardiac, branchial arch and lateral mesoderm development. Mechanisms of Development, 95:231-237 (2000).

LIST OF FIGURES AND TABLES

FIGURE I-1. Overview of cardiogenesis 7

FIGURE 1-1. Amino-acid sequence alignment of dHAND..... 20

FIGURE 1-2. *dHAND* expression in staged zebrafish embryos..... 21

FIGURE 1-3. *dHAND* expression in staged *Xenopus* embryos 22

FIGURE 1-4. *eHAND* expession in staged *Xenopus* embryos..... 23

FIGURE 1-5. Expression of *dHAND* in adult *Xenopus* tissues..... 24

FIGURE 2-1. Cardiac and somite-specific expression of *Bop* in chick and mouse..... 48

FIGURE 2-2. m-Bop2 is an HDAC-dependent transcriptional repressor..... 49

FIGURE 2-3. Targeted deletion of *Bop* is embryonic lethal from cardiac enlargement..... 51

FIGURE 2-4. Single ventricle and extracellular matrix accumulation in *Bop* -/- embryos 52

FIGURE 2-5. *dHAND* is downregulated in cardiomyocyte precursors of *Bop* -/- embryos 54

FIGURE 3-1. Yeast two-hybrid library construction 90

TABLE 3-1. Identification of yeast two-hybrid clones..... 91

FIGURE 3-2. Yeast two-hybrid clones immunoprecipitate with m-Bop..... 92

FIGURE 3-3. TRB3 enhances repression by m-Bop 93

FIGURE 3-4. N-terminus of TRB3 is necessary and sufficient to interact with m-Bop..... 95

FIGURE 3-5. N-terminal deletion disupts enhanced repression by TRB3 97

FIGURE 3-6. *skNAC* and *Bop* are coexpressed..... 98

FIGURE 3-7. Targeting strategy for *skNAC* 99

FIGURE D-1. Model: Bop represses transcription of target genes..... 105

INTRODUCTION

Congenital heart disease is the leading non-infectious cause of death in children. As we continue to study the molecular determinants of cardiogenesis, it has become increasingly clear that many cardiac abnormalities are due to mutations in developmental control genes. Historically, the identification of human congenital heart disease genes has occurred through the process of chromosome mapping. It has only been in the last decade that animal models have been used to study the genes involved in cardiac development and the genetic mutations that may lead to congenital heart disease. Thus, while heart formation is a complex biological process, understanding the genetic pathways controlling this process is essential to understanding how mutations in the developmental control genes result in congenital heart disease.

Cardiac cell fate specification

Shortly after gastrulation, cells in the anterior plate mesoderm of the embryo become committed to a cardiogenic fate by inductive signals from the adjacent endoderm (Schultheiss et al., 1995). Bone morphogenetic protein-2 (BMP-2), and fibroblast growth factors (FGF) are known to play an instructive role in this process, undoubtedly among others yet to be identified (Schultheiss et al., 1997; Andree et al., 1998; Reifers et al., 2000). In vertebrates, the heart-forming region of the embryo or the cardiac crescent (Figure 1), is bordered by repressive signals mediated by Wnt family members (Tzahor and Lassar, 2001). Cells of the cardiac crescent express the Wnt antagonists, *Crescent* and *Dkk1*, which overcome these repressive signals allowing the cells to commit to a cardiac fate (Schneider

and Mercola, 2001; Marvin et al., 2001). Induction of the heart-forming region is marked by expression of the homeodomain factor, *Nkx2*.5.

Cardiac morphogenesis and looping

Once the cells of the cardiac crescent have assumed a cardiogenic fate, these cells converge along the ventral midline of the embryo forming a beating linear heart tube composed of two cell layers. The outer layer called the myocardium is separated from the inner layer of cells, the endocardium, by extracellular matrix secreted by the myocardial cells (Hurle et al., 1980). The heart tube is patterned along the anterior-posterior axis in a segmental fashion delineating future chambers and regions of the heart (Figure 1). In vertebrates, the heart tube undergoes rightward looping critical for proper orientation of the ventricles and proper alignment of the heart chambers with the great vessels. As the heart tube loops, the chambers balloon out from the outer curvature of the heart (Figure 1). The molecular mechanisms underlying the process of looping are unclear, however, differentially expressed genes along the inner and outer curvature of the heart tube appear to be involved in driving this morphogenetic process. As the cardiomyocytes of the looped heart mature, the extracellular matrix between the myocardial and endocardial cell layers is degraded by enzymes synthesized by the myocardium, lessening the gap between these two cardiac cell layers. Further differentiation and morphogenesis of the looped heart tube results in formation of the four-chambered heart (Figure 1). Many of the transcription factors necessary for cardiac gene expression during differentiation and morphogenesis of the developing ventricles are detailed below.

Transcriptional control of cardiogenesis

Nkx2.5 is a direct target of BMP signaling in the cardiac crescent of the developing embryo (Liberatore et al., 2002). While looping morphogenesis is blocked in *Nkx2*.5 mutant mice, the heart tube is properly formed, suggesting a nonessential role for *Nkx2*.5 in cell fate specification (Lyons et al., 1995). Tinman, the Drosophila ortholog of Nkx2.5, directly activates transcription of the *Mef2* gene (Gajewski et al., 1998). Inactivation of *Mef2c* in mice results in embryonic lethality at the looping heart tube stage and hypoplasatic left and right ventricles (Lin et al., 1997). MEF2 factors are direct activators of myocyte differentiation genes and mice homozygous-null for the *Mef2c* gene fail to express a subset of muscle structural genes.

The GATA factors are also implicated in early embryonic control of the cardiac muscle gene program and formation of the linear heart tube. Three GATA family members, *GATA4*, -5, and -6 are expressed in different cardiac cell lineages at various times during development (Laverriere et al., 1994; Jiang and Evans, 1996). GATA binding sites in the enhancer region of *Nkx2*.5 direct early cardiac gene expression of *Nkx2*.5 in the cardiac crescent (Lien et al., 1998; Searcy et al., 1998). Likewise, Nkx2.5 directly binds multiple cardiac enhancers upstream of the *GATA6* gene (Molkentin et al., 2000). While these two factors can regulate one another's expression, they also physically interact to activate specific sets of downstream target genes (Durocher et al., 1997; Lee et al., 1998; Sepulveda et al., 1998). GATA factors also cooperate with MEF2 factors in cardiomyocyte differentiation and early morphogenesis of the heart tube (Morin et al., 2000). Heterozygous human mutations

of GATA4 or Nkx2.5 can cause congenital heart anomalies (Schott et al., 1998; Garg et al., 2004).

A number of factors are required for the transcriptional control of morphogenesis and patterning in the vertebrate heart. During mouse development, the basic helix-loop-helix (bHLH) transcription factors dHAND and eHAND are initially expressed throughout the heart tube before becoming restricted to predominantly the right and left ventricular segments, respectively (Srivastava et al., 1995). Targeted deletion of mouse *dHAND* results in hypoplasia of the right ventricle and embryonic lethality at approximately E9.5 (Srivastava et al., 1997). The presence of only one ventricular chamber in zebrafish is paralleled with the presence of only one *HAND* gene, *dHAND* (Angelo et al., 2000). Expression of *dHAND* in the developing zebrafish heart is essential for formation of the ventricular chamber suggesting a role for eHAND in higher organisms as one ventricular chamber evolved into two, a right ventricle and a left ventricle (Yelon et al., 2000).

Cardiac chamber-specific expression of the *HAND* genes suggests the presence of *cis*-regulatory elements that can decipher the left from the right ventricle. Expression of *dHAND* in the right ventricle is dependent on two GATA binding sites in the enhancer region of this gene (McFadden et al., 2000). Because GATA factors are not expressed in a chamber-specific fashion, the presence of an unidentified chamber-specific coactivator is a likely candidate to cooperate with GATA factors in activating transcription of *dHAND*.

Irx4, a member of the *iroquois* family of homeobox genes is expressed specifically in the primitive ventricular segment of the heart tube and persists in the ventricular chambers as development proceeds (Bao et al., 1999). Inactivation of *Irx4* in mouse revealed an

expansion of atrial markers and repression of ventricular markers of differentiation in the heart (Bruneau et al., 2001). These data suggested a role for Irx4 in promoting ventricular gene expression and suppressing atrial identity in the ventricles of the heart. *Irx4* is partially downregulated in the *dHAND*-null mouse identifying a role for this molecule in differentiation of the right ventricle as well (Yamagishi et al., 2001; Bruneau et al., 2000).

The T-box gene, *Tbx5*, is initially expressed in the precardiac mesoderm of the embryo, and becomes restricted to the posterior segments of the heart tube including the primitive atria, left ventricular segment, and the sinus venosa (Bruneau et al., 1999). Targeted deletion of *Tbx5* in mouse results in hypoplastic atria and left ventricle, and atrial and ventricular septal defects (Bruneau et al., 2001). These data suggest a possible role for Tbx5 in specification of atrial versus ventricular cell fate along the anterior-posterior axis of the heart tube. Cooperative transcriptional regulation of this process is suggested by the physical interaction of Tbx5 and Nkx2.5 and the coexpression of these molecules in the developing heart (Hiroi et al., 2001; Bruneau et al., 2001). Recent reports have also suggested a role for cooperative transcriptional control of target genes through physical interaction of Tbx5 and GATA4 (Garg et al., 2003).

Multiple layers of complexity govern the regulation of transcription in a living organism, including the process of chromatin remodeling. The basic unit of chromatin is the nucleosome, which is comprised of 146 base pairs of DNA wrapped around two copies each of histones H2A, H2B, H3 and H4. Compaction of nucleosomes through histone-histone and histone-DNA interactions limits access to genomic DNA creating a structure that is impenetrable to transcription factors. Histone tails are free from this compact structure and

modification of the tail allows for reorganization of chromatin structure. Specific residues within the histone tails are subject to post-translational modifications including acetylation, methylation, phosphorylation and ubiquitination.

Acetylation of specific lysine residues on histone tails occurs through the enzymatic activity of histone acetyl transferases (HATs). This post-translational event relaxes chromatin structure allowing gene transcription to take place. Reversal of this process by histone deacetylases (HDACs) promotes condensation of chromatin and transcriptional repression. Some SET domain-containing proteins can methylate specific unacetylated lysine residues on the histone tail resulting in more permanent silencing of gene transcription. With the identification of Bop, we reported the first cardiac-specific histone deacetylase-mediated and SET domain-containing transcriptional repressor (Gottlieb et al, 2002).

While many of the genes involved in transcriptional control of cardiogenesis have been identified, in large part, the mechanisms by which these genes function remain a mystery. This has led to a variety of methods and large-scale screens to identify partners that physically interact with essential transcriptional regulators, as well as methods to identify target genes regulated by the cardiac transcription factors. Identification of novel genes that function during cardiac development as well as novel activities of known cardiac-specific and ubiquitously expressed genes will continue to provide insight into the mechanisms by which the known regulators of cardiac gene expression function.

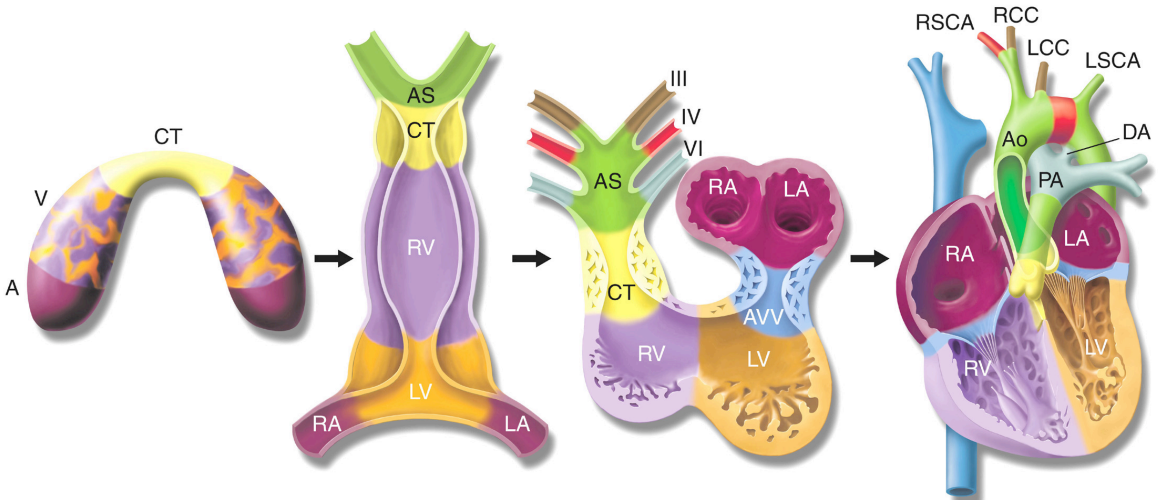

Srivastava and Olson, Nature 2000.

Figure 1. Overview of cardiogenesis.

REFERENCES

Andree, B., Duprez, D., Vorbusch, B., Arnold, H.H. & Brand, T. BMP-2 induces ectopic expression of cardiac lineage markers and interferes with somite formation in chicken embryos. *Mech Dev* **70**, 119-31 (1998).

Angelo, S. et al. Conservation of sequence and expression of Xenopus and zebrafish dHAND during cardiac, branchial arch and lateral mesoderm development. *Mech Dev* **95**, 231-7 (2000).

Bao, Z.Z., Bruneau, B.G., Seidman, J.G., Seidman, C.E. & Cepko, C.L. Regulation of chamber-specific gene expression in the developing heart by Irx4. *Science* **283**, 1161-4 (1999).

Bruneau, B.G. et al. Chamber-specific cardiac expression of Tbx5 and heart defects in Holt-Oram syndrome. *Dev Biol* **211**, 100-8 (1999).

Bruneau, B.G. et al. Cardiac expression of the ventricle-specific homeobox gene Irx4 is modulated by Nkx2-5 and dHand. Dev Biol 217, 266-77 (2000).

Bruneau, B.G. et al. Cardiomyopathy in Irx4-deficient mice is preceded by abnormal ventricular gene expression. *Mol Cell Biol* **21**, 1730-6 (2001).

Bruneau, B.G. et al. A murine model of Holt-Oram syndrome defines roles of the T-box transcription factor Tbx5 in cardiogenesis and disease. *Cell* **106**, 709-21 (2001).

Durocher, D., Charron, F., Warren, R., Schwartz, R.J. & Nemer, M. The cardiac transcription factors Nkx2-5 and GATA-4 are mutual cofactors. *Embo J* **16**, 5687-96 (1997).

Gajewski, K., Kim, Y., Lee, Y.M., Olson, E.N. & Schulz, R.A. D-mef2 is a target for Tinman activation during Drosophila heart development. *Embo J* **16**, 515-22 (1997).

Garg, V. et al. GATA4 mutations cause human congenital heart defects and reveal an interaction with TBX5. *Nature* **424**, 443-7 (2003).

Gottlieb, P.D. et al. Bop encodes a muscle-restricted protein containing MYND and SET domains and is essential for cardiac differentiation and morphogenesis. *Nat Genet* **31**, 25-32 (2002)

Hiroi, Y. et al. Tbx5 associates with Nkx2-5 and synergistically promotes cardiomyocyte differentiation. *Nat Genet* **28**, 276-80 (2001).

Hurle, J.M., Icardo, J.M. & Ojeda, J.L. Compositional and structural heterogenicity of the cardiac jelly of the chick embryo tubular heart: a TEM, SEM and histochemical study. *J Embryol Exp Morphol* **56**, 211-23 (1980).

Jiang, Y. & Evans, T. The Xenopus GATA-4/5/6 genes are associated with cardiac specification and can regulate cardiac-specific transcription during embryogenesis. *Dev Biol* **174**, 258-70 (1996).

Laverriere, A.C. et al. GATA-4/5/6, a subfamily of three transcription factors transcribed in developing heart and gut. *J Biol Chem* **269**, 23177-84 (1994).

Lee, Y. et al. The cardiac tissue-restricted homeobox protein Csx/Nkx2.5 physically associates with the zinc finger protein GATA4 and cooperatively activates atrial natriuretic factor gene expression. *Mol Cell Biol* **18**, 3120-9 (1998).

Liberatore, C.M., Searcy-Schrick, R.D., Vincent, E.B. & Yutzey, K.E. Nkx-2.5 gene induction in mice is mediated by a Smad consensus regulatory region. *Dev Biol* **244**, 243-56 (2002).

Lien, C.L. et al. Control of early cardiac-specific transcription of Nkx2-5 by a GATA-dependent enhancer. *Development* **126**, 75-84 (1999).

Lin, Q., Schwarz, J., Bucana, C. & Olson, E.N. Control of mouse cardiac morphogenesis and myogenesis by transcription factor MEF2C. *Science* **276**, 1404-7 (1997).

Lyons, I. et al. Myogenic and morphogenetic defects in the heart tubes of murine embryos lacking the homeo box gene Nkx2-5. *Genes Dev* **9**, 1654-66 (1995).

Marvin, M.J., Di Rocco, G., Gardiner, A., Bush, S.M. & Lassar, A.B. Inhibition of Wnt activity induces heart formation from posterior mesoderm. *Genes Dev* **15**, 316-27 (2001).

McFadden, D.G. et al. A GATA-dependent right ventricular enhancer controls dHAND transcription in the developing heart. *Development* **127**, 5331-41 (2000).

Molkentin, J.D. et al. Direct activation of a GATA6 cardiac enhancer by Nkx2.5: evidence for a reinforcing regulatory network of Nkx2.5 and GATA transcription factors in the developing heart. *Dev Biol* **217**, 301-9 (2000).

Morin, S., Charron, F., Robitaille, L. & Nemer, M. GATA-dependent recruitment of MEF2 proteins to target promoters. *Embo J* **19**, 2046-55 (2000).

Reifers, F., Walsh, E.C., Leger, S., Stainier, D.Y. & Brand, M. Induction and differentiation of the zebrafish heart requires fibroblast growth factor 8 (fgf8/acerebellar). *Development* **127**, 225-35 (2000).

Schneider, V.A. & Mercola, M. Wnt antagonism initiates cardiogenesis in Xenopus laevis. *Genes Dev* **15**, 304-15 (2001).

Schott, J.J. et al. Congenital heart disease caused by mutations in the transcription factor NKX2-5. Science 281, 108-11 (1998).

Schultheiss, T.M., Xydas, S. & Lassar, A.B. Induction of avian cardiac myogenesis by anterior endoderm. *Development* **121**, 4203-14 (1995).

Schultheiss, T.M., Burch, J.B. & Lassar, A.B. A role for bone morphogenetic proteins in the induction of cardiac myogenesis. *Genes Dev* **11**, 451-62 (1997).

Searcy, R.D., Vincent, E.B., Liberatore, C.M. & Yutzey, K.E. A GATA-dependent nkx-2.5 regulatory element activates early cardiac gene expression in transgenic mice. *Development* **125**, 4461-70 (1998).

Sepulveda, J.L. et al. GATA-4 and Nkx-2.5 coactivate Nkx-2 DNA binding targets: role for regulating early cardiac gene expression. *Mol Cell Biol* **18**, 3405-15 (1998).

Srivastava, D., Cserjesi, P. & Olson, E.N. A subclass of bHLH proteins required for cardiac morphogenesis. *Science* **270**, 1995-9 (1995).

Srivastava, D. et al. Regulation of cardiac mesodermal and neural crest development by the bHLH transcription factor, dHAND. *Nat Genet* **16**, 154-60 (1997).

Tzahor, E. & Lassar, A.B. Wnt signals from the neural tube block ectopic cardiogenesis. *Genes Dev* **15**, 255-60 (2001).

Yamagishi, H. et al. The combinatorial activities of Nkx2.5 and dHAND are essential for cardiac ventricle formation. *Dev Biol* **239**, 190-203 (2001).

Yelon, D. et al. The bHLH transcription factor hand2 plays parallel roles in zebrafish heart and pectoral fin development. *Development* **127**, 2573-82 (2000).

CHAPTER 1: Conservation of Sequence and Expression of Xenopus and Zebrafish *dHAND* During Cardiac, Branchial Arch and Lateral Mesoderm Development

INTRODUCTION

dHAND and *eHAND* are related basic helix-loop-helix transcription factors that are expressed in the cardiac mesoderm and in numerous neural crest-derived cell types in chick and mouse. To better understand the evolutionary development of overlapping expression and function of the *HAND* genes during embryogenesis, we cloned the zebrafish and *Xenopus* orthologues. Comparison of dHAND sequences in zebrafish, *Xenopus*, chick, mouse and human demonstrated conservation throughout the protein. Expression of *dHAND* in zebrafish was seen in the earliest precursors of all lateral mesoderm at early gastrulation stages. At neurula and later stages, *dHAND* expression was observed in lateral precardiac mesoderm, branchial arch neural crest derivatives and posterior lateral mesoderm. At looping heart stages, cardiac *dHAND* expression remained generalized with no apparent regionalization. Interestingly, no eHAND orthologue was found in zebrafish. In *Xenopus*, *dHAND* and *eHAND* were co-expressed in the cardiac mesoderm without the segmental restriction seen in mice. *Xenopus dHAND* and *eHAND* were also expressed bilaterally in the lateral mesoderm without any left-right asymmetry. Within the branchial arches, *XdHAND* was expressed in a broader domain than *XeHAND*, similar to their mouse counterparts. Together, these data demonstrate conservation of *HAND* structure and expression across species.

RESULTS

The bHLH transcription factors dHAND and eHAND (deciduum/extra-embryonic membrane, heart, autonomic nervous system, neural crest-derived cell types), also called HAND2 and HAND1 (Srivastava et al., 1995; Cserjesi et al., 1995; Hollenberg et al., 1995; Cross et al., 1995) respectively, share high homology within their bHLH regions and are encoded by genes with similar intron-exon organization. The dHAND proteins from mouse and chick share greater than 95% homology, while eHAND is much less conserved across species (Srivastava et al., 1995). In chick, *dHAND* and *eHAND* are co-expressed in the heart and loss-of-function studies in chick suggest some genetic redundancy (Srivastava et al., 1995). In mice, cardiac expression of *dHAND* and *eHAND* is complementary in the right (pulmonic) and left (systemic) ventricles, respectively. Consistent with an essential role for dHAND in the right ventricle, *dHAND*-null mouse embryos display hypoplasia of the right ventricle (Srivastava et al., 1997). *dHAND* and *eHAND* are also expressed in post-migratory neural crest cells that populate the pharyngeal arches and aortic arch arteries. Here, they play a role in development of the pharyngeal arches and in remodeling of the aortic arch arteries (Thomas et al., 1998; Srivastava et al., 1997), derivatives of the primitive gill arches of fish and amphibians.

Although zebrafish have only one atrium and one ventricle that pumps blood in series through the gills and systemic circulation, we searched for zebrafish orthologues of dHAND and eHAND. A 30-36 hour post fertilization (hpf) zebrafish cDNA library was screened at low stringency using the bHLH region of chick dHAND. Numerous clones were obtained, however sequencing revealed only a single cDNA species. The sequence of these clones

most closely matched known dHAND sequences in chick (Srivastava et al., 1995), mouse (Srivastava et al., 1995) and human (Russell et al., 1998). Because only a dHAND orthologue, zdHAND, was found, we searched for evidence of a relative that might share sequence similarity with eHAND, but found none. Zebrafish genomic DNA was digested and subjected to electrophoresis and Southern analysis was performed using zdHAND as a probe under low stringency conditions. In spite of analysis with multiple restriction enzymes, no evidence was found of cross-hybridization of the zdHAND probe with other relatives (data not shown), suggesting that only one HAND gene might be present in the zebrafish genome.

In contrast to zebrafish, *Xenopus* has two atrial and one ventricular chamber resulting in a partly divided circulation. To identify potential orthologues of the HAND genes in *Xenopus*, a stage 28 embryonic *Xenopus* cDNA library was screened under conditions of low stringency using the bHLH region of chick dHAND. Two distinct populations of clones were identified. Sequence analysis revealed four overlapping clones that shared high sequence identity with mouse and chick dHAND. Three other clones were sequenced and encoded the *Xenopus* orthologue of eHAND as previously reported (Sparrow et al., 1998). No other related family members were found in this screen. As a result, we believe the novel clones represent the *Xenopus* orthologue of dHAND and will refer to it as XdHAND.

The amino acid sequence of zdHAND and XdHAND was almost entirely conserved within the bHLH region (Fig. 1A) compared to human, mouse and chick dHAND. Interestingly, cross species comparisons revealed that even outside the bHLH region, the proteins were highly conserved. Overall, zdHAND and XdHAND were 87% and 94%

identical, respectively, to mouse and human dHAND. XdHAND shared only 56% homology with XeHAND (Fig. 1B). It is notable that zdHAND contains a proline residue rather than a conserved glycine residue in the basic region. Although XdHAND and XeHAND also contain a glycine at this position, mouse and chick eHAND have a proline residue, similar to zdHAND, in the basic region. Because the basic region of bHLH proteins is the DNA-binding domain and typically interacts with the canonical E box DNA binding site (CANNTG) (Murre et al., 1989), a proline residue may alter the DNA-binding specificity of bHLH proteins. Proteins containing a proline residue in the basic region often bind a slightly different N box (CACNAG) and sometimes serve as transcriptional repressors (Oshako et al., 1994). In addition, N-terminal of the bHLH is a region of conserved polyalanines. This polyalanine tract, although initially reported as a polyhistidine tract in mouse and chick (Srivastava et al., 1995), was found to be conserved in all other species upon repeated sequencing. Polyalanine tracts are found in several transcriptional repressors, including engrailed and Kruppel (Licht et al., 1990; Han and Manley, 1993a; Han and Manley, 1993b), and are essential for their repressor activities. Finally, the carboxyl terminus of the protein is almost entirely conserved between XdHAND and XeHAND (Fig. 1B) and across multiple species, suggesting a functional role for this region.

Whole mount in situ hybridization was performed on zebrafish embryos ranging from the 75% epiboly stage (8 hpf) to 48 hpf to compare the expression of *zdHAND* to that of other species. *zdHAND* expression was first seen at 8hpf in a circumferential pattern in the lateral mesoderm (Fig. 2A). At 12 hpf, *zdHAND* continued to be expressed in the anterior and posterior lateral plate mesoderm which is partly detached from the yolk at this stage (Fig.

2B). By 18-20 hpf, the bilateral cords of cardiac primordia fuse at the midline forming an aortic ring which is defined by the cardiac marker, *Nkx2*.5. A dorsal view of the embryo at this stage showed *zdHAND* expression in the cardiac ring and in a layer of lateral mesoderm surrounding the cardiac region (Fig. 2C and 2G), as well as in the posterior lateral mesoderm (not shown). At 24 hpf, *zdHAND* expression was seen throughout the nascent cardiac tube and in bilaterally symmetric clusters of ventrolateral cells that condense to form branchial arch mesoderm which gives rise to jaw and pharyngeal bones (Fig. 2D). *zdHAND* expression continued bilaterally in the posterior lateral mesoderm (Fig. 2E and 2H). At 36-48 hpf, *zdHAND* expression was seen in defined branchial arch mesoderm populations in a pattern complementary to that of *Nkx2.3* which is expressed in the endoderm of the pharyngeal pouches (Fig. 2F and 2I) (Lee et al., 1996). Histologic analysis of the cardiac region at the looped stage showed strong *zdHAND* expression throughout the heart tube (Fig. 2J), consistent with its earlier cardiac expression. Overall, the domains of *zdHAND* expression were remarkably similar to those observed in both chick and mouse and may be indicative of a conserved role and regulation of this gene between species.

To continue to investigate the expression of *dHAND* and *eHAND* across species, whole mount in situ hybridization was performed on *Xenopus* embryos from stage 15 (early neurulation) to stage 47 (tadpole). At stage 15, there was faint expression of *XdHAND* in the antero-ventral mesoderm (data not shown). By stage 20, after neural tube closure, expression of *XdHAND* was apparent in the ventro-lateral mesoderm of the mid-embryo with punctate expression in anterior clusters of cells that were subepidermal and may represent migrating neural crest cells (Fig. 3A). By stage 24, or early tailbud stage, the expression pattern of

XdHAND had expanded to include lateral plate mesoderm in the mid-embryo and the heart anlage in the ventral midline (Fig. 3B). The punctate groups of subepidermal cells persisted at this stage. Expression in the lateral plate mesoderm at stage 24 was symmetric along the left-right axis in all embryos tested (Fig. 3B). By the late tail bud stages (stage 28-30), the region of *XdHAND* expression in the lateral mesoderm had expanded into a symmetrical arc of ventral and lateral expression, which fused in the midline where the straight heart tube had formed. The branchial arches had high levels of *XdHAND* expression (Fig. 3C). Linear bands of punctate expression leading to the branchial arches and anterior cardiac region were again observed, similar but not identical to the migratory pattern described previously for neural crest cells (Vallin et al., 1998). By stage 33, the heart had begun to loop and *XdHAND* expression was present in the heart, lateral mesoderm and branchial arches (Fig. 3D). At stage 37, expression in the looped heart was evident as was branchial arch expression (Fig. 3E). *XdHAND* was most abundant in the heart and outflow tract at stage 47 (Fig. 3F).

Xenopus eHAND (Sparrow et al., 1998) was previously described to diverge in its expression pattern with left-right asymmetry in the lateral mesoderm, and absence of branchial arch expression. Although the sequence of XeHAND obtained in this study was identical to that reported, our analysis of gene expression differed in some respects. Expression of *XeHAND* was similar to *XdHAND* at stage 15, with mRNA apparent in the anterior and ventral mesoderm near the heart primordia (Fig. 4A and 4B). At stage 22 there was a central band of *XeHAND* expression in the lateral plate mesoderm that was confined to the mid-embryo (Fig. 4C). It extended more dorsally but less anteriorly than *XdHAND* expression. Like XdHAND, the left and right lateral plate mesoderm had expression of

XeHAND in all embryos studied, and no LR asymmetries of expression were observed. *XeHAND* expression was not observed in the branchial arch precursors at stage 22. Expression of *XeHAND* in the heart anlage and lateral plate mesoderm during stages 28-33 was similar to the expression pattern of *XdHAND* (Fig. 4D) with no asymmetries. In contrast to *XdHAND*, however, there was no punctate expression noted in the subepidermal region anteriorly. Branchial arch expression of *XeHAND* was present at stage 33 but was more medial than *XdHAND* (Fig. 4E). These subdomains of *XdHAND* and *XeHAND* in the branchial arches were reminiscent of the pattern observed in chick (Srivastava et al., 1995) and mouse (Thomas et al., 1998). At heart looping stages (stage 37) the myocardium and cardiac outflow tract expressed *XeHAND* uniformly (Fig. 4F). In the tadpole (stage 47), *XeHAND* expression was like that of *XdHAND*, with expression in the heart and cardiac outflow tract (Fig. 4G).

Analysis of *XdHAND* expression in adult *Xenopus* revealed specific expression in several adult tissues (Fig. 5). Unlike adult mouse, *XdHAND* was detectable in the adult heart. Interestingly, transcripts were also observed in the liver and spleen, but not in skeletal muscle or ovary.

DISCUSSION

The cardiovascular systems of organisms have evolved with increasing complexity in order to adapt to specific environments. The remarkable conservation of dHAND's amino acid sequence in species ranging from fish to humans is indicative of a critical role for this transcription factor throughout evolution. Recent identification of a dHAND deletion in a

zebrafish mutant exhibiting cardiac defects supports a conserved role for dHAND (Yelon et al., 2000). Analysis of the function of zebrafish and Xenopus HAND proteins may provide additional insights into the molecular mechanisms underlying the early steps of cardiogenesis.

METHODS

Zebrafish and *Xenopus* cDNA library screen

The bHLH region of chick dHAND was radiolabeled and used to screen 1.2 x 10^6 recombinants from a 30-36 hr whole embryo zebrafish lgt11 cDNA library (gift of K. Zinn) or 2.0 x 10^5 recombinants from stage 28 *Xenopus* cDNA library at low stringency according to previously described methods (Benton and Davis, 1977). Positive clones were plaque purified, subcloned into plasmid vectors and sequenced.

Whole mount RNA *in situ* hybridization

Xenopus embryos were obtained as described previously (Lohr et al., 1997) and RNA probe synthesis and whole-mount *in situ* hybridization were performed using a standard protocol (Harland et al., 1991; Sive, et al, 1996). Antisense XdHAND riboprobe was synthesized using a BamH1 linearized plasmid and T7 RNA polymerase. Antisense XeHAND riboprobe was synthesized using a Xho1 linearized plasmid and T3 RNA polymerase. *Xenopus* embryos were staged according to Niewkoop and Faber (1967) and embryos from stage 15 (early neurulation) to stage 47 (tadpole) were used for *in situ* hybridization.

In situ hybridization of various staged zebrafish embryos was performed as previously described (Lee et al., 1996). Antisense RNA probes were synthesized by in vitro transcription of full-length zebrafish dHAND cDNA as above.

Histologic analysis

Embryos were dehydrated and embedded in paraffin after whole-mount in situ hybridization. Transverse sections were made at 5-7 micron intervals. Sections were not counter-stained in order to preserve visibility of labeled RNA transcripts.

Reverse transcriptase polymerase chain reaction

RNA from adult male Albino frogs was obtained by isolating the heart, liver, spleen, ovary, and skeletal muscle. Reverse transcribed RNA was used to generate cDNA for polymerase chain reaction (PCR) amplification of XdHAND. Primer pairs were as follows: 5'-ATG AGT CTG GTT GGG GGG TTT C-3'; 5'-GTC CTG CCT TTG GTT TTC TTA TCG-3'.

PCR conditions were: 94°C for 5 min, 25-35 cycles of 94°C for 15 sec, 55°C for 30 sec, and 72°C for 30 sec. A final extension was done at 72°C for 10 min. Non reverse-transcribed RNA samples were used as negative controls. RNA quantity and quality was assessed by amplification of EF-1□. A range of amplification cycles was performed to provide semi-quantitative results.

Figure 1. Amino-acid sequence alignment of dHAND. Amino acid sequence comparison of zebrafish, *Xenopus*, chick, mouse and human dHAND is shown (A). Identical amino acids are shaded in boxes. Similar residues are in unshaded boxes. The basic and helix-loop-helix (HLH) domains are indicated in brackets. Polyalanine tract is marked with asterisk (*). Comparison of XdHAND and XeHAND sequence is also shown (B). Zebrafish dHAND (accession no. 228334) and *Xenopus* dHAND (accession no. 228335) nucleotide sequences have been submitted.

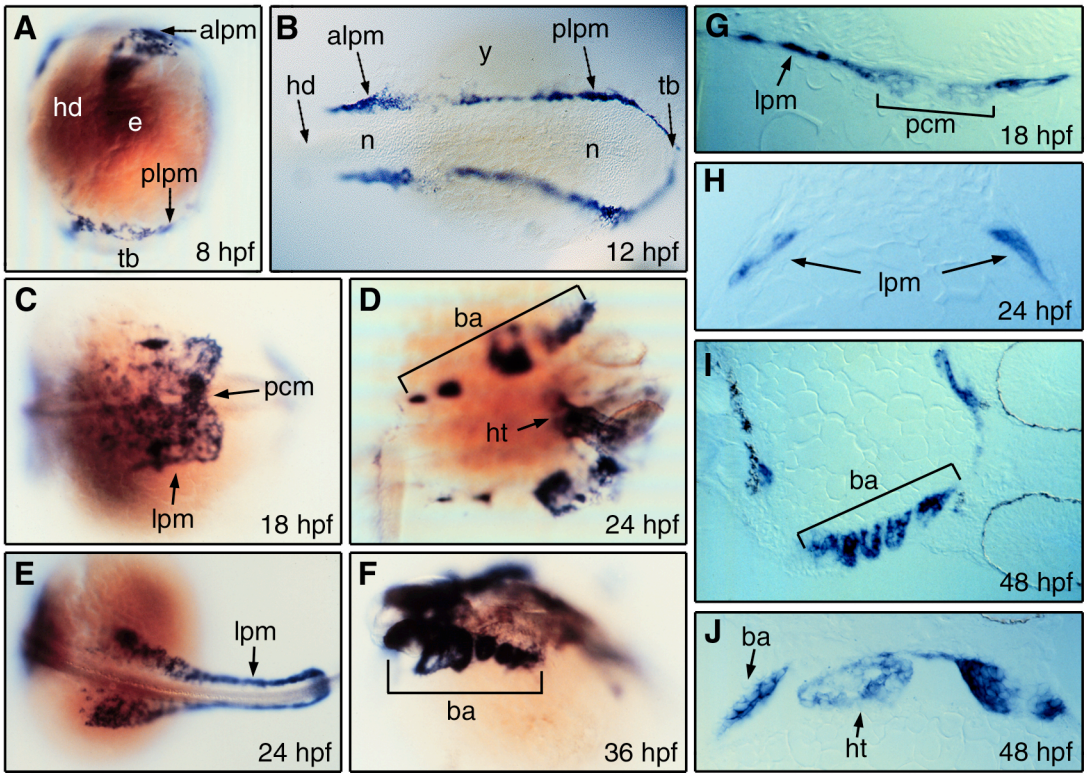

Figure 2. *dHAND* expression in staged zebrafish embryos. Whole-mount in situ hybridization (A-F) revealed expression of *dHAND* in the lateral plate mesoderm (lpm), pre-cardiac mesoderm (pcm), branchial arches (ba) and in the heart (ht). As early as 8 hours post fertilization (hpf), expression was evident circumferentially in the anterior lateral plate mesoderm (alpm) and posterior lpm (plpm) in an oblique head-on view (A); positions of head (hd), eye (e) and tailbud (tb) are shown. At 12 hpf expression was again seen in the alpm and plpm (B); embryo is oriented with the head to the left and the tailbud to the right. Notochord (n) and yolk (y) are also noted. Expression in the pcm became evident at 18 hpf (C) and persisted into the heart tube at 24 hpf (D) seen ventrally, when branchial arch expression also became apparent. The embryo at 24 hpf demonstrated bilaterally symmetric expression of *dHAND* in the lateral plate mesoderm (E) in a dorsal view of the caudal region. Branchial arch expression persisted at 36 hpf (F) in the rostral region as seen dorsally. Transverse sections of 18 (G) and 24 (H) hpf embryos in the rostral and caudal regions, respectively, confirmed expression in the pcm and lpm. (I) demonstrates branchial arch expression of *zdHAND* at the histological level. (J) shows expression of *zdHAND* throughout the heart tube.

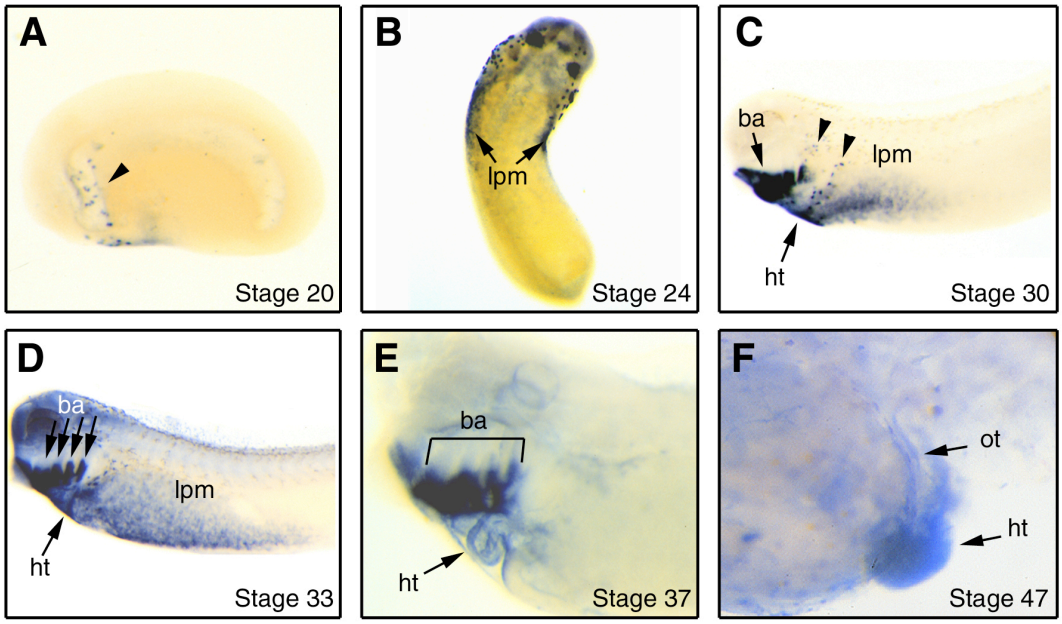

Figure 3. *dHAND* expression in staged *Xenopus* embryos. Whole-mount in situ hybridization in *Xenopus* embryos revealed *dHAND* expression in punctate subepidermal cells (arrowheads) as early as stage 20 (A). The punctate cells later appeared to be migrating to the branchial arches and heart (C). *dHAND* expression was observed in the branchial arches throughout their development (C-E). *dHAND* was expressed bilaterally in the lateral plate mesoderm (lpm) at stage 24 through stage 33 (B-D). High magnification of the anterior embryo better demonstrated expression in the looped heart tube and branchial arches at stage 37 (E). Even higher magnification of the cardiac region (F) demonstrated expression in the heart tube (ht) and outflow tract (ot) at stage 47 without any chamber restriction.

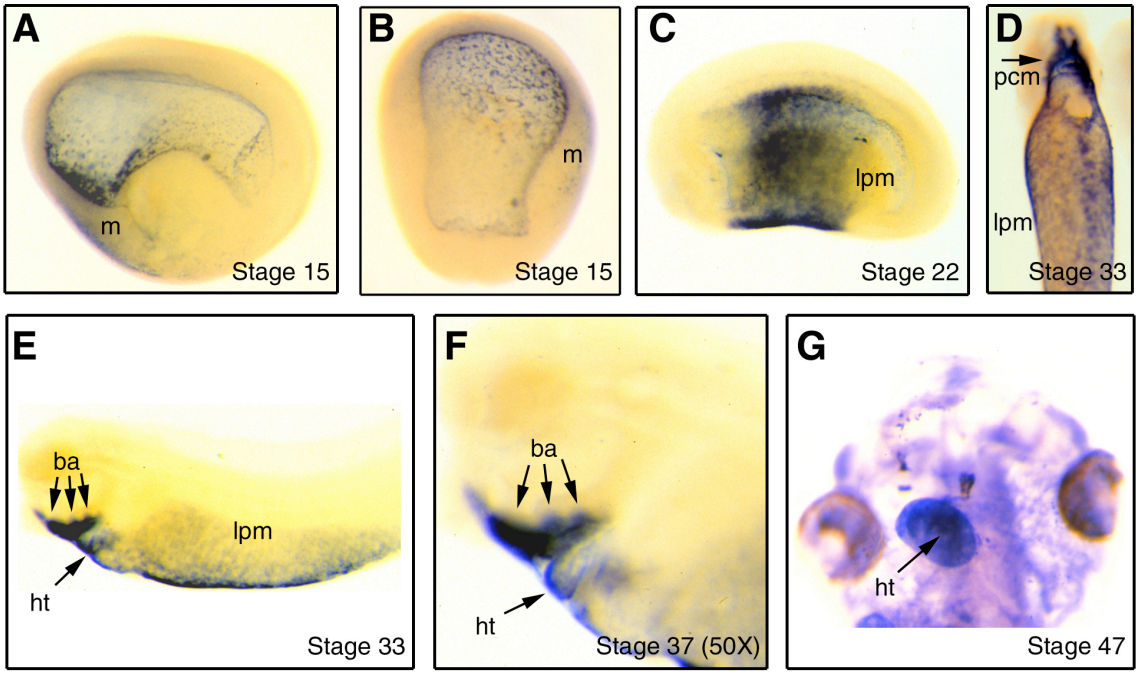

Figure 4. *eHAND* expression in staged *Xenopus* embryos. *eHAND* expression in stage 15 *Xenopus* embryos was evident in the antero-lateral mesoderm (m) in lateral (A) and frontal (B) views. Bilaterally symmetric expression in the lateral plate mesoderm (lpm) was observed at stage 22 (C) and stage 33 in a ventral view (D). Expression in the precardiac mesoderm (pcm) became apparent at stage 30-33 (D). In a lateral view at stage 33 (E), branchial arch (ba) expression was observed in addition to the heart (ht) and lateral plate mesoderm expression. Magnification of the anterior region (F) better illustrated branchial arch and heart expression. High levels of heart expression were seen at stage 47 (G).

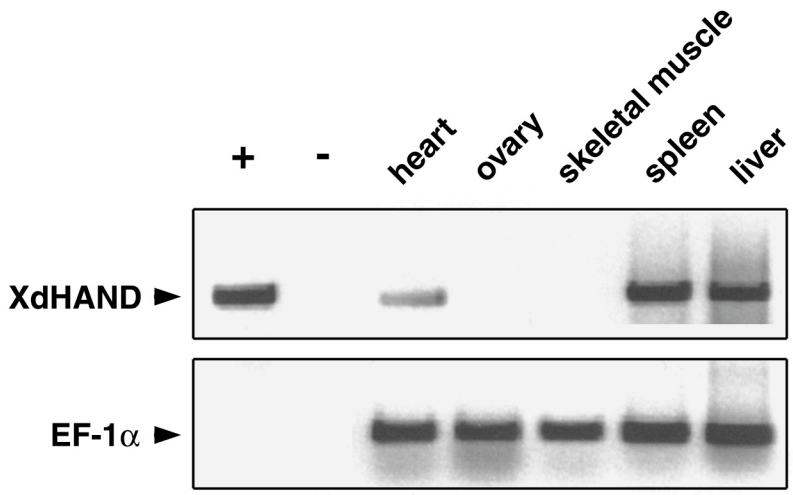

Figure 5. Expression of *dHAND* in adult *Xenopus* tissues. Reverse transcriptase polymerase chain reaction was performed on total RNA extracted from adult *Xenopus* organs as indicated. *XdHAND* was detected in the adult heart, spleen and liver, but not in the ovary or skeletal muscle. Non-reverse transcribed RNA was used as a negative control (-) and XdHAND cDNA as positive control (+). RNA quality and quantity was assessed by amplification of the ubiquitous transcript, EF-1□.

REFERENCES

Benton, W.D., and Davis, R.W. (1977) Screening lambda gt recombinant clones by hybridization to single plaques in situ. *Science*, **196**:180-182.

Cross, J.C., Flannery, M.L., Blanar, M.A., Steingrimsson, E., Jenkins, N.A., Copeland, N.G., Rutter, W.J., Werb, Z. (1995) Hxt encodes a basic helix-loop-helix transcription factor that regulates trophoblast cell development. *Development* **121**:2513-2523.

Cserjesi, P., Brown, D., Lyons, G.E. and Olson, E.N. (1995) Expression of the novel basic helix-loop-helix gene eHAND in neural crest derivatives and extraembryonic membranes during mouse development. *Dev Biol* **170**:664-678.

Han K, Manley JL. (1993a) Transcriptional repression by the *Drosophila* even-skipped protein: definition of a minimal repression domain. *Genes & Dev*. **7**:491-503.

Han K, Manley JL. (1993b) Functional domains of the *Drosophila* engrailed protein. *EMBO J*. **12**:2723-2733.

Harland, R.M. (1991) In situ hybridization: an improved whole-mount method for *Xenopus* embryos. *Methods Cell Biol* **36**:685-95.

Hollenberg, S.M., Sternglanz, R., Cheng, P.F., Weintraub, H. (1995) Identification of a new family of tissue-specific basic helix-loop-helix proteins with a two-hybrid system. *Mol Cell Biol* **15(7)**:3813-22.

Lee, K.H., Xu Q, Breitbart RE. (1996) A new tinman-related gene, nkx2.7, anticipates the expression of nkx2.5 and nkx2.3 in zebrafish heart and pharyngeal endoderm. *Dev Biol* **180(2)**:722-31.

Licht JD, Grossel MJ, Figge J. Hansen UM. (1990) *Drosophila* Kruppel protein is a transcriptional repressor. *Nature*. **346**:76-79.

Lohr, J.L., Danos, M.C., Yost, H.J. (1997) Left-right asymmetry of a nodal-related gene is regulated by dorsoanterior midline structures during *Xenopus* development. *Development* **124(8)**:1465-72.

Murre, C., McCaw, P., Vaessin, H., Claudy, M., Jan, L. Y., Jan, Y.N., Cabrera, C.V., Buskin, J.N., Hauschka, S.D., Lassar, A.B., Weintraub, H., and Baltimore, D. (1989) Interactions between heterologous helix-loop-helix proteins generate complexes that bind specifically to a common DNA sequence. *Cell* **58**:537-544.

Oshako, S., Hyer, J., Panganiban, G., Oliver, I., and Caudy, M. (1994) Hairy function as a DNA-binding helix-loop-helix repressor of *Drosophila* sensory organ formation. *Genes & Dev*. **8**:2743-2755.

Russell MW, Kemp P, Wang, L, Brody LC, Izumo S. (1998) Molecular cloning of the human HAND2 gene. *Biochimica et Biophysica Acta*. **1443**:393-399.

Sive, H., Bradley, L. (1996) A sticky problem: the *Xenopus* cement gland as a paradigm for anteroposterior patterning. *Dev Dyn* **205(3)**:265-80.

Sparrow DB, Kotecha S, Towers N, Mohun TJ. (1998) *Xenopus* eHAND: a marker for the developing cardiovascular system of the embryo that is regulated by bone morphogenetic proteins. *Mech Dev*. **71**:151-163.

Srivastava, D., Cserjesi, P. and Olson, E.N. (1995) A new subclass of bHLH proteins required for cardiac morphogenesis. *Science* **270**:1995-1999.

Srivastava, D., Thomas, T., Lin, Q., Kirby, M.L., Brown, D. and Olson, E.N. (1997) Regulation of cardiac mesodermal and neural crest development by the bHLH transcription factor, dHAND. *Nat Genet* **16**:154-160.

Thomas, T., Kurihara, H., Yamagishi, H., Kurihara Y, Yazaki Y, Olson EN, Srivastava D. (1998) A signaling cascade involving endothelin-1, dHAND and msx1 regulates development of neural-crest-derived branchial arch mesenchyme. *Development* **125**:3005-3014.

Vallin, J., Girault J.M., Thiery J.P., Broders F. (1998) *Xenopus* cadherin-11 is expressed in different populations of migrating neural crest cells. *Mech Dev*. **75(1-2)**:171-4.

Yelon D., Ticho B., Halpern M.E., Ruvinsky I., Ho R.K., Silver L.M., and Stainier D.Y.R. (2000) Parallel roles for the bHLH transcription factor HAND2 in zebrafish heart and pectoral fin development. *Development* (in press).

CHAPTER 2: *Bop* encodes a muscle-restricted MYND and SET domain-containing protein essential for cardiac differentiation and morphogenesis

INTRODUCTION

An understanding of early cardiogenesis is necessary for future interventions in heart disease, a leading cause of death in adults and children. The transcriptional regulation of cardiogenesis has been explored in considerable detail but the mechanisms controlling early steps of cardiomyocyte differentiation and maturation are largely unknown [1-2]. Cardiogenic precursors are specified in an anterior mesoderm field during early embryogenesis in response to secreted signals from the adjacent endoderm. Subsequently, a monolayer of cardiomyocytes produces a dense extracellular matrix (ECM) necessary for reciprocal signaling between the myocardial and endocardial layers of the developing heart tube [3]. Further differentiation of cardiomyocytes results in degradation of the ECM and invasion of more differentiated and less proliferative trabecular myocytes into the ECM. As this occurs, the linear heart tube forms a loop that begins to distinguish individual cardiac chambers and results in proper alignment of the inflow and outflow tracts of the heart.

As cardiomyocytes mature, distinct transcriptional programs emerge that regulate specific cardiac chambers. The discovery of distinct cis-acting elements governing gene expression in specific chambers first suggested the presence of such programs [4]. Evidence of chamber-specific trans-acting factors was revealed by the absence of a right ventricular segment in mice lacking the basic helix-loop-helix (bHLH) transcription factor, dHAND [5], and the left ventricle-specific expression of the closely-related factor, eHAND [5-6].

Subsequently, numerous chamber-specific transcription factors have been described [7-9]. The evidence for segmental regulation of cardiac transcription provides a mechanistic framework in which to consider congenital heart defects (CHD) in humans, which typically affect only a single chamber or region of the heart.

The recent discovery of proteins involved in chromatin regulation has revealed an additional mechanism of transcriptional regulation. Covalent acetylation of specific lysine residues found on histone tails by histone acetyltransferases (HATs) promotes chromatin relaxation and transcription, while deacetylation by histone deacetylases (HDACs) in a reverse reaction results in chromatin condensation and silencing of gene transcription [10-12]. Some chromatin remodeling proteins that share a highly conserved SET domain, originally described in the proteins Su(var)-39, Enhancer of zeste and Trithorax, can methylate unacetylated lysine residues on histone tails, resulting in more permanent silencing of transcription [13-14] or, in some cases, activation of transcription [15]. However, no cardiac-specific function for SET domain-containing proteins has been described previously.

Here, we describe the activity of mBop, a protein that contains a SET domain and also a MYND domain, the latter reported to be involved in recruitment of HDACs and transcriptional repression [16-17]. We isolated *Bop* through a novel subtractive hybridization approach to identify early cardiac-specific genes in chick embryos. First discovered in cytotoxic T cells (CTL) and adult heart and skeletal muscle [18], we show that *Bop* is expressed specifically in cardiac and skeletal muscle precursors and in cardiomyocytes throughout chick and mouse development, beginning prior to cardiac differentiation. m-Bop can interact with HDACs and can function as a transcriptional repressor. Targeted deletion of *Bop* in

mice revealed its essential role in ventricular cardiomyocyte maturation and right ventricular development. *dHAND* expression in cardiac precursors was dependent upon *Bop*, revealing a likely mechanism, in part, for right ventricular hypoplasia and ventricular maturation defects in *Bop* mutants. These results reveal an essential role for the cardiac-restricted MYND and SET domain-containing protein, mBop, in cardiomyocyte differentiation and chamber-specific development.

RESULTS

Isolation of chicken m-Bop by subtractive hybridization

In chick embryos, bilaterally symmetric cardiac precursors become specified by Hamburger and Hamilton (HH) stage 5 (ref 19) and express the early cardiac-specific gene, Nkx2.5 (ref 20-21). In an effort to discover genes that might be essential for the early period of cardiac specification and differentiation, a subtractive hybridization approach was taken to isolate genes expressed specifically in the cardiac precursors at HH stage 5. To avoid cloning genes expressed in the nearby neural field or abundant sarcomeric transcripts, we developed a modification of PCR-based subtractive hybridization that allowed enrichment of transcripts common to two RNA populations but absent in a third RNA pool. Using this new method, which we termed subtractive and selective PCR amplification (SSPA), we attempted to isolate genes expressed in both the presumptive heart field (stage 5) and in the straight heart tube (stage 10), but not in the posterior, non-cardiogenic region of the embryo. Ninety-nine percent of cDNA clones isolated by this modified method were anchored by unique adaptors, indicating that genes expressed in both desired tissues were isolated. This

modification allowed for efficient isolation of numerous non-sarcomeric early cardiac-specific genes, which will be described elsewhere (O. Nakagawa, E.N. Olson, D. Srivastava, in preparation).

One of the sequences isolated in this screen had homology to a mouse gene known as *Bop* (CD8b-opposite) whose expression had been previously described in cytotoxic T cells (tBop), adult heart and adult skeletal muscle (skmBop, here to be renamed m-Bop) [18,22]. Low stringency screening of an embryonic chick library for the full-length cDNA revealed the presence of two closely related species, each of which shared 90% amino-acid similarity with mouse m-Bop1 (genbank accession no. U76373) or mouse m-Bop2 (genbank accession no. U76374), respectively. Based on the similarity with its mouse orthologues, we presume these cDNAs represent chick m-Bop1 (genbank accession no. 410781) and chick m-Bop2 (genbank accession no. 410782). M-Bop1 and m-Bop2 are encoded by the same gene (*Bop*[22]) and represent isoforms that differ only by a 13 amino-acid insertion due to alternative splicing. Because of the similarity between the two, we will refer to both isoforms collectively as m-Bop.

Bop is expressed specifically in cardiac and skeletal muscle precursors

To examine the expression of *Bop* during embryogenesis, whole-mount and section in situ hybridization was performed. In chick, *Bop* transcripts were detectable in the heart field at stage 5 by RT-PCR (data not shown) and by in situ hybridization at stage 7, prior to the onset of cardiomyocyte differentiation (Fig. 1a). Cardiac expression of *Bop* continued in the straight heart tube (stage 10) and throughout cardiogenesis (Fig. 1b,c). Expression in the

myotome of the somites, which later contributes to skeletal muscle, was also abundant (Fig. 1c). Similar studies of mouse *Bop* during embryogenesis revealed conservation of cardiac-specific gene expression as early as embryonic day (E) 7.75, continuing throughout development (Fig. 1d-f). By radioactive section in situ hybridization, mouse *Bop* transcripts were localized to the myocardial, but not endocardial, layer of the developing heart and persisted in post-natal cardiomyocytes (Fig. 1g-i). Expression of *Bop* was uniform in all chambers of the heart and was also detected in the myotome of the somites (Fig. 1h).

The m-Bop2 isoform encoded by *Bop* is a 472 amino acid protein that contains a MYND domain, with its two predicted zinc fingers, and a SET domain, both of which have been implicated in chromatin remodeling (Fig. 2a). The SET domain of m-Bop is split into two segments (a S-ET domain [15]) separated by the MYND domain and other sequences. The MYND domain and the "ET" portion of the S-ET domain are also present in a thymus and cytotoxic T cell-specific *Bop* isoform (tBop) [22]. The MYND domain of mBop is most similar to that found in the ETO protein (also called CBFA2T1), which is translocated in human leukemias (t(8;21)) and is involved in recruitment of HDACs and transcriptional silencing (Fig. 2b) [16-17]. SUVAR-39, which contains a conserved SET domain, possesses histone methyl transferase (HMT) activity that is dependent upon several conserved amino acid residues within the SET domain [13]. m-Bop shares most of these essential residues, all within the "ET" region, as well as the C-terminal cysteine-rich region, with SUVAR-39 (Fig. 2c).

m-Bop2 can function as a transcriptional repressor

Because MYND and SET domains can promote chromatin remodeling and transcriptional repression, we examined the subcellular localization of m-Bop2 to determine whether it could function as a transcriptional regulator. Immunocytochemistry was performed using a hamster anti-mouse Bop monoclonal antibody generated against the carboxy-terminal half of the protein shared by all Bop isoforms[22]. In undifferentiated myoblasts, *Bop* was expressed in both cytoplasm and nucleus (Fig. 2d).

To test for transcriptional repressor activity, a system was used in which a luciferase reporter gene was activated by a fusion protein of the LexA DNA-binding domain fused to the potent activation domain of the viral coactivator protein,VP16 (LexA-VP16)[23]. Interaction of GAL4-binding sites, located between the Lex A-binding sites and the reporter, with a GAL4-m-Bop2 fusion protein consistently inhibited luciferase expression in a dose-dependent fashion compared to LexA-VP16 alone or both LexA-VP16 and GAL4-DBD (Fig. 2e). This effect is unlikely to be due to steric hindrance as other GAL4-fusion proteins did not demonstrate similar repression of LexA-VP16 (data not shown). Using the reverse constructs, a LexA-m-Bop2 fusion protein suppressed transcriptional activation by GAL4-VP16 in a similar fashion (data not shown).

A second assay for the effect of m-Bop2 on transcriptional activity made use of a luciferase reporter gene under the influence of a minimal SV40 promoter. A series of SV40-luciferase reporters were used that contained zero or five copies of the GAL4-UAS upstream of the SV40 promoter at various distances (Fig. 2f). In transient transfections of 10T1/2 cells, GAL4-m-Bop2 consistently inhibited transcription in a dose-dependent fashion,

regardless of the distance between the GAL4 binding sites and the SV40 promoter. This suggests that m-Bop2 represses transcription by an active mechanism, rather than by simply interfering with the transcriptional machinery. The m-Bop1 isoform repressed transcription in a comparable manner to m-Bop2 (data not shown). The above experiments suggest that m-Bop2 can function as a transcriptional repressor.

Transcriptional repression by m-Bop2 requires HDAC activity

Since m-Bop2 has repressor activity and contains a MYND domain similar to that shown in the ETO protein to recruit HDAC activity[24], we used the potent HDAC inhibitor, trichostatin A (TSA)[25] to test whether m-Bop2 might repress transcription by recruiting HDACs. Addition of 150 M TSA significantly abrogated GAL4-m-Bop2 repression of SV40 promoter-driven luciferase expression in 10T1/2 cells, suggesting that the effect of m-Bop2 on reporter gene expression is mediated at least in part by recruitment of HDAC activity (Fig. 2g).

To understand the mechanism of TSA-mediated inhibition of m-Bop2 activity, we tested the ability of m-Bop2 and HDAC to physically associate *in vivo*. Extracts of 293T cells transiently transfected with plasmids expressing GAL4-m-Bop2 or GAL4-DBD together with FLAG epitope-tagged HDACs (HDAC1, HDAC2 or HDAC3), were generated. Immunoprecipitation of cell lysates with a BOP-specific monoclonal antibody followed by western blot with anti-FLAG antibody demonstrated co-precipitation of all three class I HDACs with GAL4-m-Bop2 but not Gal4-DBD (Fig. 2h). anti-BOP mAb also co-precipitated FLAG-tagged class II HDACs, HDAC4 and HDAC5, from cells cotransfected

with GAL4-m-Bop2 but not GAL4-DBD (data not shown). Conversely, anti-FLAG antibody co-precipitated GAL4-m-Bop2 from lysates of 293T cells overexpressing GAL4-m-Bop2 and FLAG-HDAC1 but not GAL4-m-Bop2 alone (data not shown). Taken together, the above results suggest that m-Bop2 suppresses transcription, at least in part by recruitment of HDAC activity.

Bop mutant mice show ventricular hypoplasia and expanded extracellular matrix

The tissue and developmental expression pattern of *Bop* and its role as a transcriptional regulator prompted investigation of its *in vivo* function using mice lacking a functional *Bop* gene. Targeted inactivation of *Bop* was accomplished by replacement of exons 2 and 3, which encompass the MYND domain, with the neomycin resistance gene through homologous recombination (Fig. 3a, see Materials and Methods). Mice heterozygous for the mutant *Bop* allele were apparently normal and fertile. However, genotyping of 112 progeny of heterozygous intercrosses indicated that 71 (63%) were heterozygous and 41 (37%) contained only wild-type alleles (Fig 3b). No evidence for stillborn pups was seen, suggesting that embryos lacking a functional *Bop* allele died *in utero*.

Females from timed heterozygous matings were sacrificed to determine the day of embryonic death. Embryos homozygous for the mutant *Bop* allele were growth retarded by E9.5 and were dead by E10.5 (Fig. 3 d-g). No *Bop* mRNA transcripts were detectable by RT-PCR from *Bop* mutant hearts at E9.5, indicating the absence of any residual spliced message (Fig. 3c). Gross examination of *Bop* mutant embryos at E9.5 revealed an enlarged

heart with a more severe effect evident in the ventricle compared to atrium (Fig. 3f). In addition, there appeared to be a single left-sided ventricular chamber (Fig. 3g).

Histologic analysis of *Bop* mutant hearts by serial transverse section along the anterior-posterior axis revealed that, although the hearts were enlarged compared to wild-type, the lumen of the heart was not dilated (Fig. 4a-f). Rather, the enlargement was secondary to a tremendous expansion of ECM, known as cardiac jelly, between the myocardial and endocardial layers of the developing heart (Fig. 4d-f). In addition, at no level of section were two distinct ventricular chambers detectable as in wild-type (Fig. 4b), and the single ventricular chamber was directly connected to the outflow tract (Fig. 4e). The atrium was relatively unaffected with normal amounts of ECM (Fig. 4f). Finally, formation of trabeculae, the finger-like myocardial projections indicative of cardiomyocyte differentiation and maturation, was limited in *Bop* mutants.

To understand the mechanism underlying ECM expansion in *Bop* mutants, we examined the composition and nature of ECM in hearts lacking *Bop*. Using electron microscopy and antibodies to numerous components of normal ECM, including fibronectin, collagen and hyaluronan, the ECM in mutant hearts appeared to be relatively normal in composition, but expanded compared to wild-type (Fig. 4g,j and data not shown), although effects of hydration may also contribute. Because the enzyme hyaluronic acid synthase 2 (Has2) is necessary for ECM production [26], we hypothesized that this gene might be upregulated in the absence of *Bop*. However, section in situ hybridization revealed no change in the level of *Has2* transcripts in *Bop* mutant hearts (Fig. 4h,k). Together, these data

suggest that *Bop* may not directly regulate genes involved in production or degradation of the ECM but rather may affect a more general process reflected by the accumulation of ECM.

Cardiomyocyte maturation defect in *Bop* mutant mice

Because cardiomyocytes undergo a critical maturation step between E8.0 and E9.5 that is manifested by a transition from production to degradation of ECM[27], we assessed the degree of cardiomyocyte maturation by using several markers of cardiomyocyte differentiation in *Bop* mutants. Expression of markers of early cardiomyocyte differentiation, including *myosin light chain 2V* (*MLC2V*) [28] and *myosin light chain 2A* (*MLC2A*) [29], that are expressed prior to cardiomyocyte contractions, were normal in *Bop*-null embryos (Fig. 5a,e and data not shown). *eHAND*, a left ventricular marker, was expressed normally in *Bop* mutants and was detected throughout the ventricular chamber (Fig. 5b,f). In contrast, *dHAND*[30], which is necessary for right ventricular formation, was not detectable in the hearts of E9.0 *Bop*-null embryos, although normal expression was observed in the pharyngeal arches and lateral mesoderm (Fig. 5c,g). *dHAND* expression in *Bop* mutants was examined at a slightly earlier time point than the wild-type embryos shown in an attempt to capture potential *dHAND* expression in a rudimentary right ventricle. To test whether this result simply reflected the absence of a right ventricle in the *Bop* mutant, embryos were examined at earlier stages, prior to cardiac formation. In E7.75 embryos, *dHAND* was selectively downregulated in the precardiac mesoderm (cardiac crescent) of *Bop* mutants (Fig. 5d,h). Expression of *dHAND* was intact bilaterally in the lateral mesoderm, providing an internal control for RNA integrity in the *Bop*-null embryo. This result indicates that

mBop regulates cardiac expression of *dHAND* well before organogenesis or any visible phenotype in the *Bop* mutant.

The absent or decreased level of *dHAND* expression in the heart was confirmed by radioactive section in situ hybridization which demonstrated decreased *dHAND* expression in cardiomyocytes of *Bop* mutants compared to wild-type (Fig. 5i,n). Expression of the transcription factor Nkx2.5 in tissue sections of *Bop* mutants was normal, providing a control for intact gene expression in the *Bop*-null heart (Fig. 5j,o). To further assess the effects of *dHAND* downregulation in *Bop* mutants, we considered whether expression of any dHAND-dependent genes might be altered in the absence of *Bop*. *Irx4*, a ventricular-specific homeobox gene, was recently shown to be partially downregulated in mice lacking *dHAND* [31]. In the *Bop* mutant ventricle, *Irx4* transcripts were detectable but downregulated compared to wild-type littermates, consistent with the downregulation of *dHAND* (Fig. 5k,p). Expression of other transcription factors were equal in wild-type and *Bop* mutants on serial sections (Fig. 5j,o,l,q), suggesting that alteration in RNA integrity was not the cause of decreased *Irx4* expression.

Although whole-mount in situ hybridization suggested that the predominant portion of the residual ventricle was molecularly a left ventricle, we interrogated this with higher resolution using section in situ hybridization. *Tbx5*, which is normally expressed at highest levels in the atria and left ventricle [32], was expressed at comparable levels in the *Bop* mutant and wild-type heart (Fig. 5l,q), consistent with the conclusion that the majority of the single ventricle in the absence of *Bop* is molecularly a left ventricle. However, a small region of cells leading into the outflow tract of the Bop-null heart displayed lower levels of Tbx5

expression (Fig. 5q), similar to the lower expression level in wild-type right ventricle (Fig. 5l), suggesting that these cells may represent remnants of the right ventricle. To distinguish if this subset of cells represent outflow tract or right ventricle, eHAND expression, which marks only left ventricle and outflow tract (Fig. 5m), was examined. The cells exhibiting lower Tbx5 expression did not have detectable eHAND transcripts (Fig. 5r), indicating that a rudimentary, hypoplastic right ventricle was present. Not surprisingly, 5 ± 1 out of 40 cells in the anterior region of the E9.0 *Bop*-null looping heart tube were undergoing apoptosis, visualized by TUNEL assay, compared to 0 of 80 cells in a comparable region in wild-type hearts ($n=4$, $p < .05$). While the hypoplasia of a right ventricular segment, similar to *Bop* mutants, has been well-documented in *dHAND* mutants[33], the space between endocardium and myocardium is not as prominent as in *Bop* mutants (Fig. 5t,u). However, this space was increased in E9.5 *dHAND*-null hearts, compared to wild-type littermates (Fig. 5s,t) and was in sharp contrast to the minimal ECM detected in mice lacking *Nkx2.5* (Fig. 5v) or *Mef2c* (data not shown) at E9.5.

DISCUSSION

Here, we have cloned chick *Bop* through a novel screen searching for early cardiac-specific genes, and have demonstrated that the *Bop* gene plays a critical role in mouse cardiogenesis. *Bop* is expressed early in development, being detected in the anterior half of Hamilton and Hamburger (HH) stage 5 chick embryos and in the precardiac mesoderm (cardiac crescent) of E7.75 mouse embryos. m-Bop is the first cardiac and muscle-specific MYND or SET domain-containing protein identified and can function as an HDAC-

dependent transcriptional repressor. Targeted deletion of *Bop* in mice has shown that it is required for expression of *dHAND* in the precardiac, but not lateral, mesoderm and that *Bop* is necessary for cardiomyocyte maturation and right ventricular morphogenesis.

Selective and Subtractive PCR Amplification (SSPA)

Classical subtractive hybridization is an efficient method to identify differences in the transcriptional profile between tissues, however it is limited by its ability to compare transcripts in only two RNA pools. We have successfully devised an efficient method to compare RNA species present in two populations but absent from a third. While we have applied this method to clone early cardiac-specific genes, including *Bop*, SSPA will likely be useful to profile other dynamic developmental events.

Cardiomyocyte maturation defects in *Bop* mutant mice

The paucity of trabeculations, expansion of ECM and the downregulation of *dHAND* in *Bop* mutant cardiomyocytes are consistent with a disruption of differentiation into a more mature cardiomyocyte. Although there are no specific molecular markers for the maturation of cardiomyocytes between the straight heart tube and the looped heart tube stages, there are clear morphologic changes that normally occur. The early heart tube is mostly composed of an ECM that is secreted by a monolayer of myocardial cells and later degraded predominantly by more differentiated cardiomyocytes[27]. The degree of expansion of ECM observed in *Bop* mutants exceeds that seen in any previously described mouse mutant and may be secondary to an arrest of the transition from a partially differentiated to a more

mature cardiomyocyte. Alternatively, it is formally possible that m-Bop directly affects gene transcription of a unique set of genes involved in the production or degradation of ECM including proteases or inhibitors of proteases. However, in the absence of detectable differences in the composition of the ECM or synthetic enzymes in *Bop* mutants, and in the presence of *dHAND* downregulation, we currently favor the more general interpretation involving a role for m-Bop in a critical step in cardiomyocyte differentiation, manifested as improper management of the ECM.

Chamber-specific functions of *Bop*

Although *Bop* is expressed throughout the chambers of the heart, its function during mouse cardiogenesis is relatively specific to the ventricular chambers. It is remarkable that the *Bop* mutant atrial chamber had no expansion of ECM. Within the ventricles, the right ventricular cardiomyocytes appeared to be more severely affected but the residual left ventricular myocytes also had a block in their further differentiation. This phenotype was similar to, although more severe than, the small right ventricle in *dHAND* mutants [5,33]. While it is possible that hemodynamic alterations could contribute to the ultimate phenotype observed in any mouse model of cardiac defects, the similarities between *Bop* and *dHAND* mutants and the early (E7.75) failure of *dHAND* expression in the precardiac mesoderm in the absence of *Bop* suggest a more specific role for *Bop* in ventricular development. A GATA-dependent enhancer upstream of *dHAND* can direct cardiac gene expression of *dHAND* in vivo [34]. Whether m-Bop directly or indirectly regulates *dHAND* through this GATA site or through yet unknown sites remains to be determined. However, it is more

likely that m-Bop regulates an intermediate since m-Bop functions as a transcriptional repressor, although it is formally possible that m-Bop could also function as an activator given appropriate co-factors.

m-Bop as a regulator of chromatin modification

m-Bop contains a MYND domain homologous to that of the ETO protein whose fusion with the AML1 protein in chronic myelogenous leukemia converts AML1, normally a transcriptional activator, into a transcriptional repressor [24]. The MYND domain of ETO is essential for this conversion and appears to function by recruiting the nuclear co-repressor, N-CoR, and the Sin3/HDAC complex to DNA sites specified by AML1 binding [16,17]. Similarly, we show that m-Bop can function as a transcriptional repressor by interacting with HDACs. It will be interesting to determine if m-Bop's subcellular localization is regulated or whether m-Bop functions in a complex with other muscle-specific transcription factors that interact with HDAC, such as MEF2 factors[35]. Our preliminary data indicates that m-Bop can interact with the muscle-specific transcription factor, skNAC, although the significance of this interaction remains to be determined.

SET domain proteins are also believed to regulate chromatin structure[36]. Although the mechanism through which most SET domain proteins achieve this is unknown, the SET domain-containing human SUV39H1 and murine Suv39h1 proteins, have recently been shown to modulate higher-order chromatin structure and hence, gene expression, by means of intrinsic histone methyl-transferase (HMT) activity [13,36]. Whether the S-ET domain of m-Bop contains intrinsic HMT activity or serves some other function is yet to be determined.

However, analysis of sequence databases reveals a number of genes in yeast, plants, *Drosophila* and mammals that contain S-ET domains with intervening sequences containing MYND domains, similar to *Bop* (Sim et a., 2002), suggesting a conserved function for this combination of domains.

Our findings indicate that *Bop* regulates a critical maturation step necessary for ventricular cardiomyocyte development and right ventricular formation. To our knowledge, m-Bop is the first cardiac and muscle-specific SET or MYND domain-containing protein identified and, as such, may be part of a muscle-specific module for regulation of higher order chromatin structure.

METHODS

Cloning of chicken m-Bop cDNA

A modification of the PCR Select (Clontech) method of subtractive hybridization, subtractive and selective PCR amplification (SSPA) resulted in cloning of a 391 bp fragment of chick Bop from stage 5 and 10 chick hearts. Briefly, cDNA pools from stage 5 presumptive heart fields (tester 1), including all three germ layers, or stage10 straight heart tube (tester 2) were ligated with different oligonucleotide adaptors and were separately hybridized with excess cDNA from the non-cardiogenic posterior region of stage 5 embryos (driver). The two hybridization samples were mixed and further hybridized to allow complementary single stranded DNA to anneal. Double stranded DNA with complementary strands derived from both tester pools was preferentially amplified by PCR using primers designed to anneal to the unique adaptors ligated on the two tester populations. A 64-74h

chick embryonic heart lambda cDNA library (Stratagene) was screened using the 391 bp ^{32}P-labeled chick Bop fragment, cloned by SSPA, under conditions of low stringency in hybridization buffer consisting of 30% formamide, 6X SSPE, 0.5% SDS, and 100 g/ml denatured salmon sperm DNA at 42°C overnight as previously described[30]. Filters were washed with 2X SSC, 0.1% SDS at 42°C for 10 min followed by 0.1XSSC, 0.1%SDS at 65°C for 15 min. Positive clones were purified, excised into pBluescript plasmids, sequenced by automated sequencing and analyzed by BLAST search.

Whole-mount and section *in situ* hybridization

For whole-mount in situ hybridization, digoxygenin-labeled RNA probes were prepared by in vitro transcription. Mouse or chick embryos from E7.5 to E10.5 or stage 5 to 24, respectively, were isolated in phosphate-buffered saline (PBS) and the pericardium was removed. Embryos were fixed in 4% paraformaldehyde/PBS at 4°C overnight. Whole-mount in situ hybridization was performed as previously described[37]. For section in situ hybridization, ^{35}S-labeled antisense riboprobes were generated by in vitro transcription and in situ hybridization was performed on E9.0-E12.5 mutant and wild-type embryos, and adult heart as previously described [30].

Cell culture and transient transfections

C3H 10T1/2, C2C12, and 293T cells (ATCC) were grown in DMEM (Life Technologies, Frederick, MD) supplemented with 10% fetal bovine serum at 37° C in an atmosphere of 5% CO_2 in air. 293T and 10T1/2 cells were transfected using FuGENE6

reagent (Boehringer Mannheim). For luciferase assays, cells were harvested 48 h after transfection. The total DNA concentration was held constant by adding the GAL4-DBD expression plasmid. The pL8G5-luciferase reporter contains eight LexA-binding sites upstream of five copies of the GAL4-UAS site. The pGL2-5XGAL4-SV40 luciferase reporter (J. Milbrandt) contains five copies of the GAL4-UAS upstream of the SV40 promoter. For TSA inhibition assays, cells were placed in media with or without 150 μM TSA (Calbiochem) 24 h after transfection. For immunoprecipitation experiments, 2 X 10^6 293T cells were transfected with FLAG-tagged HDAC1, -2 or -3 (S.L. Schreiber), GAL4-DBD, and GAL4-mBop2 in various combinations. A total of 8 ug of DNA and 24 ul FuGENE6 was used in each transfection. Cells were lysed in RIPA buffer containing protease inhibitors 48 h after transfection.

Luciferase assays

Cell lysates were analyzed with a Dynex microtiter luminometer. Relative light units obtained from the pL8G5-luciferase reporter (Luciferase Assay Kit, Promega) were normalized by transfection efficiency and protein concentration. Transfection efficiency was determined by FACS (FACSCalibur, Becton Dickinson) analysis of cells co-transfected with the pEGFP-N2 expression plasmid (Clontech). Relative light units obtained from the pGL2-5XGAL4-SV40 reporter (Dual Luciferase Assay System, Promega) were normalized to a co-transfected pRL-TK expression plasmid. Percent activity was determined in relation to the GAL4-DBD. Three independent experiments were performed to calculate the mean and standard error.

Immunoprecipitation and western blotting

Cell lysates were incubated with a BOP monoclonal or FLAG M2 (Sigma) antibody for 1 h at 4°C, followed by a 1 h incubation with protein-A sepharose beads (Sigma). After extensive washing, the precipitated proteins were analyzed by SDS-PAGE and transferred to nitrocellulose. Membranes were probed with the FLAG M2 or BOP monoclonal antibody. Western blots were developed with the enhanced chemiluminescence (ECL) analysis system (Amersham, U.K.).

Targeted deletion of *Bop*

A construct was designed to replace two exons encoding the putative zinc fingers and an adjacent domain (labeled exons 2 and 3, respectively) with an oppositely-directed neomycin resistance (*neo*) gene (Fig. 3A). Genomic fragments of 4.5 kb and 0.5 kb located upstream of exon 2 and downstream of exon 3, respectively, were cloned into the OSDUPDEL 1 vector (kindly provided by N. Maeda and O. Smithies). Transfected SM1 ES cells were selected with G418 and gancyclovir, and correctly targeted integrations were identified by Southern hybridization. Correct integration of the short arm was indicated by a 2.2 kb *Xmn* I/*Kpn* I fragment that hybridized with both *probe 1* and a *neo* probe, and a 2.8 kb wild type *Xmn* I/*Xmn* I fragment that hybridized only with *probe 1*. Correct integration of the long arm was indicated by the presence of a 9-10 kb *Kpn* I/*Kpn* I fragment that hybridized with *probe 2*, and the absence of a 4.5 kb *Kpn* I/*Kpn* I fragment that could result only from the continued presence of the vector multicloning site. PCR genotyping of progeny was performed using primers KO4s (5'-TCATGAGATGGGCATGAGCC-3') and

KO5as (5'-GCATACGCACATGTGCTCGC-3') to detect the wild type allele, and KO4s and NEOs (5'-GCCCGGTTCTTTTTGTCAAGACCG-3') to detect the targeted allele. RNA from E9.0 *Bop*-null or wild-type hearts were used for RT-PCR using primers to exons 1 and 4.

Four correctly-targeted ES cell lines were derived, two of which were injected into E3.5 C57BL/6 blastocysts and transferred to (B6/D2)F1 pseudopregnant females. Two founders were obtained that passed the targeted allele to their progeny through the germline.

Histochemistry

Wild-type and *Bop* mutant embryos were harvested at E9.25, fixed in 4% paraformaldehyde, and processed for cryostat sectioning. The frozen sections were washed twice in PBS for 5 min each and once in 10% H2O2 for 5 min followed by two 5 min washes with water and one 5 min wash with PBS. The sections were incubated for 1hr with 8 g/ml of b-PG (biotinylated fragments of proteoglycan) [38] in 10% calf serum/PBS, and washed 5 times in PBS for 1 min each. A 1:500 dilution of horseradish peroxidase (HRP)-conjugated streptavidin in 10% calf serum/PBS was added to the sections and incubated for 15 min, followed by five 1 min washes in PBS. One tablet of DAKO DAB chromagen was dissolved in 10 ml 0.05M Tris pH7.6. The DAB chromagen was applied to the sections twice for 5 min each followed by two 5 min washes in water.

TUNEL assay

Terminal deoxynucleotide end-labeling (TUNEL) was performed on transverse sections of four E9.0 *Bop* mutant or wild-type embryos at the level of the outflow tract as previously described[33].

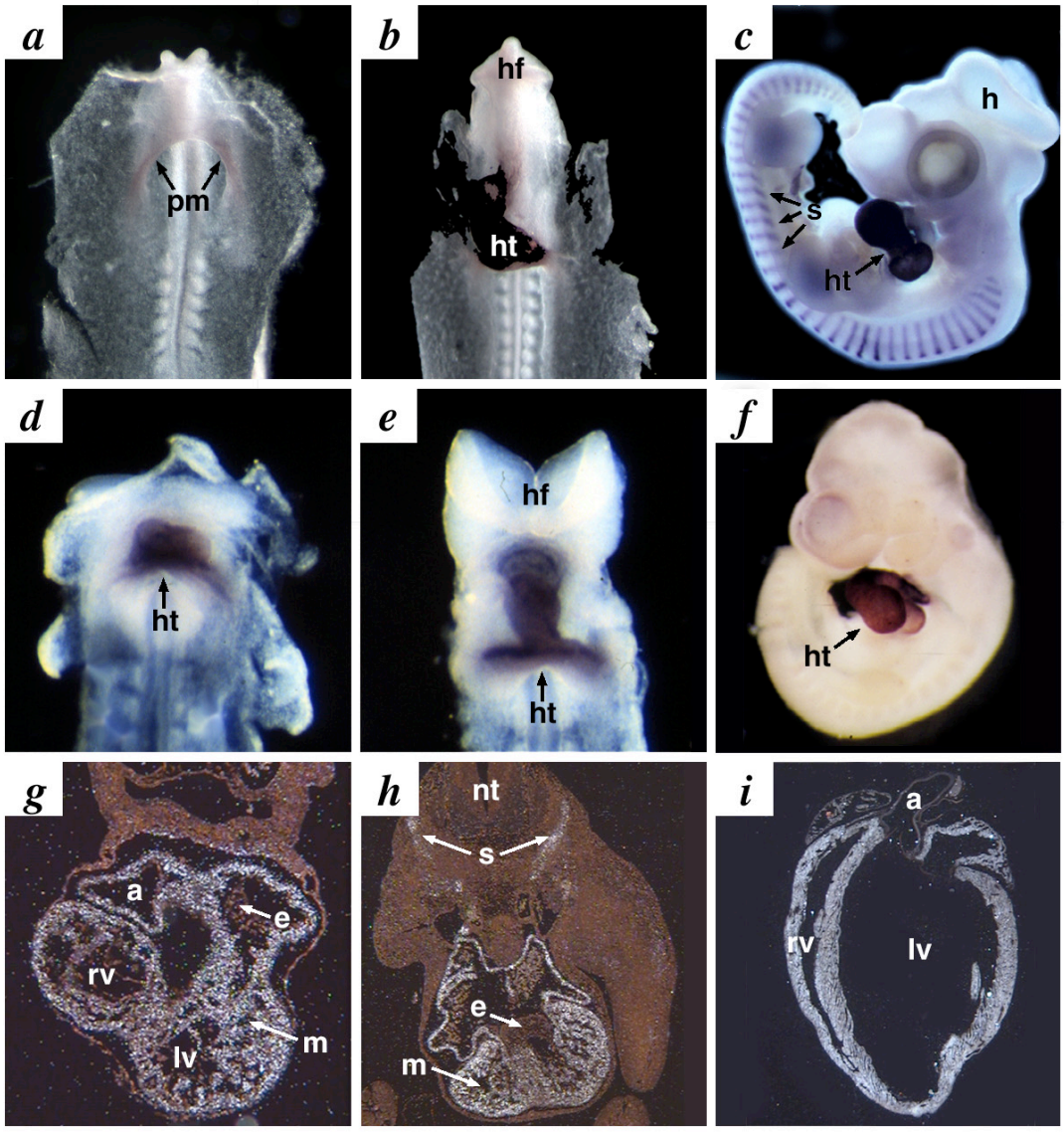

Figure 1. Cardiac and somite-specific expression of *Bop* in chick and mouse. Whole-mount in situ hybridization demonstrated *Bop* expression in chick beginning at HH stage 7 in the precardiac mesoderm (pm) (a), followed by heart (ht) restricted expression at stage 10.0 (b). By stage 20 in chick, expression of *Bop* was seen in the heart and somites (s) (c). Heart-specific expression of *Bop* was seen in mouse at E7.75 (d), E8.0 (e), and E10.5 (f), by whole-mount in situ hybridization. Transverse section in situ analysis revealed expression of mouse *Bop* specifically in the myocardium (m) of the heart at E9.5 (g), as well as in the somites (s), at E12.5 (h). No expression of *Bop* was observed in the endocardium (e) (g,h). Section in situ hybridization revealed *Bop* expression in the adult mouse heart (i). a, atria; e, endocardium; hf, head-fold; h, head; lv, left ventricle; nt, neural tube; rv, right ventricle.

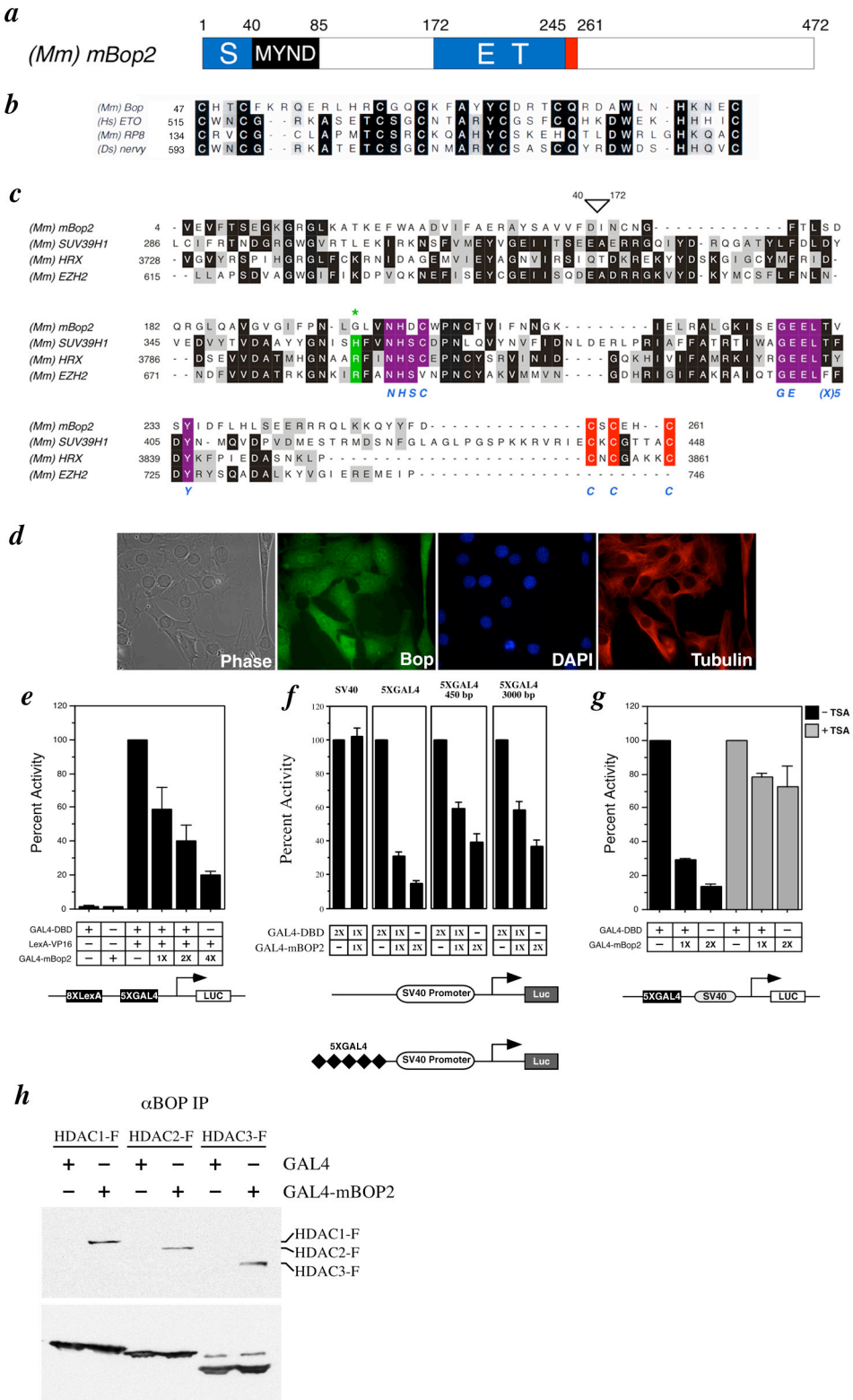
a
(Mm) mBop2
1 40 85 172 245 261 472
S MYND E T
b
(Mm) Bop 47
(Hs) ETO 515
(Mm) RP8 134
(Ds) nervy 593
c
40 172
(Mm) mBop2 4
(Mm) SUV39H1 286
(Mm) HRX 3728
(Mm) EZH2 615
(Mm) mBop2 182
(Mm) SUV39H1 345
(Mm) HRX 3786
(Mm) EZH2 671
NHSC
GE (X)5
(Mm) mBop2 233
(Mm) SUV39H1 405
(Mm) HRX 3839
(Mm) EZH2 725
Y
C C C
261
448
3861
746
d
Phase
Bop
DAPI
Tubulin
e
Percent Activity
GAL4-DBD
LexA-VP16
GAL4-mBop2
8XLexA
5XGAL4
LUC
f
SV40
5XGAL4
5XGAL4 450 bp
5XGAL4 3000 bp
Percent Activity
GAL4-DBD
GAL4-mBOP2
SV40 Promoter
Luc
5XGAL4
SV40 Promoter
Luc
g
− TSA
+ TSA
Percent Activity
GAL4-DBD
GAL4-mBop2
5XGAL4
SV40
LUC
h
αBOP IP
HDAC1-F HDAC2-F HDAC3-F
GAL4
GAL4-mBOP2
HDAC1-F
HDAC2-F
HDAC3-F

Figure 2. m-Bop2 is an HDAC-dependent transcriptional repressor. (a) Predicted protein structure of m-Bop2 with positions of MYND and S-ET domains indicated. Conserved cysteine-rich region is indicated in red. (b) Comparison of the MYND zinc finger domain of mouse m-Bop2 with other MYND domain-containing proteins. (c) Comparison of the m-Bop2 S-ET domain with other SET domain-containing factors. Conserved residues are shaded in black; similar residues are shaded in gray; residues necessary for histone methyl-transferase (HMT) activity are indicated in purple or red.. An asterisk marks a prominent difference between m-Bop2 and SUV39H1 at a residue that affects HMT activity [13]. Location of MYND domain is indicated by open arrowhead (d) Immunocytochemistry of C2C12 cells with BOP monoclonal antibodies. Nuclear or cytosolic regions are indicated by DAPI or tubulin staining, respectively. (e) C3H/10T1/2 cells were transiently transfected with the pL8G5-luc reporter along with the indicated LexA or GAL4 mammalian expression vectors. GAL4-m-Bop2 was co-transfected with LexA-VP16 in increasing amounts (1X = 0.3 ug). The relative luciferase activity was normalized for transfection efficiency by co-transfection with GFP and FACS analysis. (f) 5XGAL4-SV40-Luciferase reporter co-transfected with or without GAL4-m-Bop2. Distance of 5XGAL4 sites from SV40 promoter are shown. (g) 10T1/2 cells were transfected with GAL4-DBD or GAL4-m-Bop2 along with 5XGAL4-SV40-luc (1 ug=1X) as indicated. TSA (150 □M) was added 24 hours after transfection. Results in (e-g) are shown as the mean percentage and standard error of normalized activation from three separate experiments. (h) 293T cells were transfected with FLAG-tagged HDAC1, -2 or -3 along with GAL4-DBD or GAL4-m-Bop2. Proteins from cell lysates were immunoprecipitated with a BOP-specific monoclonal antibody, separated by SDS-PAGE, and immunoblotted with a FLAG-specific antibody. Input is shown in lower panel.

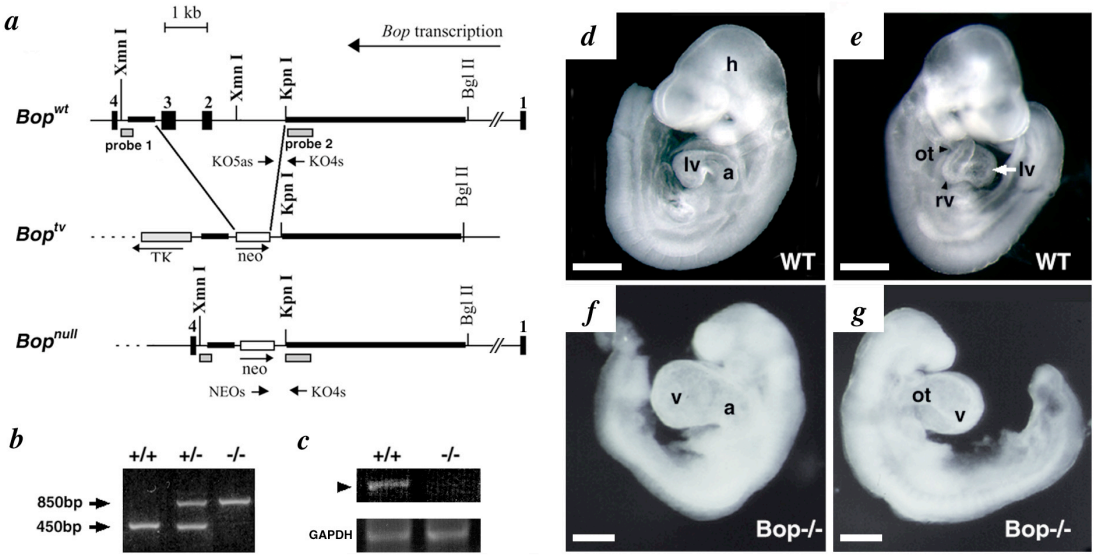

Figure 3. **Targeted deletion of *Bop* is embryonic lethal from cardiac enlargement.** (a) Organization of the *Bop* wild-type (*Bop*^{wt}) allele, and targeting vector (*Bop*^{tv}). Homologous recombination resulted in replacement of exons 2 and 3 of *Bop* by the neomycin resistance gene (Neo) as shown in the *Bop*-null allele (*Bop*^{null}). (b) Genotyping of the wild-type (+/+), heterozygous (+/-) and homozygous (-/-) null loci for the *Bop* gene. (c) RT-PCR for Bop transcripts in wild-type or Bop-null hearts. Left and right lateral views of wild-type (d,e) and *Bop* mutant (f,g) embryos at E9.5 are shown. Gross analysis of mutant embryos showed growth retardation, an enlarged ventricular chamber (v), and a single ventricular segment compared to wild-type embryos. Scale bars represent 400 uM. a, atria; h, head; lv, left ventricle; ot, outflow tract; rv, right ventricle.

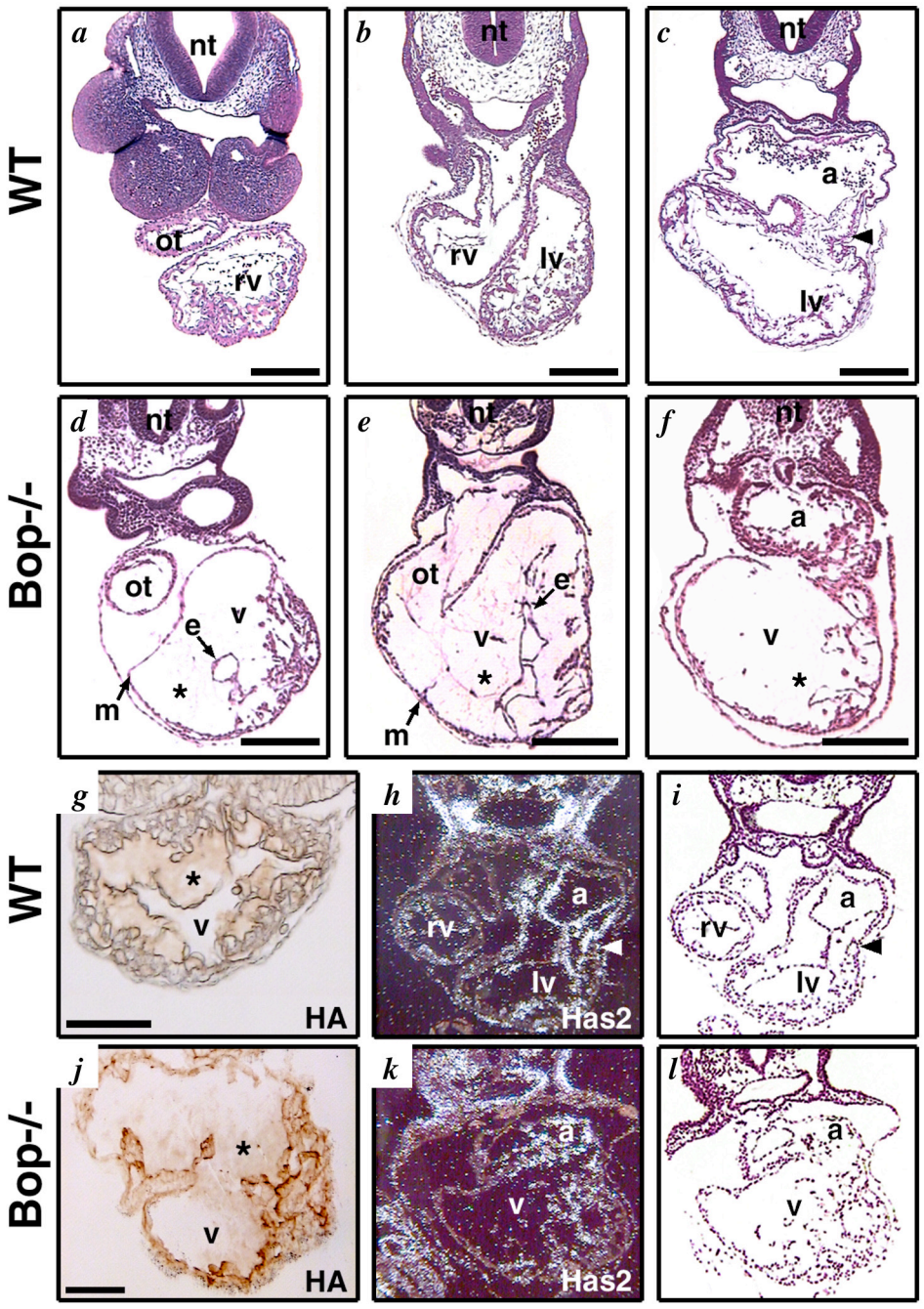

Figure 4. Single ventricle and extracellular matrix accumulation in *Bop* -/- embryos. Transverse hematoxylin and eosin (H&E) sections of wild-type and *Bop* mutant embryos at the level of the outflow tract (ot) (a,d) or ventricular chambers (v) (b,e), showed reduced trabeculae, an enlarged single ventricular chamber filled with extracellular matrix (*)

between the endocardial (e) and myocardial (m) cell layers (d-f), and a non-distinct right-sided ventricle (rv) (e) compared to wild-type embryos (b). Note the small lumen inside the endocardial layer (d,e). Transverse section at the level of the atria showed a normal-size atrial chamber (a) in the *Bop* mutant embryo (f) compared to the wild-type embryo (c). Scale bars represent 100 uM. Histochemistry using a biotinylated hyaluronan-binding protein showed similar levels of hyaluronan (asterisk) in the ECM of E9.5 *Bop* mutant embryos (j), compared to wild-type embryos (g). E8.5 wild-type embryo is shown since minimal ECM is present in E9.5 wild-type hearts. Hyaluronan expression in cardiomyocytes was also similar in both. In situ hybridization of a transverse section of a *Bop*-null embryo showed similar expression levels of hyaluronic acid synthase 2 (Has2) (k) compared to wild-type (h). (i) and (l) represent bright field views of (h) and (k) respectively; arrowhead indicates atrioventricular canal; lv, left ventricle; nt, neural tube.

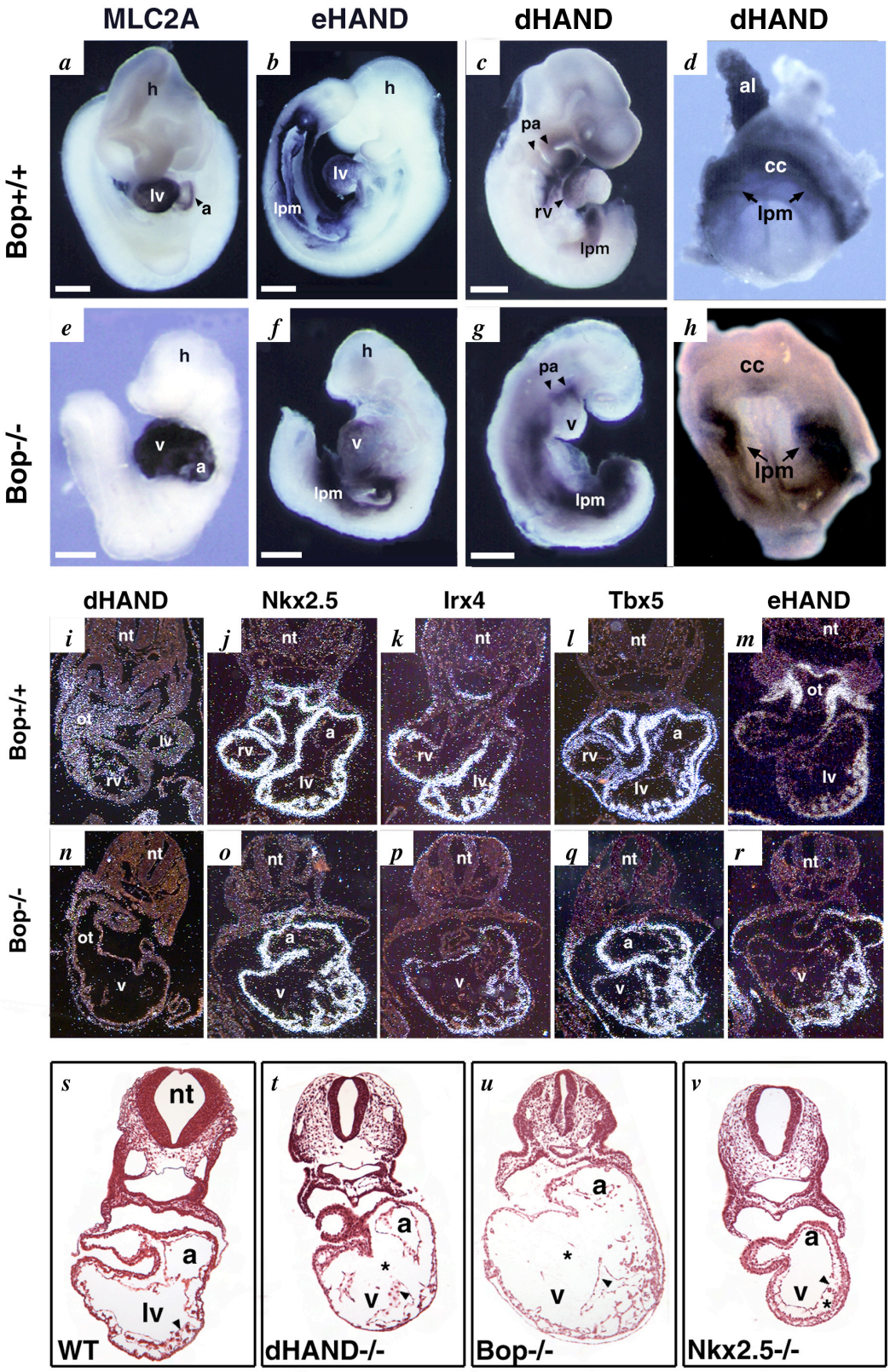
MLC2A
eHAND
dHAND
dHAND
Bop+/+
Bop-/-
a
b
c
d
e
f
g
h
h
lv
a
lpm
pa
rv
al
cc
v
dHAND
Nkx2.5
Irx4
Tbx5
eHAND
i
j
k
l
m
n
o
p
q
r
nt
ot
rv
s
t
u
v
WT
dHAND-/-
Bop-/-
Nkx2.5-/-

Figure 5. *dHAND* is downregulated in cardiomyocyte precursors of *Bop* -/- embryos. By whole-mount in situ hybridization, expression of *MLC2A* (a,e) was unchanged in *Bop* mutants compared to wild-type. *eHAND* was expressed normally in the single ventricle (v) and lateral plate mesoderm (lpm) of the *Bop* mutant embryo (f) compared to wild-type (b) while *dHAND* showed decreased expression in the ventricle of an E9.0 *Bop* mutant (g), compared to E9.5 wild-type (c); expression in the lateral plate mesoderm (lpm) and pharyngeal arches (pa) was intact. Scale bars represent 400uM. *Bop* mutant embryos were examined at E9.0 to search for expression in a rudimentary right ventricle and also were exposed longer in an attempt to reveal low levels of *Bop* expression in the heart (g). Expression of *dHAND* was decreased in the cardiac crescent (precardiac mesoderm) of E7.75 *Bop*-null embryos (h) compared to wild-type (d), but was unchanged in the bilateral lpm. Transverse section in situ hybridization of E9.0 embryos showed decreased expression of *dHAND* in the ventricular chamber (v) and outflow tract (ot) of the *Bop* mutant (n) compared to the wild-type embryo at the level of the right ventricle-outflow tract connection (i). Expression of *Nkx2.5* in the ventricle (v) and atria (a) of the *Bop*-null embryo (o), was normal compared to wild-type expression (j) by section in situ hybridization. Expression of *Irx4* appeared decreased in the single ventricular chamber of the *Bop* mutant embryo (p) compared to wild-type (k). *Tbx5* was expressed in the single *Bop* mutant ventricle (q) at levels comparable to wild-type (l). A small group of cells on the right side had lower levels of expression (q), similar to the right ventricle of wild-type (l). Serial section of *eHAND* expression was notable for lack of expression in this subset of cells but robust expression in the remainder of the ventricle (r). Wild-type demonstrates specific expression in the left ventricle and outflow tract (m); full right ventricle is not shown in this section. Transverse sections of E9.5 wild-type (s), *dHAND*-null (t), *Bop*-null (u) and *Nkx2.5*-null (v) embryos are shown at the level of the atrio-ventricular junction. Arrowheads are in the ventricular lumen and point to the endocardium. Images in (s-v) are at equal magnification. Asterisks indicate the area of ECM. al, allantois; cc, cardiac crescent; lv, left ventricle; nt, neural tube; rv, right ventricle.

REFERENCES

1. Srivastava D, Olson EN. A genetic blueprint for cardiac development. *Nature* **407**,221-6 (2000).

2. Fishman MC, Chien KR. Fashioning the vertebrate heart: earliest embryonic decisions. *Development* **124**,2099-117 (1997).

3. Hurle JM, Icardo JM, Ojeda JL. Compositional and structural heterogenicity of the cardiac jelly of the chick embryo tubular heart: a TEM, SEM and histochemical study. *J Embryol Exp Morphol* **56**,211-23 (1980).

4. Firulli AB, Olson EN. Modular regulation of muscle gene transcription: a mechanism for muscle cell diversity. *Trends Genet* **13**,364-9 (1997).

5. Srivastava D, Thomas T, Lin Q, Kirby ML, Brown D, Olson EN. Regulation of cardiac mesodermal and neural crest development by the bHLH transcription factor, dHAND. *Nat Genet* **16**,154-60 (1997).

6. Biben C, Harvey RP. Homeodomain factor Nkx2-5 controls left/right asymmetric expression of bHLH gene eHand during murine heart development. *Genes Dev* **11**,1357-69 (1997).

7. Pereira FA, Qiu Y, Zhou G, Tsai MJ, Tsai SY. The orphan nuclear receptor COUP-TFII is required for angiogenesis and heart development. *Genes Dev* **13**,1037-49 (1999).

8. Bao ZZ, Bruneau BG, Seidman JG, Seidman CE, Cepko CL. Regulation of chamber-specific gene expression in the developing heart by Irx4. *Science* **283**,1161-4 (1999).

9. Nakagawa O, Nakagawa M, Richardson JA, Olson EN, Srivastava D. HRT1, HRT2, and HRT3: a new subclass of bHLH transcription factors marking specific cardiac, somitic, and pharyngeal arch segments. *Dev Biol* **216**,72-84 (1999).

10. Cheung P, Allis CD, Sassone-Corsi P. Signaling to chromatin through histone modifications. *Cell* **103**,263-71 (2000).

11. Marmorstein R, Roth SY. Histone acetyltransferases: function, structure, and catalysis. *Curr Opin Genet Dev* **11**,155-61 (2001).

12. Khochbin S, Verdel A, Lemercier C, Seigneurin-Berny D. Functional significance of histone deacetylase diversity. *Curr Opin Genet Dev* **11**,162-6 (2001).

13. Rea S, Eisenhaber F, O'Carroll D, Strahl BD, Sun ZW, Schmid M, Opravil S, Mechtler K, Ponting CP, Allis CD, Jenuwein T. Regulation of chromatin structure by site-specific histone H3 methyltransferases. *Nature* **406**,593-9 (2000).

14. Nakayama J, Rice JC, Strahl BD, Allis CD, Grewal SI. Role of histone H3 lysine 9 methylation in epigenetic control of heterochromatin assembly. *Science* **292**,110-3 (2001).

15. Jenuwein T, Allis D. Translating the histone code. *Science* **293**,1074-1080 (2001).

16. Lutterbach B, Westendorf JJ, Linggi B, Patten A, Moniwa M, Davie JR, Huynh KD, Bardwell VJ, Lavinsky RM, Rosenfeld MG, Glass C, Seto E, Hiebert SW. ETO, a target of t(8;21) in acute leukemia, interacts with the N-CoR and mSin3 corepressors. *Mol Cell Biol* **18**,7176-84 (1998).

17. Gelmetti V, Zhang J, Fanelli M, Minucci S, Pelicci PG, Lazar MA. Aberrant recruitment of the nuclear receptor corepressor-histone deacetylase complex by the acute myeloid leukemia fusion partner ETO. *Mol Cell Biol* **18**,7185-7191 (1998).

18. Hwang I, Gottlieb PD. Bop: a new T-cell-restricted gene located upstream of and opposite to mouse CD8b. *Immunogenetics* **42**,353-61 (1995).

19. Hamburger V, Hamilton H. A series of normal stages in the development of the chick embryo. *J Morphol* **88**,49-82 (1951).

20. Lints TJ, Parsons LM, Hartley L, Lyons I, Harvey RP. Nkx-2.5: a novel murine homeobox gene expressed in early heart progenitor cells and their myogenic descendants. *Development* **119**,419-31 (1993).

21. Komuro I, Izumo S. Csx: a murine homeobox-containing gene specifically expressed in the developing heart. *Proc Natl Acad Sci U S A* **90**,8145-9 (1993).

22. Hwang I, Gottlieb PD. The Bop gene adjacent to the mouse CD8b gene encodes distinct zinc- finger proteins expressed in CTLs and in muscle. *J Immunol* **158**,1165-74 (1997).

23. Hollenberg SM, Sternglanz R, Cheng PF, Weintraub H. Identification of a new family of tissue-specific basic helix-loop- helix proteins with a two-hybrid system. *Mol Cell Biol* **15**:3813-22 (1995).

24. Lutterbach B, Sun D, Schuetz J, Hiebert SW. The MYND motif is required for repression of basal transcription from the multidrug resistance 1 promoter by the t(8;21) fusion protein. *Mol Cell Biol* **18**,3604-11 (1998).

25. Yoshida M, Horinouchi S, Beppu T. Trichostatin A and trapoxin: novel chemical probes for the role of histone acetylation in chromatin structure and function. *Bioessays* **17**:423-30 (1995).

26. Camenisch TD, Spicer AP, Brehm-Gibson T, Biesterfeldt J, Augustine ML, Calabro A, Jr., Kubalak S, Klewer SE, McDonald JA. Disruption of hyaluronan synthase-2 abrogates normal cardiac morphogenesis and hyaluronan-mediated transformation of epithelium to mesenchyme. *J Clin Invest* **106**,349-60 (2000).

27. Bernanke DH, Orkin RW. Hyaluronate binding and degradation by cultured embryonic chick cardiac cushion and myocardial cells. *Dev Biol* **106**,360-7 (1984).

28. O'Brien TX, Lee KJ, Chien KR. Positional specification of ventricular myosin light chain 2 expression in the primitive murine heart tube. *Proc Natl Acad Sci U S A* **90**,5157-61 (1993).

29. Kubalak SW, Miller-Hance WC, O'Brien TX, Dyson E, Chien KR. Chamber specification of atrial myosin light chain-2 expression precedes septation during murine cardiogenesis. *J Biol Chem* **269**,16961-70 (1994).

30. Srivastava D, Cserjesi P, Olson EN. A subclass of bHLH proteins required for cardiac morphogenesis. *Science* **270**,1995-9 (1995).

31. Bruneau BG, Bao ZZ, Tanaka M, Schott JJ, Izumo S, Cepko CL, Seidman JG, Seidman CE. Cardiac expression of the ventricle-specific homeobox gene Irx4 is modulated by Nkx2-5 and dHand. *Dev Biol* **217**,266-77 (2000).

32. Bruneau BG, Logan M, Davis N, Levi T, Tabin CJ, Seidman JG, Seidman CE. Chamber-specific cardiac expression of Tbx5 and heart defects in Holt- Oram syndrome. *Dev Biol* **211**,100-8 (1999).

33. Yamagishi, H, Yamagishi, C, Nakagawa, O, Harvey, RP, Olson EN, Srivastava, D. The combinatorial activities of Nkx2.5 and dHAND are essential for cardiac ventricle formation. *Dev Biol*, **239**, 190-203 (2001).

34. McFadden, DG, Charite, J, Richardson, JA, Srivastava, D, Firulli, AB, Olson, EN. A GATA-dependent right ventricular enhancer controls dHAND transcription in the developing heart. *Development*, **127**,5331-5341 (2000).

35. McKinsey TA, Zhang CL, Lu J, Olson EN. Signal-dependent nuclear export of a histone deacetylase regulates muscle differentiation. *Nature* **408**,106-11 (2000).

36. Jenuwein T. Re-SET-ting heterochromatin by histone methyltransferases. *Trends Cell Biol* **11**,266-273 (2001).

37. Yamagishi, H, Garg, V, Matsuoka, R, Thomas, T, Srivastava, D. A molecular pathway revealing a genetic basis for human cardiac and craniofacial defects. *Science*, **283**, 1158-1161 (1999).

38. Green SJ, Tarone G, Underhill CB. Distribution of hyaluronate and hyaluronate receptors in the adult lung. *J Cell Sci* **90**,145-56 (1988).

CHAPTER 3: m-Bop interacts with cofactors that affect its function

INTRODUCTION

Transcriptional regulation of cardiogenesis has been investigated in much detail, but the mechanisms controlling the early stages of cardiomyocyte maturation and differentiation are largely unknown. Previously, I reported the activity of m-Bop, a protein essential for cardiomyocyte maturation and chamber-specific development (Gottlieb et al., 2002). *Bop* encodes MYND and SET domains both of which regulate transcriptional repression through distinct chromatin modifications. m-Bop functions as a histone deacetylase (HDAC) mediated transcriptional repressor, and physically associates with class I HDACs. Targeted deletion of *Bop* in mouse results in embryonic lethality at E10.5 and expansion of the extracellular matrix between the myocardium and endocardium of the developing heart, suggesting persistence of immature ventricular cardiomyocytes. Expression of *dHAND*, a bHLH factor necessary for proper development of the right ventricle (Srivastava et al., 1997) is downregulated in the heart of the *Bop* mutant embryo further suggesting an important function for *Bop* in cardiomyocyte differentiation in a chamber-specific manner.

In an effort to delineate the mechanism of m-Bop's function in developing cardiomyocytes, I used the yeast two-hybrid system to identify DNA-binding factors and other cofactors that associate with m-Bop and may be important for its role in the embryonic heart. TRB3, the mammalian ortholog of *Drosophila* Tribbles, and skeletal nascent polypeptide associated complex (skNAC) were two of the factors identified from the yeast

two-hybrid screen, both of which interacted with m-Bop by co-immunoprecipitation from cell lysates coexpressing m-Bop and the candidate factor.

Drosphila tribbles was originally identified as a novel inhibitor of mitosis and is essential for blocking mitosis in the *Drosophila* mesoderm during early gastrulation. *Tribbles* initiates a delay in ventral furrow formation when overexpressed in the *Drosophila* zygote, inhibits mitosis following microinjection of *tribbles* mRNA into cleavage stage embryos, and slows progression through G2 when overexpressed in *Drosophila* wing imaginal discs (Gro□hans and Wieschaus, 2000; Mata et al., 2000; Seher and Leptin, 2000). Exogenous expression of *tribbles* and the mitotic inducer, *string,* restores wing growth to normal, suggesting an opposing role for these two molecules in regulation of the cell cycle (Mata et al., 2000). *Tribbles* induces proteosome-mediated degradation of String, and encodes a putative serine/threonine kinase that lacks an ATP binding site and contains a variant catalytic core (Mata et al., 2000). Thus far, no detectable catalytic activity has been demonstrated for Tribbles by *in vitro* kinase assay.

Drosophila gastrulation begins with the invagination of a group of ventrally located cells that will become mesoderm. During gastrulation, the transcription pattern of *string* prefigures the pattern of mitotic domains in the embryo with the exception of the tenth domain (Edgar and O'Farrell, 1989). Unlike most domains of the embryo that express *string* and enter mitosis within twenty minutes, a delay in domain ten occurs between expression of *string* and initiation of mitosis. This delay allows for the mesodermal cells to migrate and form the ventral furrow. Only after this invagination has occurred, will mitosis resume. Premature mitosis in domain ten prevents formation of the ventral furrow, and likewise, the

process of ventral furrow formation inhibits mitosis (Edgar and O'Farrell, 1990). By inducing degradation of String protein in domain ten, Tribbles is responsible for this mitotic delay, thereby coordinating the complex processes of mitosis and morphogenesis.

Skeletal and muscle-specific nascent polypeptide associated complex (skNAC) was originally identified as the muscle-specific isoform of NAC (Yotov and St-Arnaud, 1996), a molecule that was shown to form a heterodimeric complex and bind newly synthesized polypeptide chains as they exit ribosomes (Wiedmann et al., 1994). Differential splicing-in of the 6kb second exon gives rise to the proline-rich 7kb mRNA. skNAC was shown to bind specific sequences in the myoglobin promoter and activate transcription from these sites (Yotov and St-Arnaud, 1996). Mutation of the skNAC response elements in the myoglobin promoter abrogated site-specific activation by skNAC. skNAC protein is expressed in differentiating and differentiated myotubes, but not in undifferentiated myoblasts. Overexpression of skNAC in C2C12 myoblasts gives rise to early fusion of cells into large myosacs. These results suggest a role for skNAC in differentiation of muscle cells and possibly myoblast fusion.

RESULTS

Yeast two-hybrid library construction and screening

To isolate factors that interact with m-Bop in the embryonic heart, I first constructed an embryonic day 11.5 (E11.5) mouse heart yeast two-hybrid library. The library was constructed using the Clontech Matchmaker Library Construction Kit in which a library of double-stranded cDNA fragments is generated with specific oligonucleotide sequences on the

ends. When co-transformed into yeast with a linearized vector containing the same oligo sequences, the ends of the library fragment recombine with the oligo sequences in the vector creating a circularized plasmid.

Poly(A) RNA isolated from embryonic mouse hearts was used to generate the yeast two-hybrid library, first by priming the RNA with a modified oligo (dT) primer followed by first-strand cDNA synthesis using a reverse transcriptase that extends the 3' end of the cDNA with deoxycytodine nucleotides. The SMART III Oligonucleotide (Clontech SMART technology) containing an oligo(G) sequence at its 3' end was annealed to the cDNA which was then extended at the 5' end by the reverse transcriptase (Figure 1). The cDNA was then amplified by long-distance PCR using primer sequences in the SMART III Oligo and the modified oligo (dT) primer. The resulting library of double-stranded cDNA fragments was purified to select for DNA molecules greater than 200 base pairs.

To screen for molecules that interact with m-Bop in the embryonic heart, AH109 yeast cells were used. This yeast strain was engineered to contain the HIS3, ADE2, and lacZ reporter genes downstream of the GAL4-UAS, allowing for stronger selection and a higher stringency screening. AH109 cells were made competent and transformed with the pGBKT7 plasmid containing the GAL4 DNA-binding domain fused to the full-length Bop cDNA. This plasmid also encodes the TRP1 gene whose gene product allows for growth on media lacking tryptophan. One yeast colony containing the Bop plasmid was selected, the cells were grown for large-scale transformation, made competent, and cotransformed with the library of cDNA fragments and the linearized library vector (pGADT7-Rec). The transformants were plated on quadruple dropout (QDO) plates lacking adenine, histidine,

leucine, and tryptophan. 10mM 3-amino-1,2,4-triazole (3-AT) was added to the media to suppress background by competitively inhibiting leaky His3p expression. Approximately 5.5 X 10^5 clones were screened resulting in four hundred colonies. Two hundred of the largest colonies were streaked on fresh plates and assayed for β-galactosidase activity. Colonies turning blue within one hour were grown, the DNA isolated, and the insert amplified by PCR using primer sequences within the library vector. The amplified inserts were sequenced. I identified the sequence of approximately 80 clones (Table 1).

The clones I chose to pursue were based primarily on three criteria. Clones encoding well-characterized domains were selected because they provided functional clues encoded by their sequence. Clones were chosen based on the number of times the gene sequence was isolated from the yeast two-hybrid. The third criteria included the ability to assess the functional significance of the interaction in testable assays. After careful evaluation of the clones identified from the yeast two-hybrid, I continued to investigate the following five molecules: Mfz10, MICAL, a novel helicase, TRB3 and skNAC.

Mfz10 is a member of the Frizzled family of proteins which function as cell-surface receptors for the Wnt family of secreted ligands. The molecular mechanisms of Wnt signaling have been elucidated in considerable detail and these pathways are known to regulate cell proliferation, differentiation, and embryonic development (reviewed in Dierick and Bejsovec, 1999; Wodarz and Nusse, 1998). Mfz10 is expressed in the developing heart (Malik and Shivdasani, 2000) and identification of this molecule in the yeast two-hybrid suggested a potential cytosolic role for m-Bop in Wnt signaling.

Molecule interacting with CasL (MICAL) is a multi-domain protein shown to bind vimentin and localize to intermediate filaments, suggesting a role for this factor in cytoskeletal regulation by establishing a connection between the docking molecule CasL and intermediate filaments (Suzuki et al., 2002). MICAL contains a highly conserved flavoprotein monooxygenase domain necessary for plexin-mediated axonal repulsion (Terman et al., 2002). Binding of a factor by MICAL via one of its protein interaction domains may exert a regulatory effect on the bound protein by altering the redox state of the microenvironment in which it is sequestered. For these reasons, I wanted to further investigate the interaction between MICAL and m-Bop and the possible effects of changes in redox states on m-Bop protein.

A novel superfamily I RNA helicase proved interesting due to its myocardial expression discovered by gene trap in mice (Wagner et al., 1999). This family of helicases contains proteins with both RNA and DNA helicase activity (Koonin, 1992; Schmid and Linder, 1992), suggesting a possible role for this factor in facilitating transcription and other necessary cellular functions.

TRB3 is the mammalian ortholog of *Drosophila* Tribbles (Du et al., 2003), which induces degradation of String protein, the rate-limiting regulator of mitosis. Degradation of String causes a brake in cell proliferation allowing for complex morphogenetic processes to be completed without the added complication of cell division.

Since our previous work suggested that m-Bop regulates transcription but not through direct DNA binding, I was interested in identifying a DNA-binding factor that interacts with m-Bop bringing it to the site of transcription. Further investigation into the candidate factor

skeletal nascent polypeptide associated complex (skNAC), identified a potentially interesting transcription factor shown to bind specific sequences in the myoglobin promoter.

Testing the interactions by co-immunoprecipitation

As a secondary method to test the interaction between m-Bop and each candidate factor, I subcloned the full-length Bop cDNA into a MYC-tagged expression vector. The yeast two-hybrid clones were subcloned into a FLAG-tagged expression vector. MYC-Bop and each FLAG-tagged clone were cotransfected into Cos1 cells using Fugene 6 (Roche). After thirty hours the cells were lysed and m-Bop was immunoprecipitated, run on an SDS-PAGE acrylamide gel, and analyzed by Western blot. Immunodetection using an anti-FLAG antibody revealed reproducible interactions with MICAL, skNAC, and TRB3 (Figure 2). The preliminary results warranted further investigation into the functional significance of these interactions. I focused on the DNA-binding factor skNAC, and the potential cofactor, TRB3.

PART I

Bop and *TRB3* are coexpressed in the embryo

In order for a factor to physically associate with m-Bop and function with it in the embryonic heart, the two factors must be coexpressed in the heart during development. To determine the embryonic expression of *TRB3* in mouse, *in situ* hybridization was performed on an E10.5 transverse section through the heart using an mRNA probe transcribed from the full-length TRB3 cDNA. Expression of *TRB3* was ubiquitous throughout the embryo including the heart (data not shown). TRB3 may play a universal role during murine development, suggesting that its interaction with temporal and tissue-specific factors such as m-Bop may be instrumental in its activity.

TRB3 does not affect the subcellular localization of m-Bop

Immunocytochemistry was used to investigate the subcellular localization of TRB3. Expression of TRB3 protein appeared mostly nuclear but was also detected in the cytosol of Cos1 and 10T1/2 cells. Using the same cell lines, m-Bop protein was detected in the nucleus but appeared more abundant in the cytosol. Because m-Bop functions as a transcriptional repressor, a regulatory mechanism may exist to import m-Bop protein into the nucleus to perform its function, or export m-Bop protein from the nucleus to the cytosol upon completion of its function. To determine if TRB3 affects the subcellular localization of m-Bop, TRB3 and m-Bop were coexpressed in Cos1 and 10T1/2 cells. While m-Bop and TRB3 revealed overlapping domains of protein expression in the cell, TRB3 did not appear to regulate the localization of m-Bop protein (data not shown).

TRB3 does not induce ubiquitin-mediated degradation of m-Bop

Tribbles, the *Drosophila* ortholog of TRB3, interferes with cell cycle progression by inducing proteosome-dependent degradation of String (Mata et al., 2000). Tribbles also functions as a negative regulator of the C/EBP transcription factor, Slbo, by specifically targeting it for rapid degradation via ubiquitination (Rorth et al., 2000). To determine if the interaction between TRB3 and m-Bop facilitates degradation of m-Bop, I overexpressed increasing amounts of TRB3 with constant levels of Bop in Cos1 cells to see if m-Bop protein decreased in the presence of excess TRB3. By Western blot analysis, m-Bop protein was unchanged in the presence TRB3 compared to samples expressing m-Bop alone. However, since Bop was also overexpressed in the experiment, this negative result could be attributed to a saturation of degradation machinery in the cell, in which case a slight change in protein levels may be difficult to detect. In a second experiment, I tested the ability of TRB3 to induce ubiquitin-mediated degradation of m-Bop. In the presence of proteosome inhibitors, I coexpressed TRB3, Bop and HA-tagged ubiquitin in Cos1 cells. If TRB3 caused m-Bop to become ubiquitinated, immunoprecipitation of m-Bop followed by Western blot analysis using an anti-HA antibody would detect the presence of ubiquitinated m-Bop. A negative result by Western blot revealed that the interaction between TRB3 and m-Bop does not serve to post-translationally regulate m-Bop protein in the heart by degradative means.

TRB3 does not phosphorylate m-Bop by *in vitro* kinase assay

The protein sequence encoded by *TRB3* reveals a putative serine/threonine kinase similar to the SNF1 family of serine/threonine kinases (Seher and Leprin, 2000), however

careful examination of the amino acid sequence suggests that this molecule may not be catalytically active. TRB3 contains a truncated kinase domain that lacks an adenosine 5'-triphosphate binding site (GXGXXG) and contains a variant catalytic core motif from amino acid 175 to 182 (LRDLKLRR compared to consensus HRDLKPEN). To date, Tribbles and its mammalian counterparts lack detectable kinase activity by *in vitro* kinase assay. However, to thoroughly investigate the interaction between m-Bop and TRB3, I performed an *in vitro* kinase assay to determine if TRB3 could phosphorylate m-Bop. TRB3 and Bop were coexpressed in Cos1 cells, coimmunoprecipitated and resuspended in kinase buffer with ATP, [□-^{32}P] ATP and serine/threonine phosphatase inhibitors. The reactions were run on a SDS-PAGE acrylamide gel, and phosphorylation was detected by autoradiography. Similar to previously reported results, TRB3 did not appear to phosphorylate m-Bop by *in vitro* kinase assay (data not shown).

TRB3 enhances transcriptional repression by m-Bop

Through the use of *in vitro* assays, we showed that Bop functions as a transcriptional repressor mediated in part by class I histone deacetylases (HDACs). To further establish the functional significance of the interaction between m-Bop and TRB3, I used the SV40-driven luciferase reporter to determine if TRB3 affects the function of m-Bop as a repressor. This reporter construct contains five copies of the GAL4-UAS upstream of the minimal SV40 promoter. In transient transfections of 293T cells, GAL4-m-Bop consistently inhibits transcriptional activation of luciferase by the SV40 promoter (Gottlieb et al., 2002). In a similar experiment, TRB3 was added to determine if it affected the transcriptional activity of

m-Bop. The levels of Bop in this experiment were titrated to an amount of Bop that would not repress alone but may repress with TRB3. The addition of MYC-tagged TRB3 reproducibly enhanced repression of luciferase activity by m-Bop in a dose-dependent manner (Figure 3A). To confirm that TRB3 does not enhance the activity of a repressor by non-specific means, I used a negative control experiment, which revealed that TRB3 had no effect on Hrt2-mediated repression of the Hrt2-luciferase reporter activated by Notch IC (Figure 3B) (Nakagawa et al., 2000). Taken together, these data suggest a specific role for m-Bop and TRB3 in the transcriptional repression of target genes in the embryonic heart.

N-terminus of TRB3 is necessary and sufficient for interaction with m-Bop

In an effort to characterize the interaction between m-Bop and TRB3, I mapped the region of TRB3 bound by m-Bop. Since TRB3 does not contain clearly defined functional domains, I constructed a series of N-terminal and C-terminal cDNA deletions by PCR, and subcloned them into the PCDNA3.1 vector in frame with a MYC-tag. Cotransfection of the deletion constructs with FLAG-Bop in Cos1 cells followed by immunoprecipitation of m-Bop using an anti-FLAG antibody revealed that the N-terminus of TRB3 was necessary and sufficient for its interaction with m-Bop (Figure 4).

Since TRB3 enhanced repression by m-Bop in the transcriptional reporter assay, I tested whether disruption of the interaction between m-Bop and TRB3 would abrogate the ability of TRB3 to enhance this repression. The N-terminal deletion of TRB3 and full-length Bop were coexpressed in Cos1 cells with the SV40-driven luciferase reporter construct described above. In this experiment, the full-length TRB3 positive control consistently

increased repression of luciferase activity by m-Bop while the N-terminal deletion of TRB3 had no effect (Figure 5). Taken together, these data suggest that m-Bop interacts with the N-terminus of TRB3 and it is through this interaction that TRB3 potentiates repression by m-Bop.

This work describes a novel interaction between the cardiac-specific transcriptional repressor, m-Bop, and TRB3, a factor necessary for coordinating cell division and morphogenesis during *Drosophila* development. While TRB3 has not previously been shown to regulate transcription, I showed that TRB3 specifically enhanced repression of luciferase activity by m-Bop. The N-terminus of TRB3 was necessary for its interaction with m-Bop and deletion of this region resulted in the inability of TRB3 to potentiate repression by m-Bop. This finding suggests a possible role for TRB3 as a transcriptional corepressor of m-Bop in the heart during development.

PART II

Bop and *skNAC* are coexpressed in the heart and somites

Many considerations warranted further investigation into the functional significance of the interaction between skNAC and m-Bop. Thirty-five of the eighty clones identified from the yeast two-hybrid encoded the C-terminus of skNAC, comprising approximately 44% of the identified clones. Sims et al. reported the same interaction by yeast two-hybrid using a skeletal muscle library. By mutational analysis the authors showed that the N-terminal portion of the SET domain and the MYND domain of m-Bop are necessary to interact with a PXLXP motif in the C-terminus of skNAC (Sims et al., 2002). Because of this data and the fact that skNAC was reported to bind DNA (Yotov and St-Arnaud, 1996), I decided to investigate the functional role of this interaction in the embryonic heart.

skNAC is expressed in adult heart and skeletal muscle by Northern blot analysis, and was found to be upregulated in skeletal muscle upon injury (Munz et al., 1999; Yotov and St-Arnaud, 1996). To study the developmental expression pattern of *skNAC*, *in situ* hybridization was performed on a timecourse of mouse embryo sections from E9.5- E15.5. *skNAC* was expressed throughout the myocardium of the heart and the somites beginning at the earliest stage and continuing through development, strikingly similar to the expression pattern of *Bop* (Figure 6). These overlapping patterns of expression suggested an important role for m-Bop and skNAC in the developing heart and somites.

m-Bop and the DNA-binding factor, skNAC

Because m-Bop does not appear to bind DNA, but functions as a transcriptional repressor, I was interested in identifying a DNA-binding factor that interacts with m-Bop to bring it to the site of transcription. skNAC was previously reported to bind the myoglobin promoter and transactivate downstream reporter genes (Yotov and St-Arnaud, 1996). Mutations in the binding sites of this promoter abolish skNAC binding. Using the same myoglobin promoter sequences driving luciferase, I asked if m-Bop could affect activation of luciferase by skNAC, either through repression of this activation or by cooperative activation of the reporter. In my hands, skNAC did not activate transcription of luciferase via the myoglobin promoter. After much trouble-shooting with different cell lines, various transfection reagents, incubation times and other variables, I decided to forego this experiment. There are a variety of reasons that this experiment could have failed. There may not have been enough skNAC protein in the cell to activate the reporter because skNAC did not express at detectable levels in any cell line that I tested. This is possibly due to the large size of skNAC. Additionally, the conditions for this assay may not have been optimal, or skNAC may not activate transcription through the reported sites in the myoglobin promoter.

In an effort to study the function of skNAC and its role with m-Bop in the embryonic heart, I used an *in vitro* candidate approach to determine if these two factors could affect transcription on a variety of cardiac–specific enhancers known to play important roles in the embryonic and adult heart. Plasmids containing these enhancer regions upstream of the luciferase reporter gene were used. I tested Bop and skNAC alone, together, and in

combination with the endogenous activators of the ANF, dHAND, HRT2, Nkx2.5, and SM22 enhancers. This series of experiments revealed no significant results.

Targeted deletion of *skNAC*

Failed attempts at *in vitro* methods to investigate skNAC prompted me to study this molecule by *in vivo* methods. skNAC is composed of seven exons (Figure 7). Splicing out of the large 6 kb second exon results in the □NAC isoform which is expressed in the embryo beginning around E 14.5. I devised a targeting strategy to inactivate *skNAC* by deleting the large 6 kb exon, leaving the rest of the molecule intact so that the ubiquitous □*NAC* isoform is properly transcribed (Figure 7). ES cell electroporation was performed by the transgenic core at UT Southwestern. Chong Yon Park performed Southern blot analysis on the ES cells and identified two positively targeted clones at both the 5' and 3' ends by homologous recombination. These clones generated high percentage chimeras, and successful germline transmission of the targeted allele. Mutants homozygous for the *skNAC*-null allele were underrepresented with only half the expected number at birth, suggesting embryonic lethality of *skNAC*-null mice with variable penetrance in a mixed genetic background. A number of the viable *skNAC* mutant mice appeared smaller than their wild type and heterozygote littermates. Detailed evaluation of these mice and mice in a pure genetic background are needed to fully investigate the phenotype. RT PCR within the second exon of skNAC confirmed the absence of skNAC mRNA transcript in the mutant mice compared with the wildtype mice. The □-NAC isoform was transcribed properly across all genotypes.

Because I identified skNAC as a factor that interacts with m-Bop in the embryonic heart, and *in vitro* methods to study this interaction yielded no results, I used the *skNAC* and *Bop* heterozygote mice to investigate an *in vivo* interaction for these two factors. *skNAC* heterozygote mice were bred to mice heterozygote for the *Bop* gene to determine if double heterozygote mice revealed cardiac or skeletal muscle abnormalities. In a mixed genetic background, inactivation of a single *skNAC* allele and a single *Bop* allele resulted in viable progeny. As previously mentioned, this experiment will be repeated in a pure genetic background to further investigate a genetic interaction of these two factors in mice. Additionally, *skNAC*-null mice will be crossed to *Bop* heterozygote mice to determine if one inactivated *Bop* allele can compound the *skNAC* mutant phenotype.

At present, no conclusions can be drawn from this preliminary data. While there is convincing *in vitro* data to support the idea that skNAC and m-Bop physically interact, elucidating the role of this interaction in a biological context remains challenging. Detailed characterization of the *skNAC* mutant mice and double heterozygote mice in a pure genetic background may reveal a functional role for this interaction in the heart.

DISCUSSION

In an effort to begin understanding the molecular mechanisms by which m-Bop functions in the embryonic heart, I performed a yeast two-hybrid assay to identify potential molecules that interact with m-Bop. This screen resulted in a number of interesting candidate factors, two of which I pursued. *TRB3* is the mouse ortholog of *Drosophila tribbles*, which coordinates the entry into mitosis with morphogenesis during gastrulation. I

showed that TRB3 enhanced transcriptional repression by m-Bop in luciferase reporter assays. The N-terminal region of TRB3 was necessary and sufficient to interact with m-Bop, and disruption of this interaction resulted in the inability of TRB3 to enhance m-Bop's repression. The DNA-binding factor *skNAC*, was expressed in the myocardium of the heart and somites, strikingly similar to the expression pattern of *Bop* during cardiogenesis. Due to the inability to study the interaction between skNAC and m-Bop by *in vitro* means, I performed targeted deletion of *skNAC* in mice. Preliminary results suggested that *skNAC* mutant mice are embryonic lethal with variable penetrance in a mixed genetic background.

Using the yeast two-hybrid as a tool

In recent times, with the sequencing of the human and other genomes, medical research has entered the post-genomic era, where the challenge is to understand the function of the entire range of gene products. Identifying the function of a novel protein can be a difficult feat to achieve. Since the original description in 1989, the yeast two-hybrid has provided insight into many biological pathways (Fields and Song, 1989). Understanding protein function is key to understanding how complex biological systems operate in normal physiological situations.

The yeast two-hybrid was founded on the principle that transcription factors consist of two separable modules. The DNA-binding domain is necessary for binding of the transcription factor to the promoter region by sequence specific DNA recognition, and the activation domain recruits the transcriptional machinery for mRNA production. Both of these domains are necessary for transcription, but not necessarily within the same protein.

Fusion of factor X to the GAL4 DNA-binding domain and factor Y to the activation domain will result in induction of a reporter gene downstream of the GAL4-UAS if the two proteins interact. This system allows for sensitive detection of *in vivo* protein-protein interactions and can be used to screen a library for novel interacting proteins. It can also be used to map the regions that bind by testing deletion mutants of the proteins, or to evaluate mutations in the proteins associated with disease states.

As valuable as the yeast two-hybrid system has been at identifying protein-protein interactions, there are limitations that must be considered. These experiments are performed by yeast transformation or yeast mating, processes that are both known to be inefficient. Many protein interactions are dependent on correct protein folding or posttranslational modifications. These processes may not occur properly in yeast resulting in false negatives. Some of the proteins are difficult to express in yeast while others may be toxic to the yeast cells. Inducible expression vectors may circumvent the latter. The yeast two-hybrid assay is biased by the abundance of any given mRNA and therefore does not display dipeptide combinations at physiological frequencies. It is well known that molecules interact in multiprotein complexes to perform biological functions, however the yeast two-hybrid has the capacity to detect only bimolecular associations. A protein interaction dependent on the presence of a complex of proteins would be missed. Possibly the most difficult problem to overcome is the issue of false positives. Technical false positives arise due to artificial induction of the reporter gene through direct binding of the activation domain fusion protein to DNA or the inherent ability of the DNA-binding domain fusion to activate the reporter alone. One way to minimize this is through the use of multiple reporters and by swapping

the domains fused to the two proteins. Biological false positives truly interact in yeast, but have no physiological relevance. These occur in part because proteins that do not endogenously reside in the same cellular compartment are brought together in the nucleus of yeast, allowing for an interaction that has no biological significance. Therefore, it is important to confirm that these proteins are truly expressed in the same subcellular location. The interactions can be further tested in mammalian cells by overexpression and co-immunoprecipitation, however similar issues may arise. Although there are several limitations to the yeast two-hybrid assay, this method has repeatedly been a successful way to identify biologically relevant protein-protein interactions.

While the yeast two-hybrid has been used to shed light on many biological pathways, more recent modifications of this assay have allowed researchers to expand the type of molecular interactions that can be identified by this method. The yeast one-hybrid assay is based on the same principles as the yeast two-hybrid, but screens for proteins that bind DNA (Alexander et al., 2001). One example would be the identification of factors that bind a specific gene promoter sequence (Li and Herskowitz, 1993). The ability to assess tertiary complexes has also been developed. Through these systems, proteins that act as a bridge between two other proteins, or proteins that stabilize the association of an otherwise weak protein-protein interaction can be identified (Tirode et al., 1997). A further adaptation of the three-hybrid system can identify proteins that bind specific RNA sequences or can identify the partner RNA for a RNA-binding protein (Putz et al., 1996). Additional modifications have allowed for the identification of receptor interactions with small ligands or the discovery of novel ligands for orphan receptors (Licitra and Liu, 1996). Finally, a 'reverse'

system has been developed in which factors that inhibit protein binding can be identified (Vidal et al., 1996; Vidal and Legrain, 1999). This assay has important potential for identification of novel therapeutic agents.

As a method to identify proteins that interact with m-Bop in the embryonic heart, the yeast two-hybrid has been a valuable assay, but also a challenging one. The difficulty of false positives remain and while many candidate clones may appear attractive at first glance, there must be functional assays available to study the interacting proteins in the context of a biological pathway. In retrospect, I would refine the scheme I used to eliminate and evaluate the clones from the yeast two-hybrid. To begin, the library screening I performed resulted in the growth of approximately 400 colonies on the quadruple dropout media containing 10mM 3-AT. As previously mentioned, 3-AT inhibits leaky expression of the HIS reporter gene. Replica plating these colonies onto media containing a higher concentration of 3-AT would have initially helped to reduce false positives resulting from non-specific binding. The remaining colonies would be tested for β-galactosidase activity and DNA from the blue clones would be isolated. These clones would be introduced back into the AH109 yeast strain containing the appropriate reporters, but lacking the bait plasmid containing m-Bop. Any clones that activated the reporters in the absence of the GAL4-m-Bop fusion would be eliminated. It would also be useful to swap the fusion domains, and reintroduce the new fusion proteins into yeast. DNA would be extracted from the resulting colonies, and the sequence encoded by each clone would be identified through direct sequencing. Assuming that there were a relatively small number of clones remaining, I would subclone each clone into a tagged expression vector and test the interaction by co-immunoprecipitation from cells

transiently transfected with both m-Bop and the candidate clone. Because we have shown that m-Bop functions as a transcriptional repressor, the proteins that interact with m-Bop through co-immunoprecipitation would then be studied in transcriptional assays with m-Bop. Further characterization of the interactions would depend on the identity of each protein.

The scheme I have outlined is a more systematic method to identify biologically significant protein-protein interactions when faced with a large number of colonies resulting from a yeast two-hybrid screen. There are still many candidate factors from this yeast two-hybrid that I have yet to characterize and may be important for m-Bop's biological function. Attempts to eliminate some of these factors in earlier steps may have streamlined the process of identifying true physiological interactions. A second challenge was the availability of assays to test the interactions. Many of the proteins identified in this yeast two-hybrid were not well studied and therefore provided a limited number of functional assays by which to test the interactions. Every attempt at performing the yeast two-hybrid is different and the method by which the resulting clones are pursued will vary depending on the number of colonies that result from the screen, the number of clones that are eliminated after each step, the identity of the clones, and the assays available to study the interactions.

A role for TRB3 in cardiac development

Tribbles was first reported as a novel inhibitor of mitosis in the mesoderm of domain 10 during *Drosophila* gastrulation. This allowed for proper formation of the ventral furrow during development. Reorganization of the cytoskeleton is necessary for both cell cycle division and morphogenetic processes and therefore cannot occur simultaneously, suggesting

the need for a regulatory mechanism that can coordinate the two processes. Tribbles performs this function by inducing proteosome-mediated degradation of String at the proper developmental timepoint. Flies homozygous-null for *tribbles* are lethal throughout development, suggesting that Tribbles may modulate cell proliferation at many developmental stages (Seher and Leptin, 2000). The question remains whether *tribbles* orthologs use similar mechanisms to coordinate morphogenetic movements and cell proliferation in higher organisms as well.

The interaction with m-Bop suggests a novel function for TRB3 in murine cardiac development. Interestingly, Seher and Leptin reported the inability of Tribbles to block mitosis in cell types other than the mesoderm, suggesting the presence of a cofactor in mesoderm-derived tissue that is absent in other cell types (Seher and Leptin, 2000). Neither Tribbles nor its mouse ortholog, TRB3, have been shown to be involved in transcriptional regulation, however Tribbles regulates the transcription factor Slbo (C/EBP□) through proteosome-mediated degradation (Rorth et al., 2000). m-Bop protein was unchanged in the presence of TRB3 suggesting a different role for this factor in the heart.

Through a collaborative effort, I showed that m-Bop functions as a transcriptional repressor, but we do not know what genes it directly regulates. By virtue of its interaction, TRB3 enhanced repression by m-Bop, but again, we have yet to identify endogenous target genes that are regulated by these proteins. Because Tribbles is involved in regulation of cell division, it will be interesting to determine if TRB3 and m-Bop work together in the embryonic heart to transcriptionally regulate cell cycle genes. Targeted deletion of *Bop* in mice was lethal at E10.0, and revealed persistence of immature ventricular cardiomyocytes.

The possibility remains that m-Bop and TRB3 function together to coordinate mitosis with cardiomyocyte maturation in the ventricles of the embryonic heart during development. Inactivation of *Bop* in mice would disrupt this process possibly leading to cells that need to undergo the proper morphological changes but cannot because the gene program to shut down cell division is not in place.

Although Tribbles has not been implicated in transcriptional regulation of cell cycle, many cell cycle genes are regulated by multiple mechanisms. TRB3 is located in the nucleus of the cell, and it would seem necessary that while a specific gene product was being degraded, production of that protein would also be halted. Future experiments are aimed at determining if *Bop* regulates genes involved in cell cycle by looking at cell cycle genes disregulated in *Bop* mutant embryos, and by determining the cell cycle profile of cells overexpressing *Bop*. We showed that transcriptional repression by Bop is mediated at least in part by HDACs. It will also be interesting to determine if the mechanism by which TRB3 enhances repression by m-Bop is mediated via histone deacetylase activity, or if it works through a separate mechanism entirely.

skNAC in the embryonic heart

While there is much convincing data that m-Bop and skNAC physically interact, studying the functional significance of this interaction has been challenging. *Bop* and *skNAC* have perfectly overlapping domains of expression in the embryonic myocardium suggesting a unique role for these molecules during cardiogenesis. While we know Bop is essential for

cardiovascular development, preliminary evidence suggests that skNAC may not be required during this process, however it is early to speculate.

It seems unlikely that the α*NAC* and *skNAC* isoforms serve a similar purpose in mouse development due to their disparate patterns of expression and protein size. There is no convincing evidence in the literature suggesting that these two molecules share a function, and there is still much controversy over the role of α*NAC* in the cell and whether it encodes a protein that serves a dual function. αNAC was originally identified as a ribosome-associated factor that binds unfolded polypeptide chains independent of their sequence (Weidmann et al., 1994). It was suggested by *in vitro* methods that αNAC functions in a dimeric complex as a negative regulator of translocation into the endoplasmic reticulum (Jungnickel and Rapoport, 1995; Lauring et al., 1995) and a positive regulator of translocation into the mitochondria (George et al., 1998). However, neither of these hypotheses is widely accepted, and the *in vivo* function of the ribosome-bound NAC complex is poorly understood. αNAC has also been reported to function as a developmentally regulated bone-specific transcriptional coactivator (Yotov et al., 1998; Moreau et al., 1998). Separate reports refute this data suggesting that α*NAC* is expressed at relatively high levels in many tissues (Moller et al., 1998). Additionally, there is much debate as to whether αNAC truly translocates from the cytosol to the nucleus (Beatrix et., 2000).

It is difficult to say whether details of αNAC function will provide insight into the function of skNAC. The fact that they are products of the same gene appears to be the most that these two proteins have in common thus far. skNAC can be found in the nucleus, but is predominantly cytosolic, and is reported to be a transcriptional activator based on

experiments that I have been unable to repeat. Further investigation of the *skNAC* mutant mouse in the mixed and pure genetic background may reveal an *in vivo* role for this molecule in the tissues in which it is expressed. Previous reports suggest a role for skNAC in myocyte differentiation. The fact that a number of *skNAC*-null mice are viable suggests a nonessential function for *skNAC* in the embryonic heart, but may reveal an important role for skNAC in the skeletal muscle of the developing and adult mouse. The possibility remains that the embryonic mouse heart expresses a functionally redundant gene such as □*NAC*, which may be upregulated in the absence of *skNAC*. These preliminary results suggest that the interaction between m-Bop and skNAC is not essential for the function of m-Bop in the embryonic heart. Corroborating evidence is suggested by the fact that mice heterozygote for both *Bop* and *skNAC* are viable.

METHODS

RNA isolation

Two litters of E11.5 mouse hearts were harvested and total RNA was isolated using the NucleoSpin RNA II Kit (Clontech). The tissue was homogenized in lysis buffer containing □-Mercapthoethanol, adsorbed onto a NucleoSpin RNA column, centrifuged and digested with Dnase I. The filter was washed thoroughly and the RNA was eluted from the column. From the total RNA, poly(A) RNA was isolated (MicroPoly(A) Pure kit, Ambion). Total RNA was bound to Oligo(dT) Cellulose, incubated for 1 h, washed several times and eluted. The poly(A) RNA was then precipitated and resuspended in water.

Yeast two-hybrid library construction and screening

The yeast two-hybrid library was constructed using the MATCHMAKER Library Construction Kit (Clontech). An Oligo d(T) primer was annealed to 200ng of poly(A) RNA isolated from the mouse embryonic hearts. MMLV reverse transcriptase and dNTPs were added and the sample was incubated at 42° C for 10 m to begin first strand cDNA synthesis, and add deoxycytidine residues to the 5' end of the cDNA. The SMART III Oligonucleotide (Clontech) containing an oligo(G) sequence at its 3' end was annealed to the 5' end of the cDNA and the cDNA was extended in the 3' direction resulting in a ss cDNA containing the complete 5' end of the mRNA was well as the sequence complimentary to the SMART III Oligo. This sequence served as a universal priming site in the subsequent amplification. Long-distance PCR (LD PCR) was performed using primer sequences within the SMART III Oligo and the Oligo (dT) primer. The following program was used in the Bio Rad iCycler: 1 cycle (95°, 30 sec); 22 cycles (95°, 10 sec + 68°, 6 min + y); 1 cycle (68°, 5 min). y= 5 sec x (cycle number –1). The resulting ds cDNA fragments were purified on a CHROMA SPIN+TE-400 Column to eliminate DNA molecules < 200 bp.

AH109 yeast cells were made competent by LiAc method, and transformed with pGBKT7 bait plasmid (Clontech) containing the full-length Bop cDNA. Colonies were selected on plates lacking tryptophan. Media was inoculated with one colony containing bait plasmid and was grown in culture shaking at 30° C to an OD_{600} of 0.4-0.5. The yeast was made competent by LiAc method and transformed with the ds cDNA library and the linearized backbone vector (pGADT7-Rec, Clontech). Because the linearized vector shares sequence homology with the ends of the library fragments, these two components recombine

via a double-crossover mechanism to produce the circular plasmid. Transformants were selected for on quadruple dropout medium containing 10mM 3-AT. Colonies were screened for β-galactosidase activity, and DNA was isolated from blue colonies and subject to PCR. The 5' primer (TCATCGGAAGAGAGTAG) and 3' primer (GTCACTTTAAAATTTGTAT) were used to amplify the insert. The PCR products were purified and directly sequenced.

Plasmid construction

Expression plasmids were constructed in the backbone vector PCDNA3.1 containing either a MYC or FLAG tag. Yeast two-hybrid clones were amplified using PCR primers containing Xba1 or Cla1 restriction site sequences, and cloned into the FLAG-tagged vector using Cla1, Xba1 or both restriction sites. The following TRB3 protein truncations were constructed by PCR using EcoR1 and Xho1 restriction sites: TRB3 (1-80); TRB3 (1-149); TRB3 (1-214); TRB3 (1-295); TRB3 (81-355); TRB3 (150-355); TRB3 (215-355); TRB3 (296-355). All PCR amplifications were performed with high fidelity Pfu Turbo DNA polymerase (Stratagene) and sequenced for accuracy.

Immunoprecipitation and western blotting

Cell lysates were incubated with 10 μl of a 50% slurry of protein-A/G sepharose beads for 1 h to preclear. One microgram of polyclonal MYC A14 or monoclonal FLAG M2 (Sigma) antibody was added to the supernatant for a minimum of 4 h at 4°C, followed by a 1 h incubation with 20 μl protein-A/G sepharose beads (Sigma). After four 1 mL washes with

lysis buffer, the precipitated proteins were analyzed by SDS-PAGE and transferred to PVDF membrane. Membranes were probed with the monoclonal FLAG M2, monoclonal MYC 9E10, polyclonal MYC A14, or polyclonal HA antibody (Sigma). Western blots were developed with the enhanced chemiluminescence (ECL) analysis system (Amersham, U.K.).

Whole mount and section *in situ* hybridization

For whole-mount in situ hybridization, digoxygenin-labeled RNA probes were prepared by in vitro transcription. Mouse embryos from E9.5 to E15.5, were isolated in phosphate-buffered saline (PBS) and the pericardium was removed. Embryos were fixed in 4% paraformaldehyde/PBS at 4°C overnight. Whole-mount *in situ* hybridization was performed as previously described in Chapter 2. For section *in situ* hybridization, ^{35}S-labeled antisense riboprobes were generated by *in vitro* transcription and *in situ* hybridization was performed on E9.0-E12.5 mutant and wild-type embryos, and adult heart as previously described in Chapter 2.

Cell culture and transient transcfections

C3H 10T1/2, HELA, and Cos 1, cells (ATCC) were grown in DMEM (Life Technologies, Frederick, MD) supplemented with 10% fetal bovine serum at 37° C in an atmosphere of 5% CO_2 in air. The cells were transfected using FuGENE6 reagent (Boehringer Mannheim) or Lipofectamine Plus (Invitrogen). For luciferase assays, the total DNA concentration was held constant by adding the empty PCDNA3.1 expression plasmid. Cells were harvested 30- 36 h after transfection using the lysis buffer contained in the

Promega Luciferase Kit. For immunoprecipitation experiments, Cos 1 cells were transfected with MYC-tagged m-Bop and the various FLAG-tagged yeast two-hybrid clones, or FLAG-tagged m-Bop and the MYC-tagged TRB3 deletion constructs. Cells were lysed in buffer (10 mM Tris pH 7.4, 1mM EDTA, pH 8.0, 0.5% Triton X100 in PBS) containing protease inhibitors (Roche) and PMSF 30-36 h after transfection.

Luciferase assay

Twenty microliters of cell lysates were analyzed with a Rosys Anthos Lucy2 luminometer. Relative light units obtained from the pGL2-5XGAL4-SV40 reporter (Luciferase Assay Kit, Promega) were normalized by transfection efficiency and protein concentration. Transfection efficiency was determined by spectrophotmetric analysis of cells co-transfected with the RSV-Lac Z expression plasmid. Activation was determined in relation to the pGL2-5XGAL4-SV40 reporter alone. Three independent experiments were performed to calculate the mean and standard error.

Immunocytochemistry

Cells were fixed with 3.7 % formaldehyde/PBS for 20 m at room temperature (RT) and washed three times in PBS for 5 m. The cells were permeabilized for 3 m in 0.1% triton/PBS followed by three PBS washes for 5 m. Cells were blocked for non-specific binding with 3% BSA/PBS for 1 h at RT and incubated with primary antibody (0.1 -2 □g/mL) in 1% BSA/PBS 1 h at RT. Monoclonal FLAG M2 or MYC 9E10 was used for primary antibody. Three 10 m PBS washes were followed by incubation with FITC or Cy3 -conjugated anti-mouse

secondary antibody (1:200) for 1 h. Cells were washed three times for 10 m, stained with DAPI and mounted on microscope slides.

Kinase assay

Proteins were immunoprecipitated from cell lysates as described above. The beads were washed twice with lysis buffer and twice with kinase buffer (20 mM HEPES, 20 mM MgCl, 2 mM DTT). The beads were resuspended in kinase buffer with the addition of 20 μM ATP, 1 μM okadeic acid, and [γ-^{32}P] ATP. The reaction was incubated for 30 m at 30° C. The results were run on an acrylamide gel and visualized by autoradiography.

Targeted deletion of *skNAC*

A construct was designed to replace the second exon, which confers skeletal muscle specificity to skNAC, with a neomycin resistance (*neo*) gene flanked by FRT sites. A BAC clone containing the skNAC genomic sequence was digested with Xba1 and the digested fragments were subcloned into pBluescript. The colonies containing the 5' and 3'-arm sequences were identified by colony lift and cloned into the targeting vector. 129/SvEvTAC ES cells were electroporated with linearized targeting vector and selected with G418. Correctly targeted integrations were identified by Southern hybridization. Correct integration of the 3' short arm was indicated by a 7.7 kb HpaI fragment, and a 13.5 kb wild type HpaI fragment that hybridized only with the 5' probe. Correct integration of the long arm was indicated by the presence of an 11.7 kb HIND III fragment and a 9.7 kb wild type HIND III fragment that hybridized with the 3' probe (Figure 7).

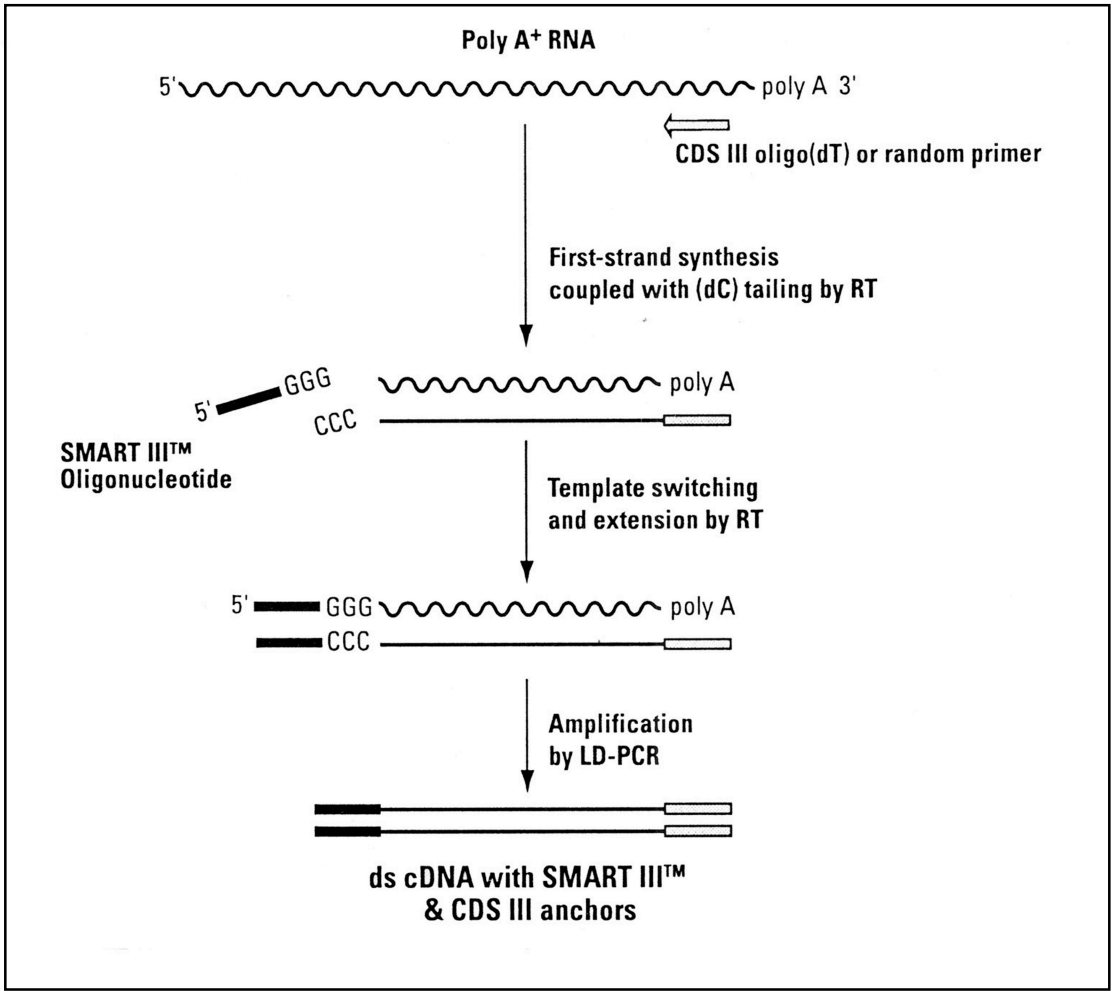

Figure 1. Yeast two-hybrid library construction. Poly(A) RNA was isolated from E11.5 embryonic mouse hearts. Using the Clontech Matchmaker Library Construction Kit, first-strand cDNA synthesis was performed first by annealing the oligo(dT) primer (CDSIII) to the poly(A) region followed by reverse transcription with the MMLV reverse transcriptase. The SMART III Oligonucleotide was annealed to the 5' end of the cDNA and the cDNA was extended by the reverse transcriptase creating ss cDNA fragments with SMART III and CDS III anchors. These sites were used to amplify the cDNA by long-distance PCR creating a library of ds cDNA fragments.

IDENTITY OF YEAST TWO-HYBRID CLONE	No. OF CLONES
SkNAC	35
TRB3	1
Novel helicase	4
MICAL	4
FKBP 8 (38)	4
mFz10	1
Splicing factor 3a	3
PGC-1beta	1
Novel nucleosome assembly protein	1
Novel melanoma associated antigen	1
Novel G protein sunbunit (Gng31g)	1
Acyl-CoA oxidase	1
Proteosome beta type 5	1
Hemoglobin, beta adult chain	1
Hemoglobin, alpha adult chain	1
Glucosidase II beta subunit	1
Fibronectin	1
Tubulin	1
Zyxin	1
Beta myosin heavy chain	1
Ubiquitin conjugating enzyme E2	1
Cytochrome C oxidase	1
Phospholipase C	1
ADP ribosylarginine	1
Mithochondrial protein	1
Ribosomal proteins	6

Table 1. Identification of yeast two-hybrid clones. The left column displays the clones identified by the yeast two-hybrid screen. The right column shows the number of times each clone was identified.

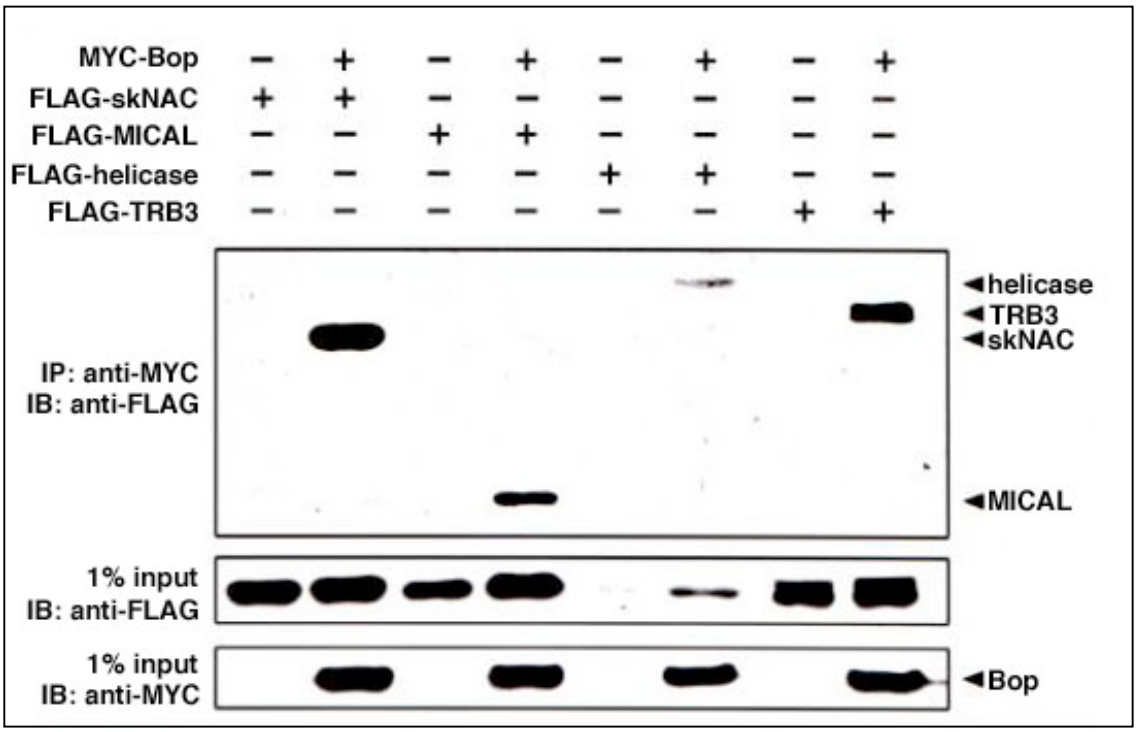

Figure 2. Yeast two-hybrid clones immunoprecipitate with m-Bop. Cos1 cells were cotransfected with a FLAG-tagged yeast two-hybrid clone and either a MYC-tagged Bop or empty vector, and incubated for 30 h. Cells were lysed and lysates were immunoprecipitated with a polyclonal MYC A14 antibody. The immunoprecipitates were run on a SDS-PAGE gel and analyzed by Western blot with a monoclonal FLAG M2 antibody shown in upper panel. skNAC, TRB3, MICAL and the novel helicase immunoprecipitated with m-Bop. Input is shown in lower two panels.

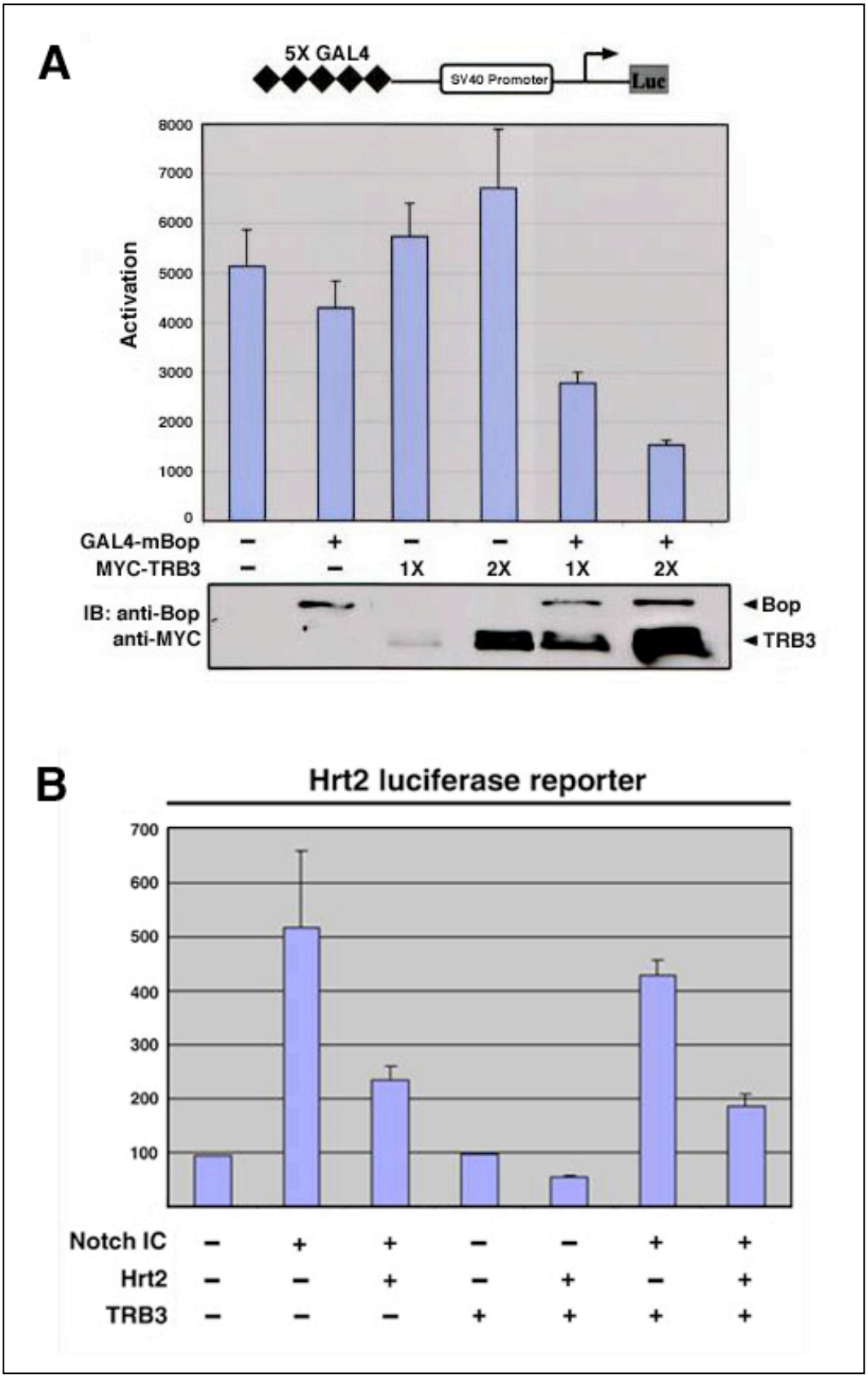
A
5X GAL4
SV40 Promoter
Luc
Activation
8000
7000
6000
5000
4000
3000
2000
1000
0
GAL4-mBop
MYC-TRB3
1X
2X
1X
2X
IB: anti-Bop
anti-MYC
Bop
TRB3
B
Hrt2 luciferase reporter
700
600
500
400
300
200
100
Notch IC
Hrt2
TRB3

Figure 3. TRB3 enhances repression by m-Bop. (A) Cos1 cells were cotransfected with an SV40-driven luciferase reporter containing 5X GAL4 DNA-binding elements, GAL4-Bop, RSV-lacZ and increasing amounts of MYC-TRB3. TRB3 enhanced repression of luciferase by m-Bop in a dose-dependent fashion, but had no effect on luciferase activity alone. Results were normalized to β-galactosidase activity and repression was determined in relation to SV40-driven luciferae activity alone. The lower panel shows protein expression of m-Bop and TRB3 in each sample by immunoblot. (B)) Cos1 cells were cotransfected with a Hrt2-driven luciferase reporter containing, Notch IC, Hrt2, TRB3, and RSV-lacZ. TRB3 had not effect on Hrt2-mediated repression of the Hrt2 reporter. Results were normalized to β-galactosidase activity.

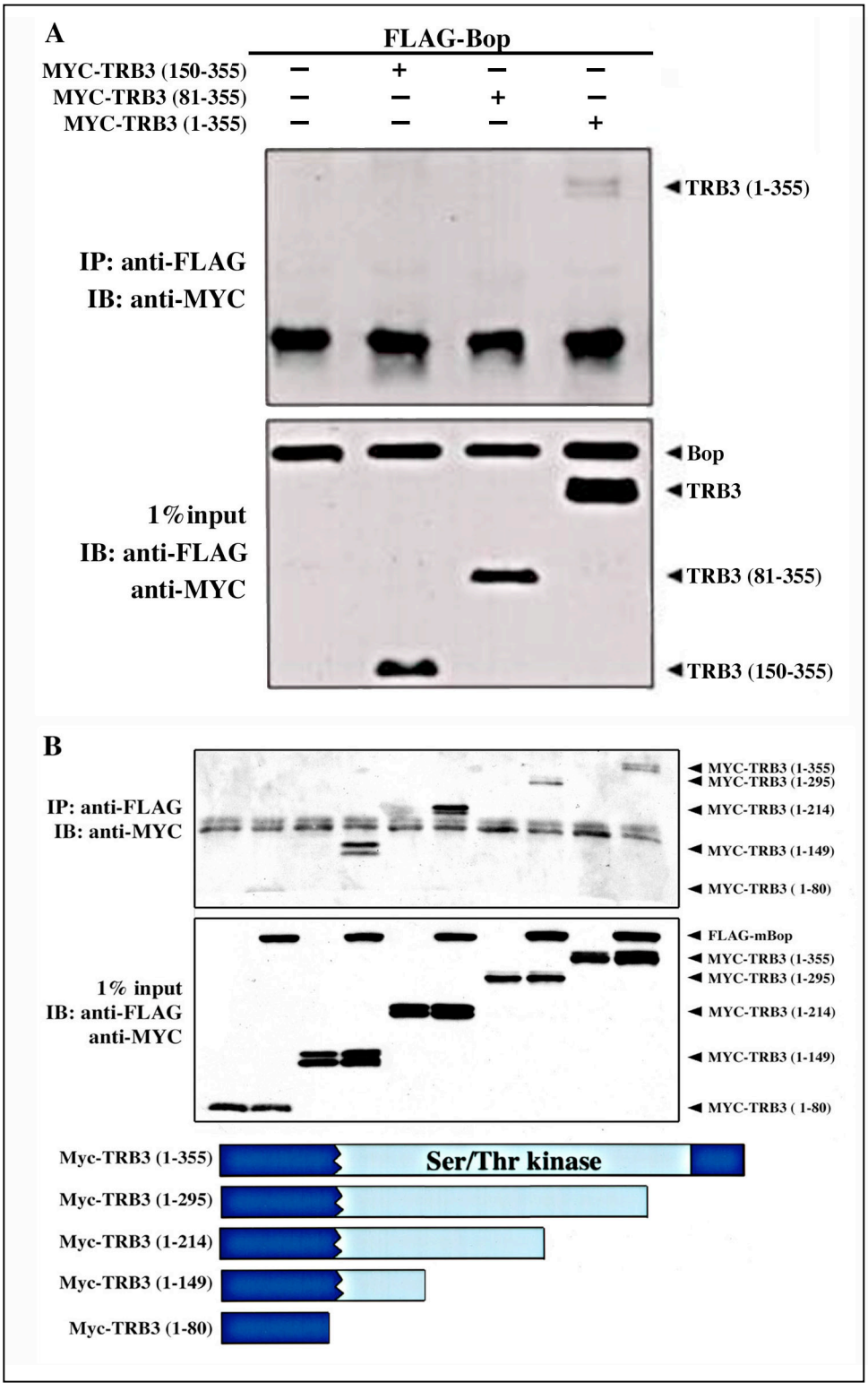
A
FLAG-Bop
MYC-TRB3 (150-355) − + − −
MYC-TRB3 (81-355) − − + −
MYC-TRB3 (1-355) − − − +
IP: anti-FLAG
IB: anti-MYC
TRB3 (1-355)
1%input
IB: anti-FLAG
anti-MYC
Bop
TRB3
TRB3 (81-355)
TRB3 (150-355)
B
IP: anti-FLAG
IB: anti-MYC
MYC-TRB3 (1-355)
MYC-TRB3 (1-295)
MYC-TRB3 (1-214)
MYC-TRB3 (1-149)
MYC-TRB3 (1-80)
1% input
IB: anti-FLAG
anti-MYC
FLAG-mBop
MYC-TRB3 (1-355)
MYC-TRB3 (1-295)
MYC-TRB3 (1-214)
MYC-TRB3 (1-149)
MYC-TRB3 (1-80)
Myc-TRB3 (1-355)
Ser/Thr kinase
Myc-TRB3 (1-295)
Myc-TRB3 (1-214)
Myc-TRB3 (1-149)
Myc-TRB3 (1-80)

Figure 4. N-terminus of TRB3 is necessary and sufficient to interact with m-Bop. N-terminal (A) and C-terminal (B) MYC-TRB3 deletion constructs were tested by co-immunoprecipitation with FLAG-Bop to map the region of TRB3 that interacts with m-Bop. Cos1 cells were cotransfected FLAG-Bop and the MYC-TRB3 deletion constructs, incubated for 30 h and lysed. Cell lysates were immmunoprecipitated using a monoclonal FLAG M2 antibody. The immunoprecipitates were run on an SDS-PAGE acrylamide gel and analyzed by Western blot with a polyclonal MYC A14 antibody. C-terminal deletions (B), but not N-terminal deletions (A) immunoprecipitated with m-Bop. Input is shown in the lower panels for both 4A and 4B.

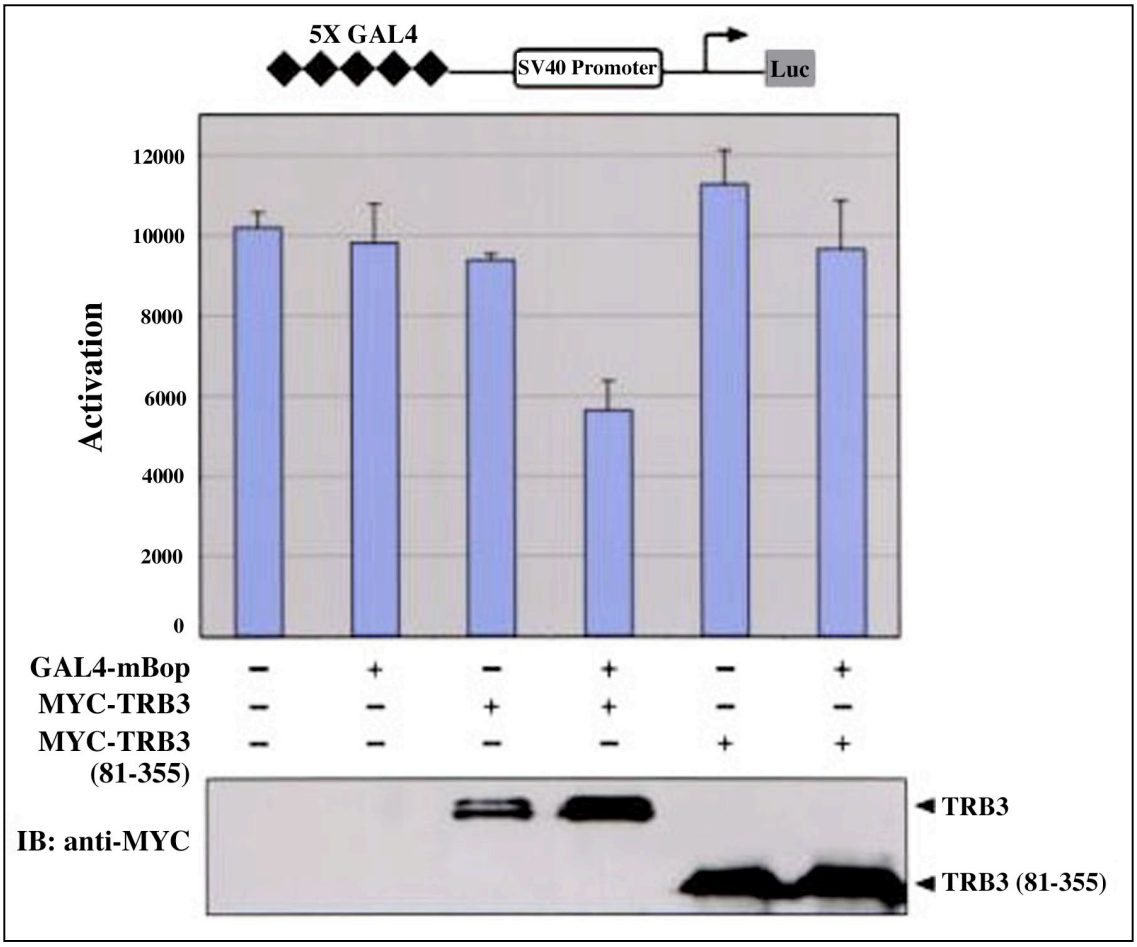

Figure 5. N-terminal deletion disupts enhanced repression by TRB3. Cos1 cells were cotransfected with the SV40-driven luciferase reporter containing 5XGAL4 DNA-binding elements, GAL4-Bop, RSV-lacZ, and either full-length MYC-TRB3 or MYC-TRB3 (81-355). Full-length TRB3, but not TRB3 (81-355) enhanced repression of luciferase by m-Bop. Results were normalized to β-galactosidase activity, and repression was determined in relation to SV40-driven luciferae activity alone. The lower panel shows protein expression of TRB3 and TRB3 (81-355) in each sample b y immunoblot.

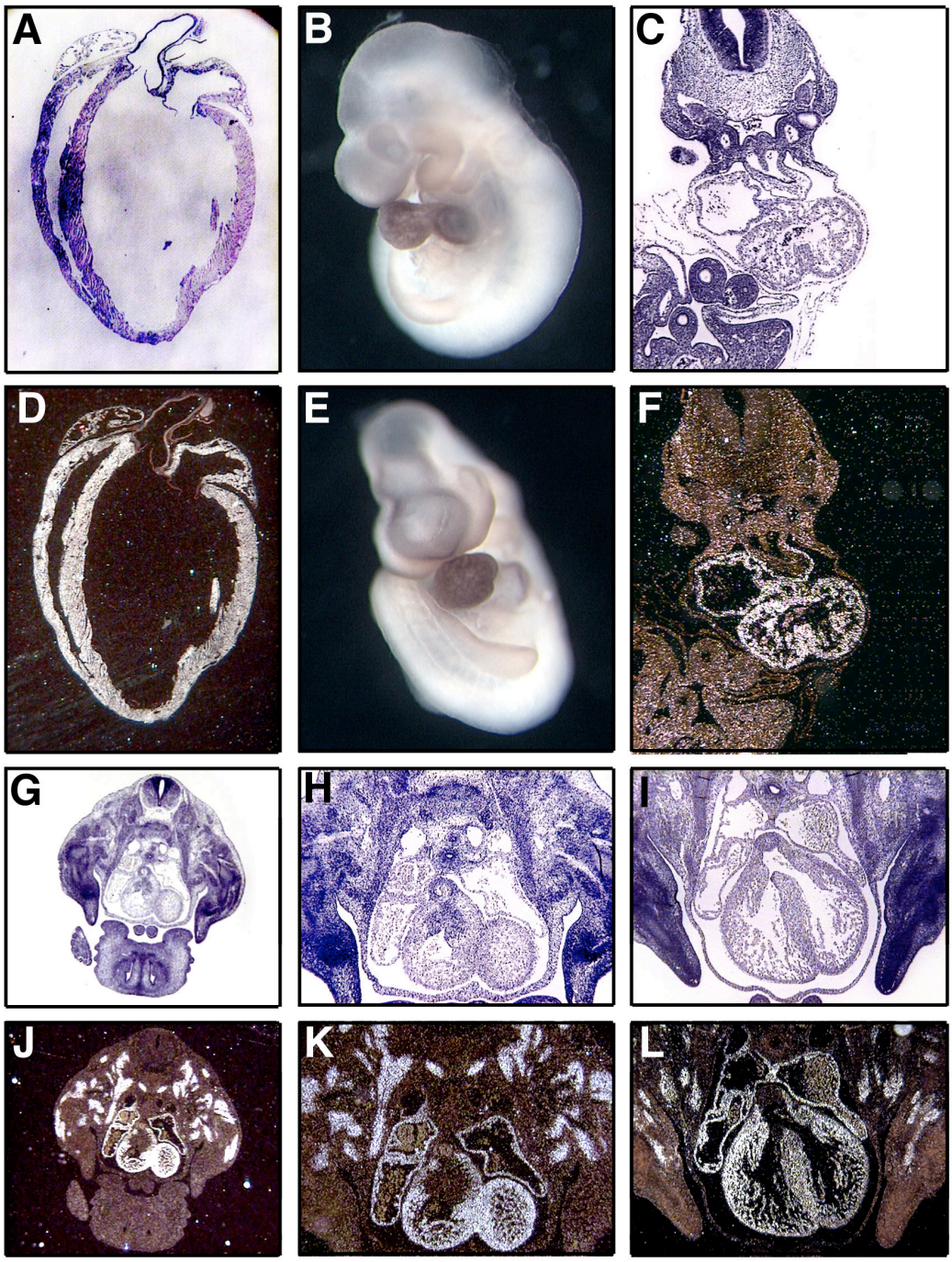

Figure 6. *skNAC* and *Bop* are coexpressed. *skNAC* is expressed in adult mouse heart by section *in situ* hybridization (D). Cardiac expression of *skNAC* at E9.5 in a left-sided (B) and frontal (E) view by whole-mount *in situ* hybridization. *skNAC* expression was observed in the myocardium of the heart and the skeletal muscle precursors at E10.5 (F), and E12.5 (J,K) similar to *Bop* expression shown at E12.5 (L) by section in situ.

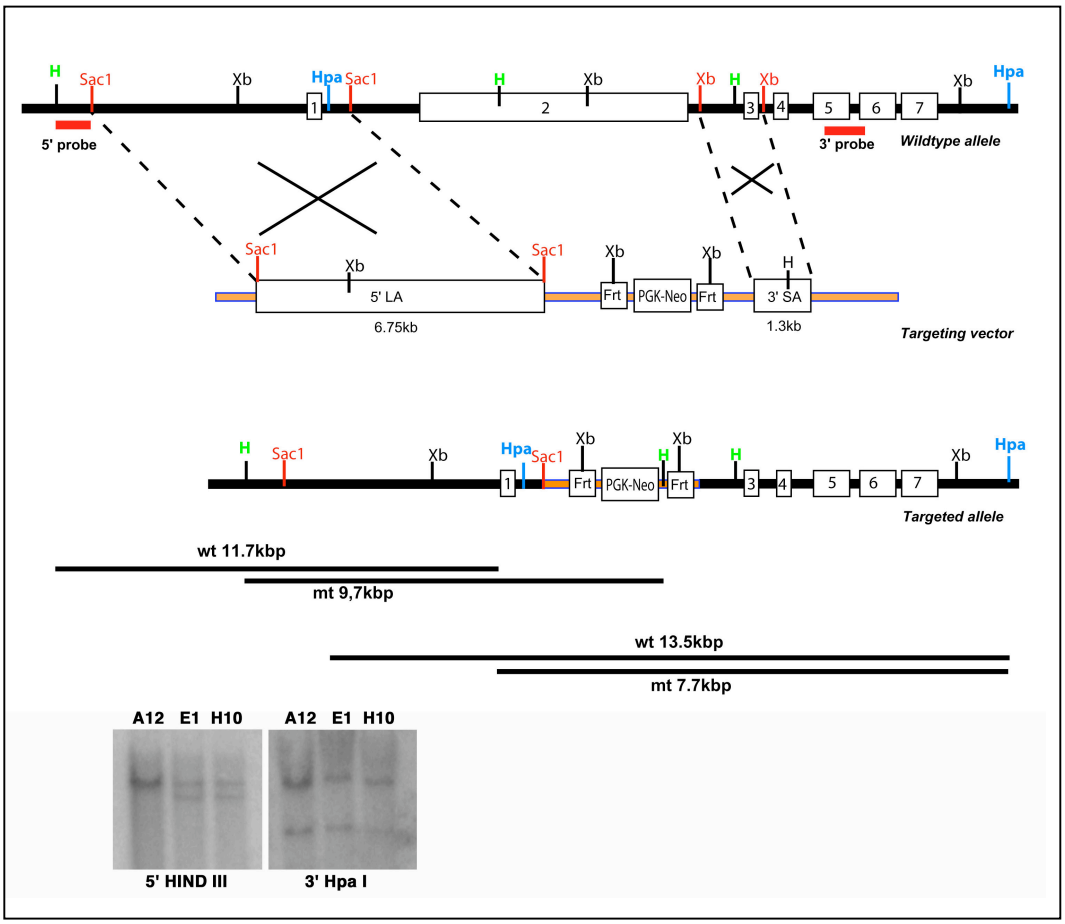

Figure 7. Targeting strategy for *skNAC*. Organization of the *skNAC* wild type allele and targeting vector. Homologous recombination resulted in replacement of exon 2 of *skNAC* by the neomycin resistance gene (Neo) flanked by FRT sites as shown in the *skNAC* targeted allele. The inset shows ES cell genotyping by Southern blot analysis. Two ES cell clones, E1 and H10, were positively targeted at the 5' and 3' ends.

REFERENCES

Alexander, M.K., Bourns, B.D. & Zakian, V.A. One-hybrid systems for detecting protein-DNA interactions. *Methods Mol Biol* **177**, 241-59 (2001).

Beatrix, B., Sakai, H. & Wiedmann, M. The alpha and beta subunit of the nascent polypeptide-associated complex have distinct functions. *J Biol Chem* **275**, 37838-45 (2000).

Dierick, H. & Bejsovec, A. Cellular mechanisms of wingless/Wnt signal transduction. *Curr Top Dev Biol* **43**, 153-90 (1999).

Du, K., Herzig, S., Kulkarni, R.N. & Montminy, M. TRB3: a tribbles homolog that inhibits Akt/PKB activation by insulin in liver. *Science* **300**, 1574-7 (2003).

Edgar, B.A. & O'Farrell, P.H. Genetic control of cell division patterns in the Drosophila embryo. *Cell* **57**, 177-87 (1989).

Edgar, B.A. & O'Farrell, P.H. The three postblastoderm cell cycles of Drosophila embryogenesis are regulated in G2 by string. *Cell* **62**, 469-80 (1990).

Fields, S. & Song, O. A novel genetic system to detect protein-protein interactions. *Nature* **340**, 245-6 (1989).

George, R., Beddoe, T., Landl, K. & Lithgow, T. The yeast nascent polypeptide-associated complex initiates protein targeting to mitochondria in vivo. *Proc Natl Acad Sci U S A* **95**, 2296-301 (1998).

Gottlieb, P.D. et al. Bop encodes a muscle-restricted protein containing MYND and SET domains and is essential for cardiac differentiation and morphogenesis. *Nat Genet* **31**, 25-32 (2002).

Grosshans, J. & Wieschaus, E. A genetic link between morphogenesis and cell division during formation of the ventral furrow in Drosophila. *Cell* **101**, 523-31 (2000).

Jungnickel, B. & Rapoport, T.A. A posttargeting signal sequence recognition event in the endoplasmic reticulum membrane. *Cell* **82**, 261-70 (1995).

Koonin, E.V. A new group of putative RNA helicases. *Trends Biochem Sci* **17**, 495-7 (1992).

Lauring, B., Sakai, H., Kreibich, G. & Wiedmann, M. Nascent polypeptide-associated complex protein prevents mistargeting of nascent chains to the endoplasmic reticulum. *Proc Natl Acad Sci U S A* **92**, 5411-5 (1995).

Li, J.J. & Herskowitz, I. Isolation of ORC6, a component of the yeast origin recognition complex by a one-hybrid system. *Science* **262**, 1870-4 (1993).
Licitra, E.J. & Liu, J.O. A three-hybrid system for detecting small ligand-protein receptor interactions. *Proc Natl Acad Sci U S A* **93**, 12817-21 (1996).

Malik, T.H. & Shivdasani, R.A. Structure and expression of a novel frizzled gene isolated from the developing mouse gut. *Biochem J* **349 Pt 3**, 829-34 (2000).

Mata, J., Curado, S., Ephrussi, A. & Rorth, P. Tribbles coordinates mitosis and morphogenesis in Drosophila by regulating string/CDC25 proteolysis. *Cell* **101**, 511-22 (2000).

Moller, I. et al. Unregulated exposure of the ribosomal M-site caused by NAC depletion results in delivery of non-secretory polypeptides to the Sec61 complex. *FEBS Lett* **441**, 1-5 (1998).

Moreau, A., Yotov, W.V., Glorieux, F.H. & St-Arnaud, R. Bone-specific expression of the alpha chain of the nascent polypeptide-associated complex, a coactivator potentiating c-Jun-mediated transcription. *Mol Cell Biol* **18**, 1312-21 (1998).

Munz, B., Wiedmann, M., Lochmuller, H. & Werner, S. Cloning of novel injury-regulated genes. Implications for an important role of the muscle-specific protein skNAC in muscle repair. *J Biol Chem* **274**, 13305-10 (1999).

Nakagawa, O. et al. Members of the HRT family of basic helix-loop-helix proteins act as transcriptional repressors downstream of Notch signaling. *Proc Natl Acad Sci U S A* **97**, 13655-60 (2000).

Putz, U., Skehel, P. & Kuhl, D. A tri-hybrid system for the analysis and detection of RNA--protein interactions. *Nucleic Acids Res* **24**, 4838-40 (1996).

Rorth, P., Szabo, K. & Texido, G. The level of C/EBP protein is critical for cell migration during Drosophila oogenesis and is tightly controlled by regulated degradation. *Mol Cell* **6**, 23-30 (2000).

Schmid, S.R. & Linder, P. D-E-A-D protein family of putative RNA helicases. *Mol Microbiol* **6**, 283-91 (1992).

Seher, T.C. & Leptin, M. Tribbles, a cell-cycle brake that coordinates proliferation and morphogenesis during Drosophila gastrulation. *Curr Biol* **10**, 623-9 (2000).

Sims, R.J., 3rd et al. m-Bop, a repressor protein essential for cardiogenesis, interacts with skNAC, a heart- and muscle-specific transcription factor. *J Biol Chem* **277**, 26524-9 (2002).

Srivastava, D. et al. Regulation of cardiac mesodermal and neural crest development by the bHLH transcription factor, dHAND. *Nat Genet* **16**, 154-60 (1997).

Suzuki, T. et al. MICAL, a novel CasL interacting molecule, associates with vimentin. *J Biol Chem* **277**, 14933-41 (2002).

Terman, J.R., Mao, T., Pasterkamp, R.J., Yu, H.H. & Kolodkin, A.L. MICALs, a family of conserved flavoprotein oxidoreductases, function in plexin-mediated axonal repulsion. *Cell* **109**, 887-900 (2002).

Tirode, F. et al. A conditionally expressed third partner stabilizes or prevents the formation of a transcriptional activator in a three-hybrid system. *J Biol Chem* **272**, 22995-9 (1997).

Vidal, M., Brachmann, R.K., Fattaey, A., Harlow, E. & Boeke, J.D. Reverse two-hybrid and one-hybrid systems to detect dissociation of protein-protein and DNA-protein interactions. *Proc Natl Acad Sci U S A* **93**, 10315-20 (1996).

Vidal, M. & Legrain, P. Yeast forward and reverse 'n'-hybrid systems. *Nucleic Acids Res* **27**, 919-29 (1999).

Wagner, D.S., Gan, L. & Klein, W.H. Identification of a differentially expressed RNA helicase by gene trapping. *Biochem Biophys Res Commun* **262**, 677-84 (1999).

Wiedmann, B., Sakai, H., Davis, T.A. & Wiedmann, M. A protein complex required for signal-sequence-specific sorting and translocation. *Nature* **370**, 434-40 (1994).

Wodarz, A. & Nusse, R. Mechanisms of Wnt signaling in development. *Annu Rev Cell Dev Biol* **14**, 59-88 (1998).

Yotov, W.V. & St-Arnaud, R. Differential splicing-in of a proline-rich exon converts alphaNAC into a muscle-specific transcription factor. *Genes Dev* **10**, 1763-72 (1996).

Yotov, W.V., Moreau, A. & St-Arnaud, R. The alpha chain of the nascent polypeptide-associated complex functions as a transcriptional coactivator. *Mol Cell Biol* **18**, 1303-11 (1998).

DISCUSSION

This work includes the identification of the essential transcriptional repressor, *Bop*, in cardiac development, and the identification of factors that interact with m-Bop in the embryonic heart. Future investigation into the physiological targets of Bop activity will provide insight into the biological pathways through which Bop functions in the heart. Epigenetic studies in *Bop*-null embryos revealed that m-Bop activates *dHAND* expression in the heart, but not directly. Since m-Bop functions as a transcriptional repressor these data suggest that m-Bop represses transcription of factor X, which represses transcription of *dHAND* (Figure 1). In the absence of *Bop*, factor X is derepressed thereby repressing *dHAND*. Differentiation and formation of the right ventricle does not occur properly in the *dHAND*-null mouse embryo. It is likely that aberrant development of the right ventricle in *Bop* mutant mice is due to disruption of this suggested pathway.

Because Bop functions as an HDAC-dependent transcriptional repressor, it is unlikely that Bop directly binds DNA. Identification of the transcription factor skNAC by yeast two-hybrid revealed a potential DNA-binding factor that interacts with m-Bop to bring it to the site of transcription and repress transcription of target genes (Figure 1). Future studies include further investigation into a genetic interaction between these two molecules and the targets of skNAC.

TRB3 coordinates mitosis with morphogenesis during *Drosophila* development. Inhibiting progression of the cell cycle allows for essential morphogenetic changes to occur in the *Drosophila* embryo. This work revealed a novel role for TRB3 as a transcriptional repressor in the embryonic heart. Whether m-Bop and TRB3 function to repress cell cycle

genes is yet to be determined. It is interesting to note that *Bop* mutants reveal a persistence of immature cardiomyocytes. We hypothesize that the expansion of extracellular matrix (ECM) in the *Bop* mutant heart may be a secondary effect of the immature cardiomyocytes. In normal development, newly formed cardiomyocytes secrete ECM, and as they mature and become fully differentiated, they synthesize enzymes that degrade the ECM. m-Bop and TRB3 may function to negatively regulate cell cycle genes in cardiomyocytes, allowing the cells to mature. In the absence of *Bop*, cardiomyocytes continue to express genes necessary for cell division, and therefore do not undergo the normal process of maturation. On the other hand, m-Bop and TRB3 may work together to repress a completely different subset of genes that play no role in regulating the balance between cardiomyocyte cell division and maturation. In either case, these two factors likely function in a complex with a DNA-binding factor since neither m-Bop nor TRB3 appear to bind DNA.

. The data presented above suggests a regulatory role for Bop as a transcriptional repressor in cardiac differentiation and morphogenesis. Because the focus of this work has been the study of factors that control cardiac gene expression during development, little attention has been paid to the possible cytosolic function of Bop. We have shown that m-Bop protein is found both in the nucleus and the cytosol of the cell, and many of the clones generated from the yeast two-hybrid suggest a potential cytosolic function for Bop in differentiating cardiomyocytes. It will be interesting to determine if m-Bop activity is an essential component of both the nucleus and the cytosol, or if the activity of m-Bop is regulated by shuttling the protein from one cellular compartment to the other.

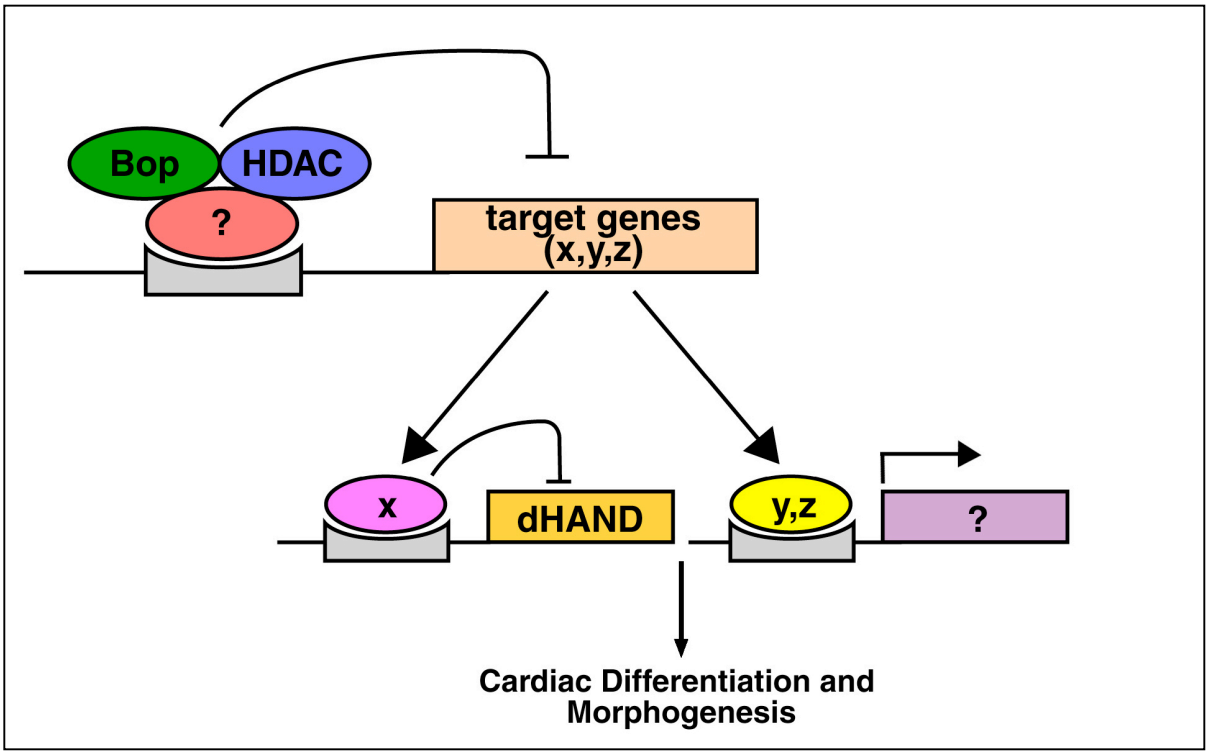

Figure 1. Model: Bop represses transcription of target genes.

ACKNOWLEDGEMENTS

First I thank my family, the people who have seen me through every stage of my life and continue to give me strength. I have learned more from my family than I could ever learn from a textbook or at the bench. My dad inspired the scientist in me, he always taught me to think independently and work hard. My mother taught me strength and compassion. Without realizing it, she always put others before herself. From my sister Christine I learned that life may take an unexpected detour, faith will light your way. My sister Kimberly has always inspired me to stand up for what I believe in. It is not just knowing what you want, it is going out and getting it. My sister Jennifer has taught me many things, most importantly, be honest with yourself.

My husband Mark deserves the most thanks for his patience during the long lab hours and weekends during our first years of marriage. His sacrifice allowed me to follow my dreams. Without his love, support, and friendship, I would not be where I am today.

Thanks to my husband's family who are continually supportive of the path I have chosen and genuinely interested in my research. Your questions have sparked many great discussions.

Thanks to all my friends from each part of my life who have been great sources of encouragement during this endeavor.

Thanks to my dissertation committee, Rueyling Lin, Daniel Garry, and Eric Olson, for all of the insightful advice and encouragement. Special thanks to my chairperson Rueyling for the lengthy discussions not only about science, but also about life.

To all the members of the Srivastava Lab, past and present, it is hard to put into words what an incredible experience it has been to work with you. Thanks for your friendships, your collaborations, and all the fun times. I have learned a tremendous amount from you all, not just in science, but in life as well.

To my mentor Deepak, thanks for giving me the opportunity to join something truly great. I am deeply grateful for the immeasurable time and energy you spent to help me reach my destination, armed with the knowledge and tools to confidently begin the next stage of my life's journey.

To the memory of Paul Gottlieb, a man that showed me anything is possible with determination and hard work. Thanks for the inspiration.

VITAE

Stephanie Angelo Pierce was born in Plainfield, New Jersey, on October 24, 1975, the daughter of Dr. Jacob B. Angelo and Mrs. Diana F. Angelo. At less than one year of age she moved with her family to Spring, Texas, and lived there until she moved to college. After graduating from Klein High School in 1994, she entered Texas A&M University, College Station, Texas, and graduated cum laude, receiving a Bachelor of Science with a double major in Biochemistry and Genetics. In August 1998, she entered The Graduate School of Biomedical Science at The University of Texas Southwestern Medical Center at Dallas to begin her doctoral studies. She joined the laboratory of Deepak Srivastava, M.D. in the summer of 1999. Stephanie married Mark Alan Pierce in May 2000.

Permanent Address: 1313 Wentworth Drive
Lewisville, Texas 75067